NASA TECHNICAL MEMORANDUM

NASA TM X-3078

NASA TM X-3078

SUBSONIC AND SUPERSONIC LONGITUDINAL STABILITY AND CONTROL CHARACTERISTICS OF AN AFT TAIL FIGHTER CONFIGURATION WITH CAMBERED AND UNCAMBERED WINGS AND UNCAMBERED FUSELAGE

by Samuel M. Dollyhigh

Langley Research Center
Hampton, Va. 23665

NATIONAL AERONAUTICS AND SPACE ADMINISTRATION • WASHINGTON, D. C. • AUGUST 1974

1. Report No. NASA TM X-3078	2. Government Accession No.	3. Recipient's Catalog No.
4. Title and Subtitle SUBSONIC AND SUPERSONIC LONGITUDINAL STABILITY AND CONTROL CHARACTERISTICS OF AN AFT TAIL FIGHTER CONFIGURATION WITH CAMBERED AND UNCAMBERED WINGS AND UNCAMBERED FUSELAGE		5. Report Date August 1974
		6. Performing Organization Code
7. Author(s) Samuel M. Dollyhigh		8. Performing Organization Report No. L-9463
		10. Work Unit No. 760-67-01-04
9. Performing Organization Name and Address NASA Langley Research Center Hampton, Va. 23665		11. Contract or Grant No.
		13. Type of Report and Period Covered Technical Memorandum
12. Sponsoring Agency Name and Address National Aeronautics and Space Administration Washington, D.C. 20546		14. Sponsoring Agency Code
15. Supplementary Notes		

16. Abstract

An investigation has been made in the Mach number range from 0.20 to 2.16 to determine the longitudinal aerodynamic characteristics of a fighter airplane concept. The configuration concept employs a single fixed geometry inlet, a 50° leading-edge-angle clipped-arrow wing, a single large vertical tail, and low horizontal tails. The wing camber surface was optimized in drag due to lift and was designed to be self-trimming at Mach 1.40 and at a lift coefficient of 0.20. An uncambered or flat wing of the same planform and thickness ratio was also tested. However, for the present investigation, the fuselage was not cambered. Further tests should be made on a cambered fuselage version, which attempts to preserve the optimum wing loading on that part of the theoretical wing enclosed by the fuselage.

17. Key Words (Suggested by Author(s)) Wind-tunnel tests, Fighter configurations, Aerodynamic characteristics	18. Distribution Statement Unclassified – Unlimited STAR Category 01

19. Security Classif. (of this report)	20. Security Classif. (of this page)	21. No. of Pages	22. Price*
Unclassified	Unclassified	96	$4.00

*For sale by the National Technical Information Service, Springfield, Virginia 22151

SUBSONIC AND SUPERSONIC LONGITUDINAL STABILITY AND CONTROL CHARACTERISTICS OF AN AFT TAIL FIGHTER CONFIGURATION WITH CAMBERED AND UNCAMBERED WINGS AND UNCAMBERED FUSELAGE

By Samuel M. Dollyhigh
Langley Research Center

SUMMARY

An investigation has been made in the Mach number range from 0.20 to 2.16 to determine the longitudinal aerodynamic characteristics of a fighter airplane concept. The configuration concept employs a single engine fed by a single fixed geometry inlet, a 50° leading-edge-angle clipped-arrow wing, a single large vertical tail, and low horizontal tails. The wing camber surface was optimized in drag due to lift and was designed to be self-trimming at Mach 1.40 and at a lift coefficient of 0.20. An uncambered or flat wing of the same planform and thickness ratio was also tested. However, for the present investigation, the fuselage was not cambered. Further tests should be made on a cambered fuselage version, which attempts to preserve the optimum wing loading on that part of the theoretical wing enclosed by the fuselage.

The results indicate that the configuration possessed reasonably linear pitching-moment characteristics over the test Mach and angle-of-attack ranges, except at Mach 0.50 where the configuration pitched down when the wing airflow separated at angles of attack above 20°. The horizontal-tail control effectiveness was found to be adequate over the test Mach range. The configuration with the supersonic cambered wing had drag polar characteristics at the higher angles of attack superior to those for the configuration with the flat wing at all Mach numbers of the test. However, the positive zero-lift pitching moment was absent; this would have enabled the cambered wing configuration to trim at high lift coefficients with relatively small or no horizontal-tail loads, and thus lower the trim drag. It was speculated that the absence of significant positive zero-lift pitching moment in the cambered wing configuration was due to the fuselage's lack of being cambered in such a way that the theoretical wing loading was preserved. Trimmed drag differences between the configuration with the two wings at Mach 1.47, 1.80, and 2.16 were fairly accurately predicted by current supersonic theoretical methods.

INTRODUCTION

As part of a research program on advanced fighter aircraft technology, the National Aeronautics and Space Administration has undertaken research related to highly maneuverable fighter aircraft. This report presents the results of wind-tunnel tests of the first in a series of generalized fighter configurations of research models of an aft tail fighter concept.

The configuration concept is as tightly packaged as possible to keep cross-sectional area low. It employs a single engine fed by a single fixed geometry inlet, and the cockpit features an inclined pilot seat. As a result, the cross-sectional area at the pilot station is greatly reduced, and the pilot is able to withstand higher sustained g loads. The wing planform is a clipped arrow with a 50° leading-edge sweep. The wing camber surface is designed for minimum drag due to lift and to be self-trimming at Mach number 1.40 and at a lift coefficient C_L of 0.20 by the method discussed in reference 1. Ideally, designing the wing this way should result in a low drag penalty associated with trimming the aircraft by keeping the necessary horizontal-tail deflections or horizontal-tail loads small. No attempt was made to camber the fuselage in order to preserve the wing loading on the part of the theoretical wing that was enclosed by the fuselage. A second wing of the same planform and thickness distribution, but with a flat camber surface, was included in the investigation as a reference.

Wind-tunnel tests on a 0.056-scale model were conducted in the Langley 8-foot transonic pressure and Unitary Plan wind tunnels at Mach numbers from 0.2 to 2.16. The results of the wind-tunnel investigation along with some supersonic analytical results are reported herein.

SYMBOLS

The force and moment coefficients are referenced to the stability axis system. The moment reference point was located at fuselage station 39.40 cm $(0.40\ \bar{c})$ for the wing apex located at 20.353 cm and at fuselage station 40.61 cm $(0.30\ \bar{c})$ for the wing apex located at 23.52 cm.

A	aspect ratio
b	wing span, cm
C_D	drag coefficient, Drag/qS
$C_{D,c}$	chamber-drag coefficient, Chamber drag/qS

$C_{D,i}$ internal-drag coefficient, Internal drag/qS

$C_{D,o}$ drag coefficient at zero lift

C_L lift coefficient, Lift/qS

C_{L_α} lift curve slope at $C_L = 0$

C_m pitching-moment coefficient, Pitching moment/qS$\bar{c}$

$C_{m,o}$ pitching-moment coefficient at zero lift

$\partial C_m/\partial C_L$ longitudinal stability parameter at $C_L = 0$

$\Delta C_D/{C_L}^2$ drag-due-to-lift parameter (determined at $C_L = 0.5$)

$\Delta C_L/\Delta\delta_h$ tail control effectiveness at zero moment, per degree

$\partial C_m/\partial\delta_h$ pitching effectiveness of horizontal tail at $C_L = 0$

c streamwise chord, cm

$\bar{c}$ wing mean geometric chord, cm

L/D lift-drag ratio

M free-stream Mach number

q free-stream dynamic pressure, N/m^2

S reference area of wing including fuselage intercept, cm^2

x longitudinal distance from leading edge of wing

y lateral distance from center line of airplane

z vertical ordinate of camber surface, positive up

α angle of attack, degrees

Γ dihedral angle, degrees

δ_h horizontal-tail deflection angle, positive when trailing edge is down, degrees

Λ leading-edge sweep angle, degrees

Subscripts:

max maximum

trim trimmed

DESCRIPTION OF MODEL

A three-view drawing of the complete model is shown in figure 1(a), and drawings of the wing, vertical tail, and horizontal tail are shown in figures 1(b) to 1(d). Some geometric characteristics are given in table I, and a photograph of the model is presented in figure 2. The configuration incorporates an uncambered fuselage with a single external compression horizontal-ramp inlet, a clipped-arrow wing, twin horizontal tails, and a single vertical tail.

The wing planform was a clipped arrow with a 50° leading-edge sweep. The taper ratio of the theoretical planform was 0.20, and the notch ratio was 0.157. The streamwise airfoil thickness distribution was a NACA 65A004.5. Two wings were tested, each having the same planform and airfoil thickness distribution but differing in camber surface. The first wing had a camber surface that was designed for minimum drag due to lift at Mach number 1.4 and $C_L = 0.2$. The camber surface was also designed so that the wing would be self-trimming about the center of gravity of the configuration at the design point ($M = 1.4$; $C_L = 0.2$) with the wing apex located at model station 20.353. The camber surface ordinates of this wing with respect to the leading edge are given in table II. The wing is hereafter referred to as the cambered wing. The second wing was uncambered and untwisted (flat) and is hereafter referred to as the uncambered wing. Both wings could be moved rearward 3.167 cm.

The configuration employed low twin horizontal tails with a 4 percent biconvex section. The horizontal tail could be deflected over a range of from -13.33° to 10° and could be removed from the model. The relatively large single vertical tail also had a 4 percent biconvex airfoil section.

TESTS AND CORRECTIONS

The tests were conducted in the Langley 8-foot transonic pressure and Unitary Plan wind tunnels. The conditions under which the tests were conducted were as follows:

Mach number	Stagnation pressure, kN/m^2	Stagnation temperature, K	Reynolds number per meter
0.2	57.46	316	2.30
.5	57.46	320	5.18
.8	57.46	321	7.05
.85	57.46	322	7.22
.90	57.46	323	7.38
.95	57.46	323	7.48
1.03	57.46	323	7.68
1.2	57.46	323	7.81
1.47	66.03 and 39.60	339	8.20 and 4.92
1.80	73.07 and 43.86	339	8.20 and 4.92
2.16	85.61 and 52.38	339	8.20 and 4.92

At Mach 1.47, 1.80, and 2.16, the Reynolds number per meter, as indicated by the lower value in the table, was reduced at angles of attack above 10° in order to stay within the balance load limits. The dewpoint was maintained sufficiently low to prevent measurable condensation effects in the test section. The angle-of-attack range was from approximately -6° to 20°. In order to insure boundary-layer transition to turbulent flow at Mach 0.2 to 1.2, 0.16-cm-wide transition strips of No. 60 grit were placed on the body 3.05 cm aft of the nose of the model, and strips of No. 80 grit were placed 1.02 cm streamwise on the wings, tails, inlet ramps, and external inlet surface. At Mach 1.47 to 2.16, strips of No. 50 grit were used to replace the strips of smaller grit used at the lower Mach numbers. These transition strips are shown to be adequate in reference 2.

Aerodynamic forces and moments on the model were measured by means of a six-component strain-gage balance which was housed within the model. The balance was attached to a sting which, in turn, was rigidly fastened to the tunnel support system. Balance-chamber static pressures were measured with pressure tubes located in the vicinity of the balance. The model internal-flow total and static pressures were measured with a rake consisting of 29 total-pressure tubes and 5 static-pressure tubes. The rake was placed flush with the base of the model and was removed during the force-measurement tests. The drag data presented herein have been corrected for internal drag and have also been corrected to the condition of free-stream static pressure in the balance chamber. Figures 3 and 4 show values of the balance chamber and internal drag

coefficients which were used to correct the drag data. Corrections to the angles of atta
of the model have been made for both tunnel-airflow misalinement and deflection of the balance and sting under load.

PRESENTATION OF RESULTS

DISCUSSION

Shown in figure 5 are the longitudinal aerodynamic characteristics of the configura
tion with the cambered wing at those Mach numbers at which control characteristics wer
investigated. The configuration exhibits reasonably linear pitching-moment characteristics at all Mach numbers of the test except at an angle of attack of approximately 21° a
Mach 0.50, where the configuration pitches downward. This behavior is presumably associated with flow separation at the wing tip. As the flow separates, the downwash on the low horizontal tail is decreased, and an increased tail load results. This presumptio
is further supported by the fact that the configuration with tail off displays a tendency fo
increased pitch as the lift-curve slope indicates that separation is beginning to occur. However, for a wing with no devices to assist in maintaining the flow, this phenomenon does not occur until the configuration has reached a relatively high angle of attack. Subsonically, there tends to be a slight increase in lift-curve slope at angles of attack of approximately 6° to 8° that can be associated with the generation of vortex lift. (The vortex-lift concept is discussed in ref. 3.) The horizontal-tail control effectiveness appears to be adequate at all Mach numbers of the test for the moment reference center

used. The longitudinal trim characteristics of the configuration with the cambered wing are shown in figure 6.

A second wing, identical to the cambered wing in planform and thickness, except that it was uncambered (or flat), was tested on the model. Its longitudinal aerodynamic characteristics are presented in figure 7. The same comments that were made about the configuration with the cambered wing are true for the configuration with the flat wing. At Mach 0.5, the downward pitch as the flow separates occurs at the same angle of attack as for the cambered wing; thus, it is indicated that the supersonic camber surface is not responsible for inducing the separation. Again, subsonically, the increase in lift-curve slope that is associated with vortex lift can be observed at an angle of attack of approximately 5°. The generation of vortex lift is much more evident on the flat wing and occurs at a lower angle of attack than on the cambered wing. Figure 8 presents the longitudinal trim characteristics for the configuration with the flat wing.

The longitudinal aerodynamic characteristics of the configuration with the cambered and flat wings are shown in figure 9. The data presented are for the configuration with zero horizontal-tail deflection at all test Mach numbers. In addition, tail-off data are presented at those Mach numbers at which control characteristics were investigated. Although no attempt was made to camber the fuselage in order to preserve the wing loading on the part of the theoretical wing that was enclosed by the fuselage, significant drag reductions from those levels for the configuration with the flat wing were encountered at higher lift coefficients for all the test Mach numbers. For the horizontal tail-off data, small differences in zero-lift pitching moments are discernible between the cambered and uncambered wing configurations over the test Mach range as well as near the design Mach number. Supersonically, the cambered wing configuration has a small positive tail-off $C_{m,o}$, but apparently the horizontal tail is slightly up loaded at zero deflection angle behind the cambered wing at zero lift. This results in a $C_{m,o}$ of zero for the cambered wing configuration with tail on at zero deflection. However, the amount of tail-off positive zero-lift pitching moment is not enough to accomplish the design goal, which specifies that the configuration be self-trimming with no tail load at Mach 1.4 at a C_L of 0.2. These results verify theoretical calculations that predicted that if the portion of the theoretical wing enclosed by the fuselage were to be flat, little positive zero-lift pitching moment would remain. The results of supersonic wind-tunnel tests on a model with a highly cambered fuselage with several different exposed wings, including a flat one, have been reported in reference 4. In this report it was shown that each configuration had substantial zero-lift pitching moment. In order to achieve the design goal that the configuration be self-trimming, it is necessary to camber the fuselage so that the theoretical wing loading is preserved.

Throughout the Mach number range of the tests, the configuration with the cambered wing had a negative lift coefficient at an angle of attack of 0°, which can be attributed to referencing the theoretical wing camber surface so that zero lift occurred at an angle of attack of 0°. However, when the highly cambered portion of the wing inboard the fuselage was not preserved, the configuration needed a positive angle of attack to achieve zero lift. Over the subsonic range, the configuration with the flat wing is slightly less stable at a positive lift condition than the configuration with the cambered wing. Since the tail-off data do not indicate as great a difference in static margin, it can be speculated that tail-loading differences account for the slightly different stability levels.

Trimmed $(L/D)_{max}$ and tail control effectiveness $\Delta C_L/\Delta\delta_h$ are plotted against Mach number in figure 10. Although tail effectiveness is less for the cambered wing configuration, a definite trimmed $(L/D)_{max}$ superiority exists throughout the test Mach number range. The superior performance is brought about by several factors. One is the better drag characteristics with lift of the cambered wing. Another is the fact that the cambered wing carries a greater percentage of the total lift relative to the horizontal tail than the flat wing does. As a result, the horizontal tail behind the flat wing is a more effective control surface, but the drag associated with the larger tail load apparently more than offsets any possible advantage in trimming the configuration.

Figure 11 presents longitudinal aerodynamic characteristics of the configuration with the cambered wing moved rearward 3.167 cm. The moment center is also moved rearward 1.210 cm to correspond to the center of gravity change brought about by moving the wing on the airplane configuration. The severity of the pitch-down that occurred at $M = 0.50$ and above $\alpha = 20^{\circ}$ has been reduced by moving the wing back. In figure 12 other characteristics are compared with those for the configuration with the cambered and uncambered wings in the forward position.

A summary plot of the variation of the more pertinent longitudinal parameters with Mach number for the configuration with the cambered wing in both forward and rearward positions and with the flat wing in the forward position is shown in figure 12. Except for the tail control effectiveness, the data are for the configurations that are untrimmed with no horizontal-tail deflection.

Correlations between the experimental and theoretical trimmed drag and tail deflection necessary to trim the configuration are given in figure 13 for the configuration with each wing in the forward position at Mach 1.47, 1.80, and 2.16. The method used in reference 5, modified to include control surfaces, was employed to calculate the camber drag, drag due to lift, and tail control characteristics. The wave drag and skin friction, calculated by methods of references 6 and 7, respectively, were added to the camber drag and drag due to lift to obtain the total drag. From examination, although the drag levels do not always conform, the theory accurately predicts the trimmed drag differences between the two wings. The tail control is accurately predicted except at Mach 1.47; the failure to predict precisely the tail control is probably responsible for this Mach number having the worst correlation in drag.

CONCLUDING REMARKS

An investigation has been made in the Mach number range from 0.20 to 2.16 to determine the longitudinal aerodynamic characteristics of a fighter airplane concept. The configuration concept employs a single engine fed by a single fixed geometry inlet, a 50° leading-edge-angle clipped-arrow wing, a single large vertical tail, and low horizontal tails. The wing camber surface was optimized in drag due to lift and designed to be self-trimming at Mach number 1.40 and at a lift coefficient of 0.20. An uncambered or flat wing of the same planform and thickness ratio was also tested. However, for the present investigation, the fuselage was not cambered. Further tests should be made on a cambered fuselage version, which attempts to preserve the optimum wing loading on that part of the theoretical wing enclosed by the fuselage.

The results indicate that the configuration possessed reasonable linear pitching-moment characteristics over the test Mach number and angle-of-attack ranges, except at Mach 0.50 where the configuration pitched down when the wing flow separated at angles above 20°. The horizontal-tail control effectiveness was found to be adequate over the test Mach range. The configuration with the supersonic cambered wing had drag polar characteristics at the higher angles of attack superior to those for the configuration with the flat wing at all Mach numbers of the test. However, the positive zero-lift pitching moment was absent; this would have enabled the cambered wing configuration to trim at high lift coefficients with relatively small or no horizontal-tail loads and thus lower the trim drag. It was speculated that the absence of significant positive zero-lift pitching moment in the cambered wing configuration was due to the fuselage's lack of being cambered in such a way that the theoretical wing loading was preserved. Trimmed drag differences between the configuration with the two wings at Mach 1.47, 1.80, and 2.16 were fairly accurately predicted by current supersonic theoretical methods.

Langley Research Center,
National Aeronautics and Space Administration,
Hampton, Va., June 21, 1974.

REFERENCES

1. Carlson, Harry W.; and Middleton, Wilbur D: A Numerical Method for the Design of Camber Surfaces of Supersonic Wings With Arbitrary Planforms. NASA TN D-2341, 1964.

2. Braslow, Albert L.; Hicks, Raymond M.; and Harris, Roy V., Jr.: Use of Grit-Type Boundary-Layer-Transition Trips on Wind-Tunnel Models. NASA TN D-3579, 1966.

3. Polhamus, Edward C.: A Concept of the Vortex Lift of Sharp-Edge Delta Wings Based on a Leading-Edge-Suction Analogy. NASA TN D-3767, 1966.

4. Dollyhigh, Samuel M.: Wing-Camber Effects on Longitudinal Aerodynamic Characteristics of a Variable-Sweep Fighter Configuration at Mach Numbers From 1.60 to 2.86. NASA TM X-2826, 1973.

5. Middleton, Wilbur D.; and Carlson, Harry W.: A Numerical Method for Calculating the Flat-Plate Pressure Distributions on Supersonic Wings of Arbitrary Planform. NASA TN D-2570, 1965.

6. Harris, Roy V., Jr.: An Analysis and Correlation of Aircraft Wave Drag. NASA TM X-947, 1964.

7. Sommer, Simon C.; and Short, Barbara J.: Free-Flight Measurements of Turbulent-Boundary-Layer Skin Friction in the Presence of Severe Aerodynamic Heating at Mach Numbers From 2.8 to 7.0. NASA TN 3391, 1955.

TABLE I.- GEOMETRIC CHARACTERISTICS

(a) Component geometry

Wing:	
A	2.759
Λ, deg	50
Γ, deg	0
$\bar{c}$, cm	19.185
b, cm	45.550
S, including fuselage intercept, cm^2	752.398
Airfoil section	NACA 65A004.5
Horizontal tails (exposed):	
A	2.586
Λ, deg	42.5
Γ, deg	0
Mean geometric chord, cm	9.025
Semispan, cm	11.026
Area, cm^2	188.038
Airfoil	4 percent biconvex
Vertical tail:	
A	3.435
Λ, deg	61
Mean geometric chord, cm	13.467
Semispan, cm	10.483
Area, cm^2	127.977
Airfoil	4 percent biconvex
Inlet area, cm^2	13.344
Exit area, cm^2	12.533
Chamber area, cm^2	12.300
Base area (excluding chamber and exit areas), cm^2	1.153

(b) Wetted areas and reference lengths

Component	Wetted area, cm^2	Reference length, cm
Wing	1181.727	16.977
Fuselage	1307.703	68.072
Vertical tail	256.970	13.469
Horizontal tails	376.070	9.004

TABLE II.- CAMBER SURFACE ORDINATES FOR CAMBERED WING

[Fuselage juncture at $\frac{y}{b/2} = 0.15$]

x/c	$\frac{z}{c}$, in percent, from leading edge at $\frac{y}{b/2}$ of –									
	0.150	0.200	0.300	0.400	0.500	0.600	0.700	0.800	0.900	1.000
0	0	0	0	0	0	0	0	0	0	0
.05	.259	.253	.313	.360	.400	.451	.521	.365	.316	.328
.10	.349	.389	.513	.612	.697	.795	.888	.799	.809	.840
.15	.356	.459	.656	.810	.942	1.067	1.199	1.148	1.155	1.383
.20	.314	.485	.759	.962	1.137	1.307	1.468	1.445	1.518	1.988
.25	.244	.474	.829	1.096	1.311	1.521	1.723	1.742	1.836	2.593
.30	.149	.442	.884	1.203	1.475	1.711	1.950	2.005	2.134	3.198
.35	.041	.394	.921	1.301	1.608	1.890	2.163	2.250	2.409	3.833
.40	-.078	.332	.943	1.381	1.741	2.057	2.362	2.479	2.684	4.469
.50	-.323	.209	.978	1.523	1.976	2.367	2.747	2.936	3.212	5.740
.55	-.439	.147	.992	1.584	2.078	2.510	2.862	3.148	3.443	6.406
.60	-.551	.085	.998	1.646	2.180	2.653	3.089	3.343	3.674	7.042
.65	-.649	.038	1.011	1.708	2.282	2.785	3.274	3.537	3.927	7.677
.70	-.740	.010	1.033	1.770	2.384	2.916	3.431	3.731	4.137	8.313
.75	-.813	-.042	1.055	1.840	2.476	3.047	3.589	3.926	4.346	8.979
.80	-.870	-.068	1.084	1.902	2.578	3.179	3.746	4.120	4.555	9.614
.85	-.912	-.071	1.123	1.973	2.681	3.310	3.903	4.298	4.742	10.250
.90	-.929	-.067	1.169	2.053	2.783	3.430	4.046	4.475	4.929	10.916
.95	-.929	-.041	1.223	2.142	2.895	3.561	4.203	4.652	5.094	11.552
1.00	-.908	.000	1.293	2.231	3.008	3.693	4.361	4.830	5.260	12.187

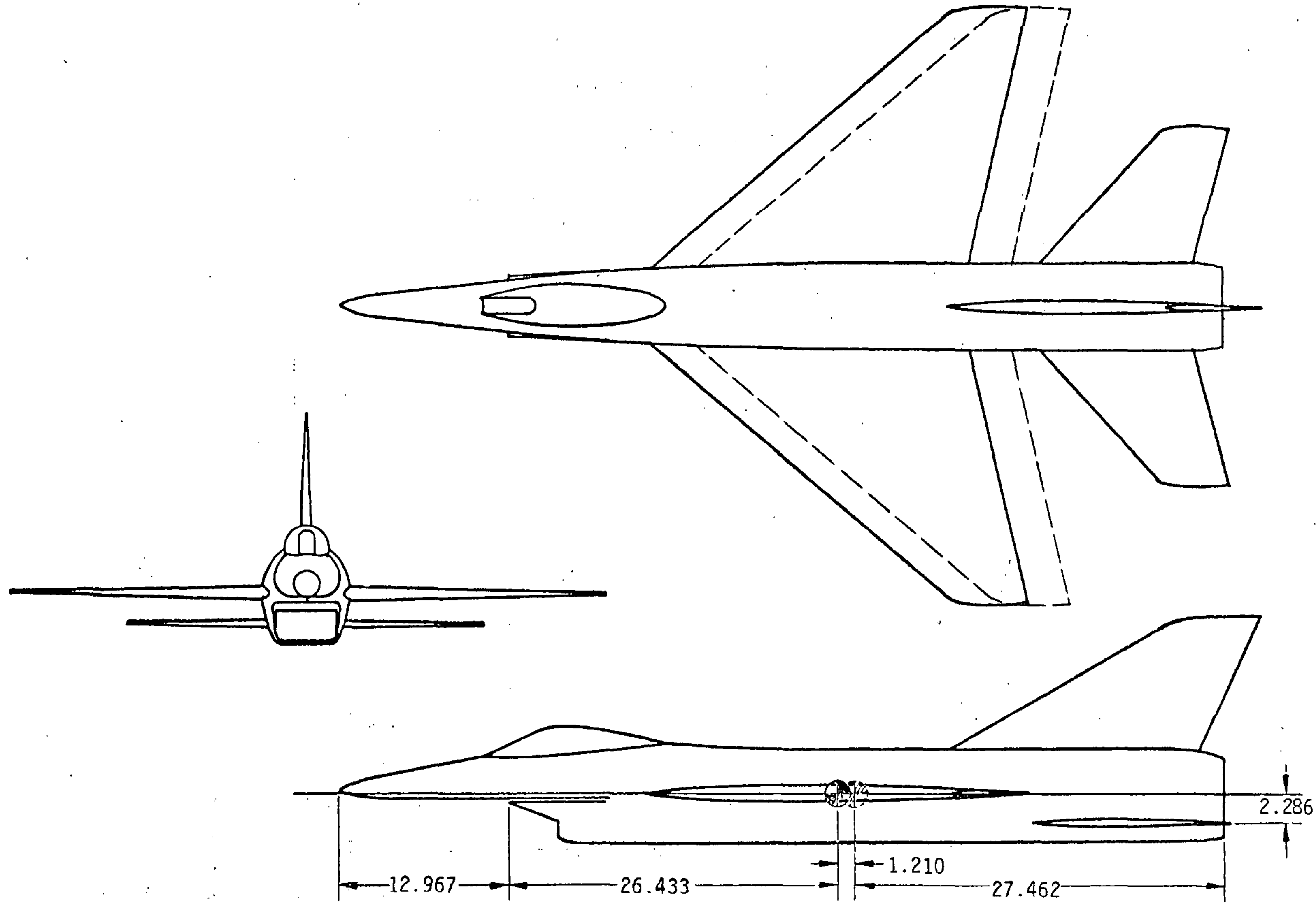

(a) Three-view drawing of complete model.

Figure 1.- Drawings of the model. Linear dimensions are in centimeters.

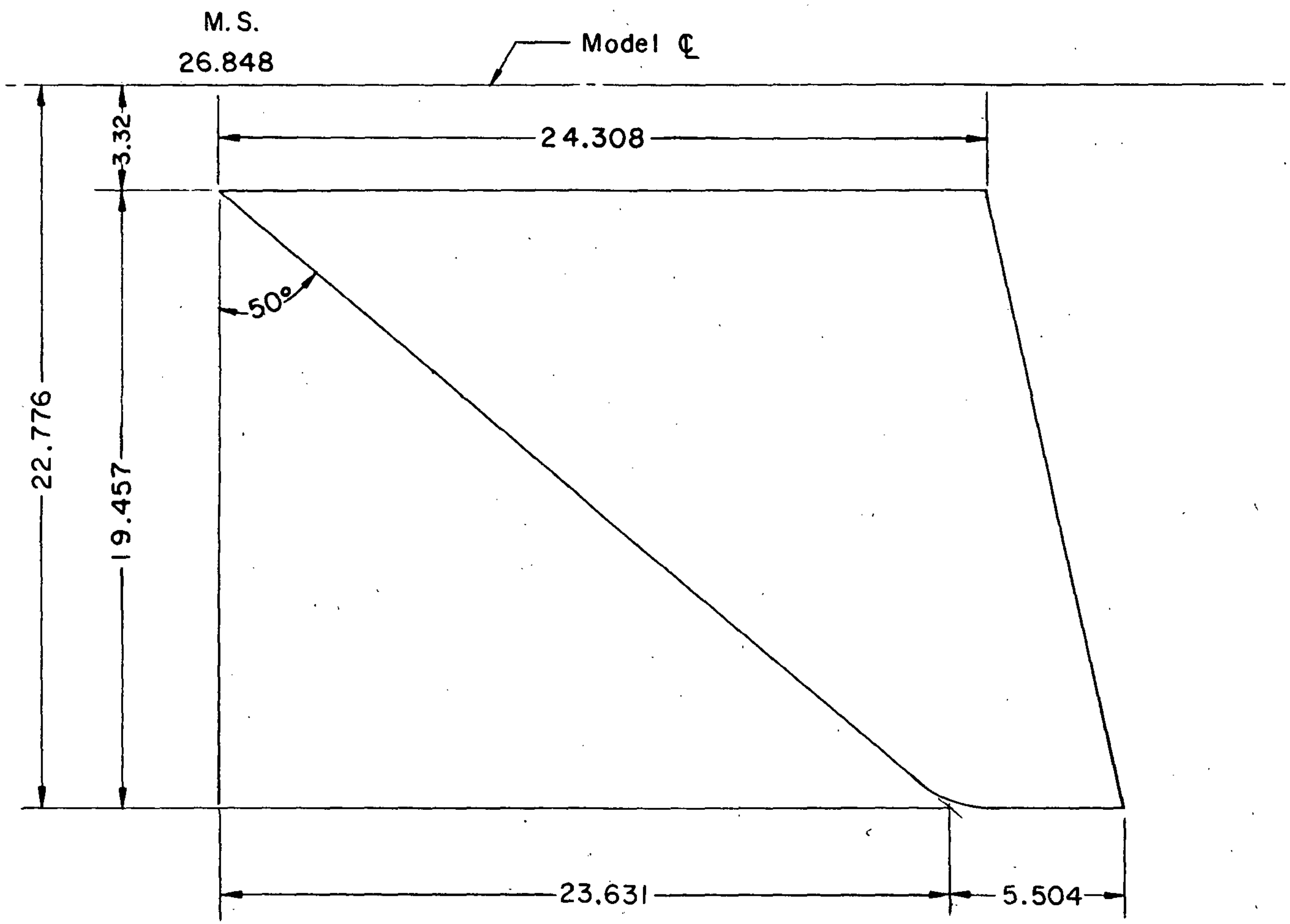

(b) Details of the wing. M.S. denotes model station.

Figure 1.- Continued.

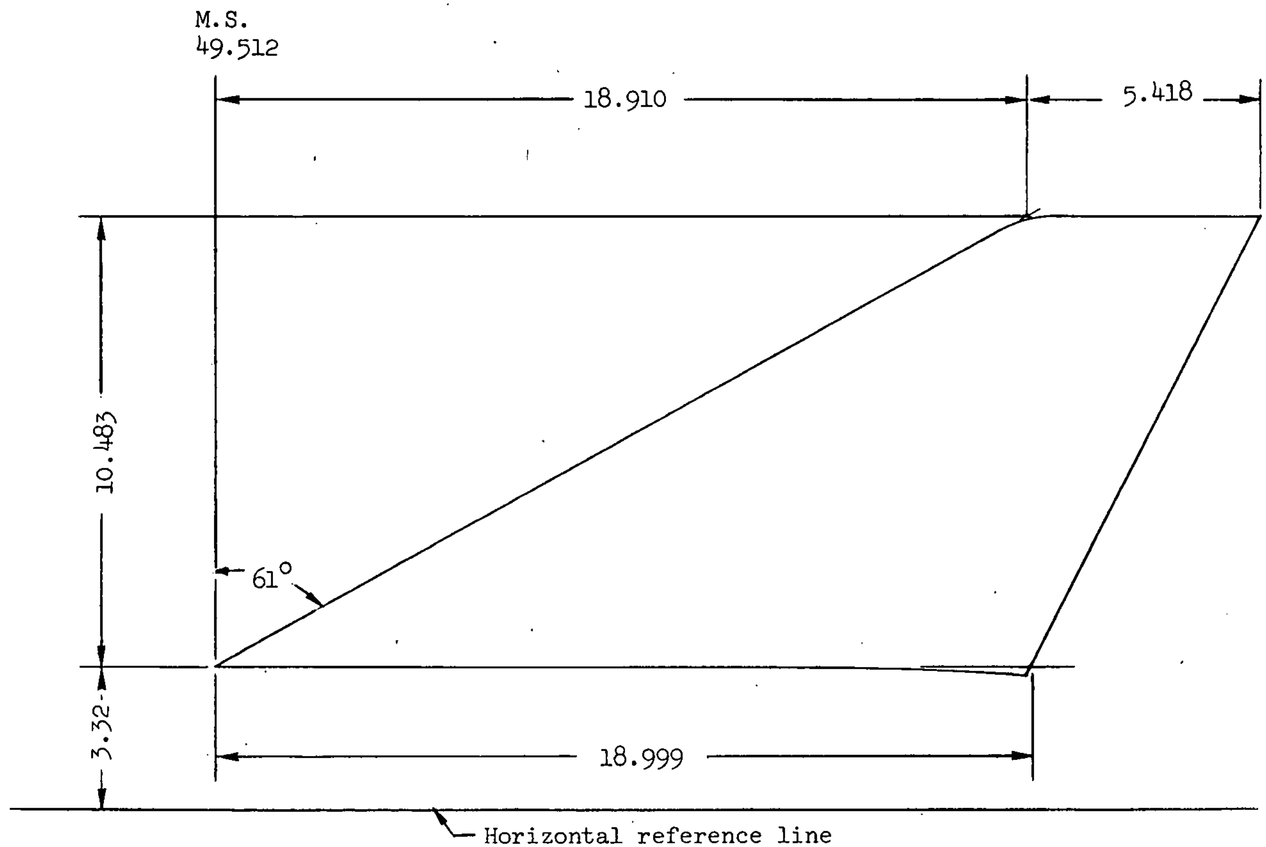

(c) Details of the vertical tail. M.S. denotes model station.

Figure 1.- Continued.

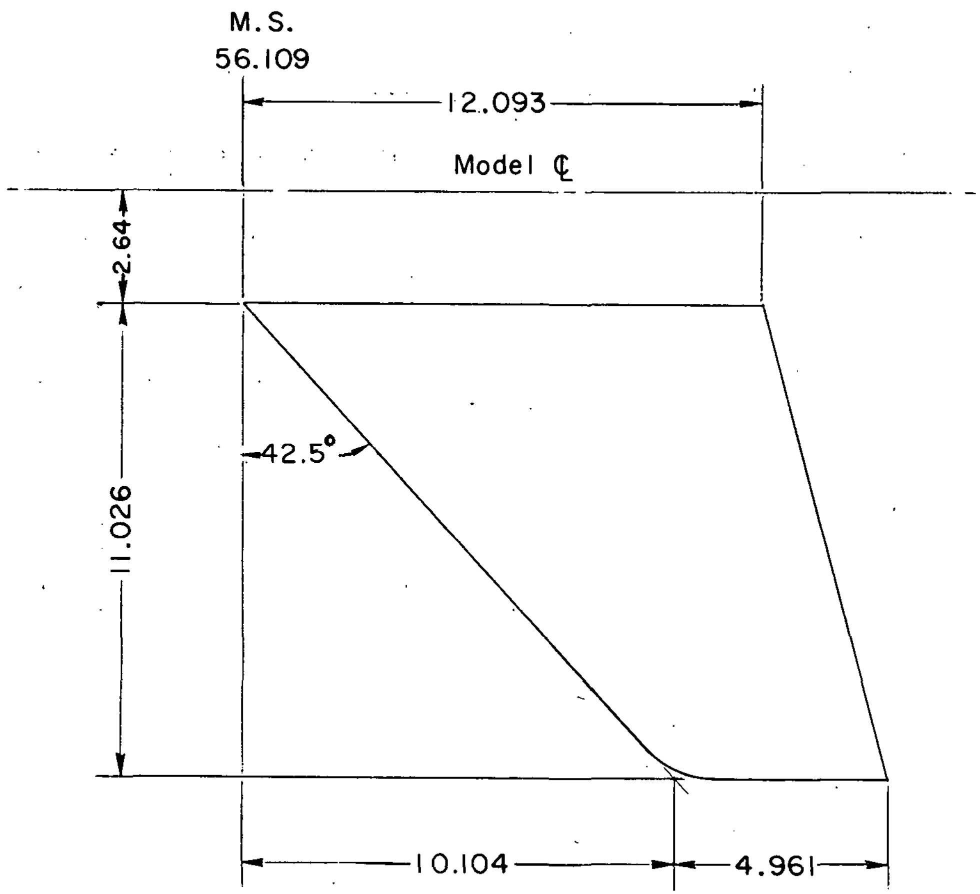

(d) Details of the horizontal tail. M.S. denotes model station.

Figure 1.- Concluded.

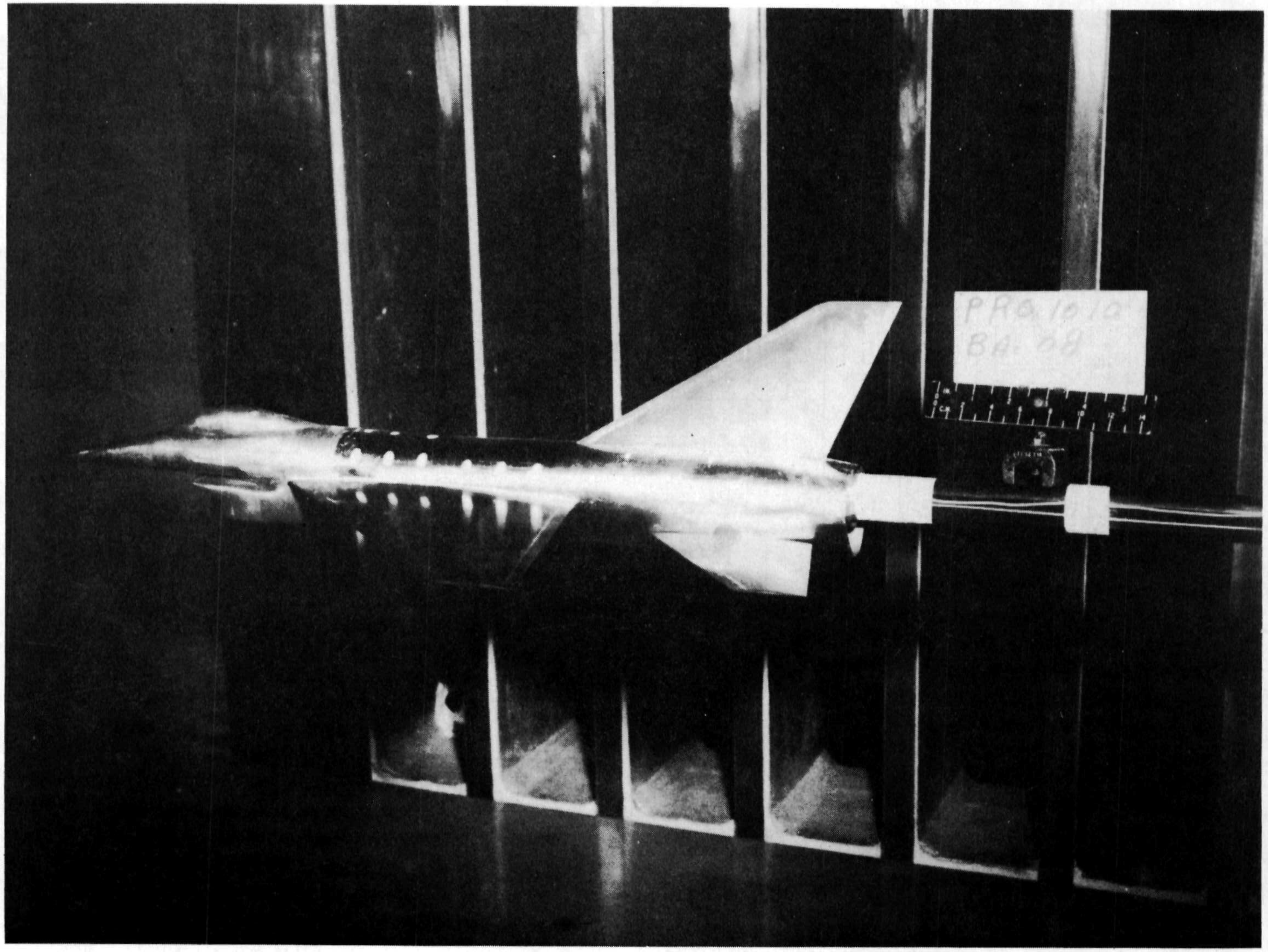

L-74-1136

Figure 2.- Photograph of the model.

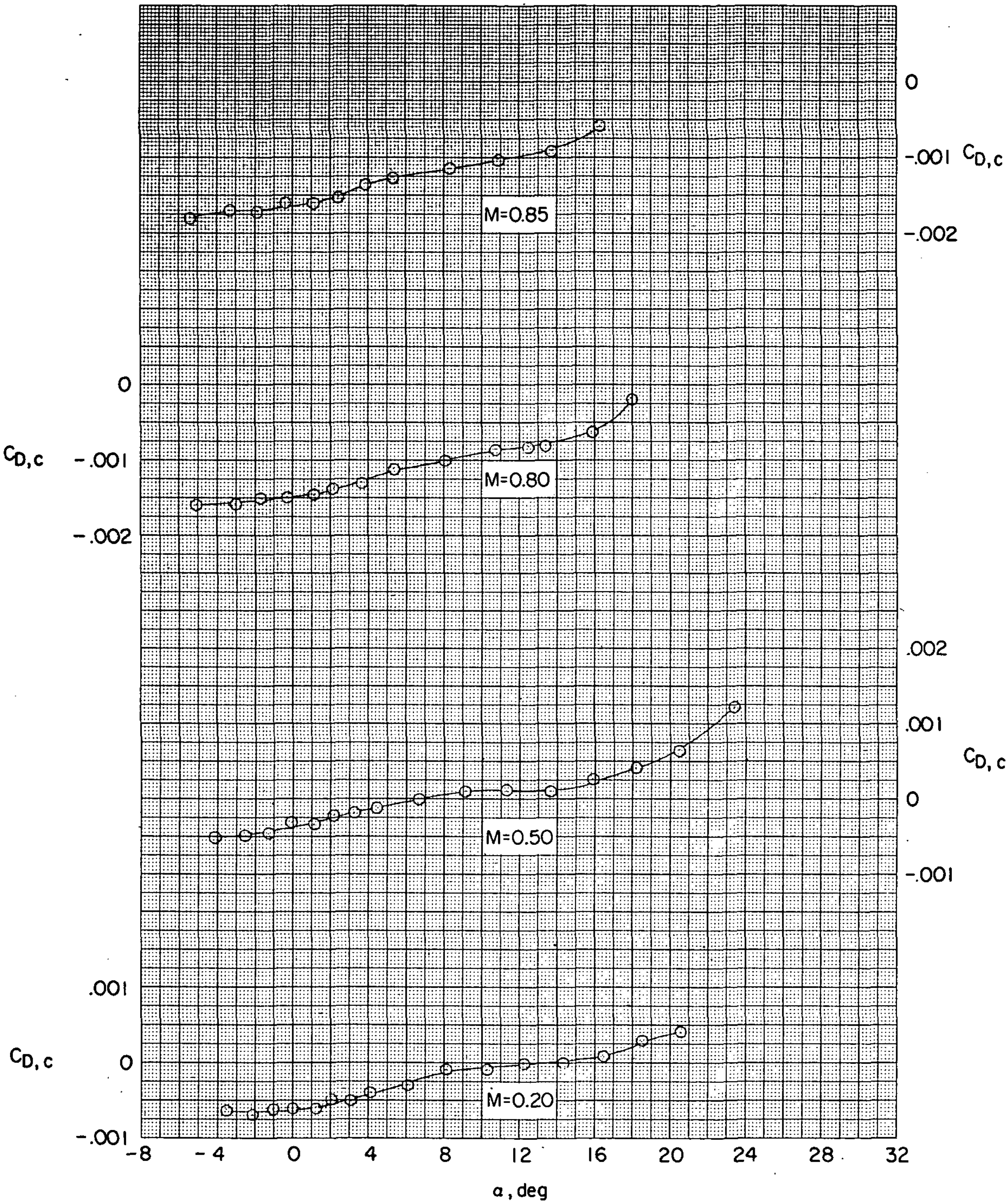

Figure 3.- Chamber drag correction.

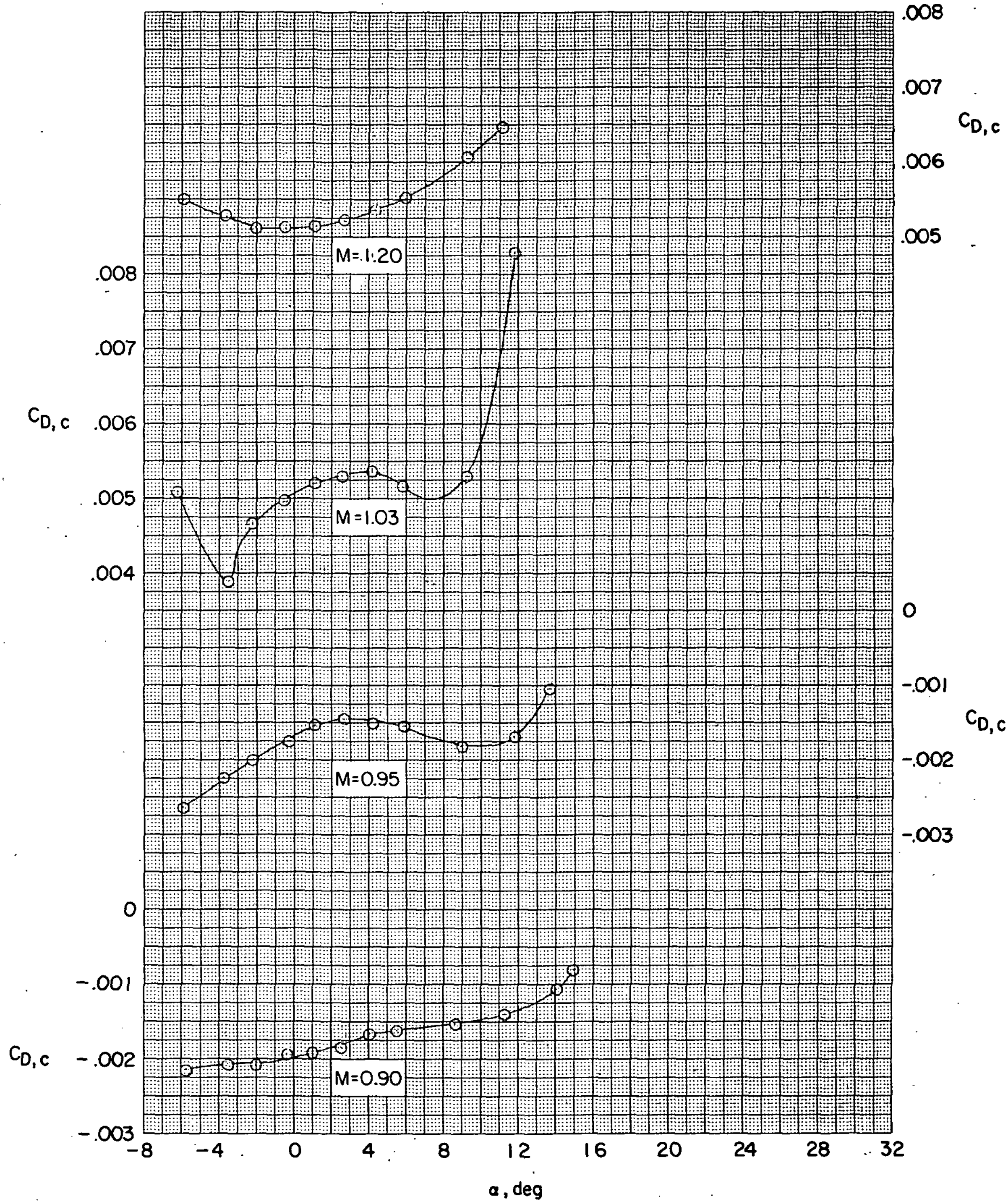

Figure 3.- Continued.

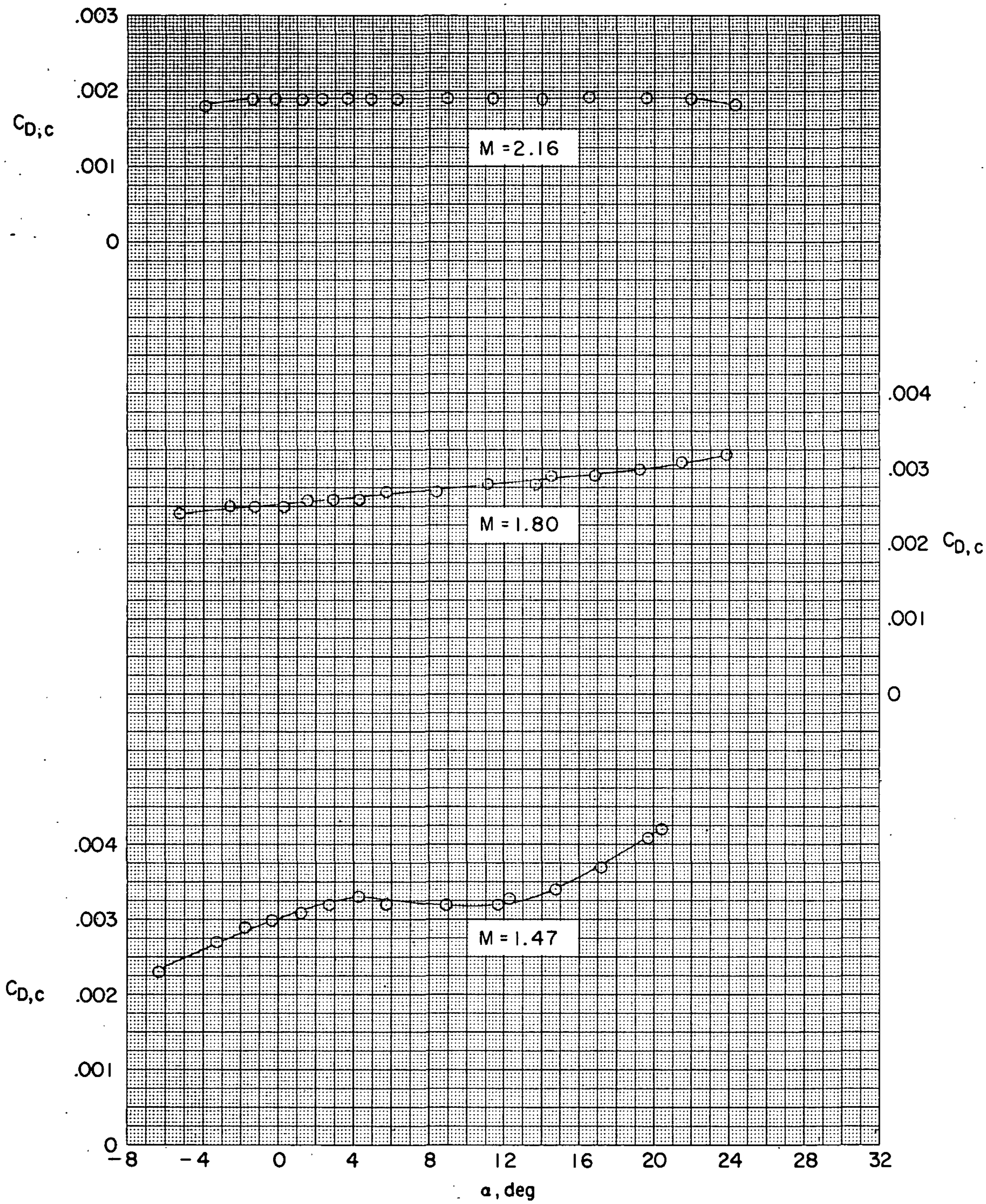

Figure 3.- Concluded.

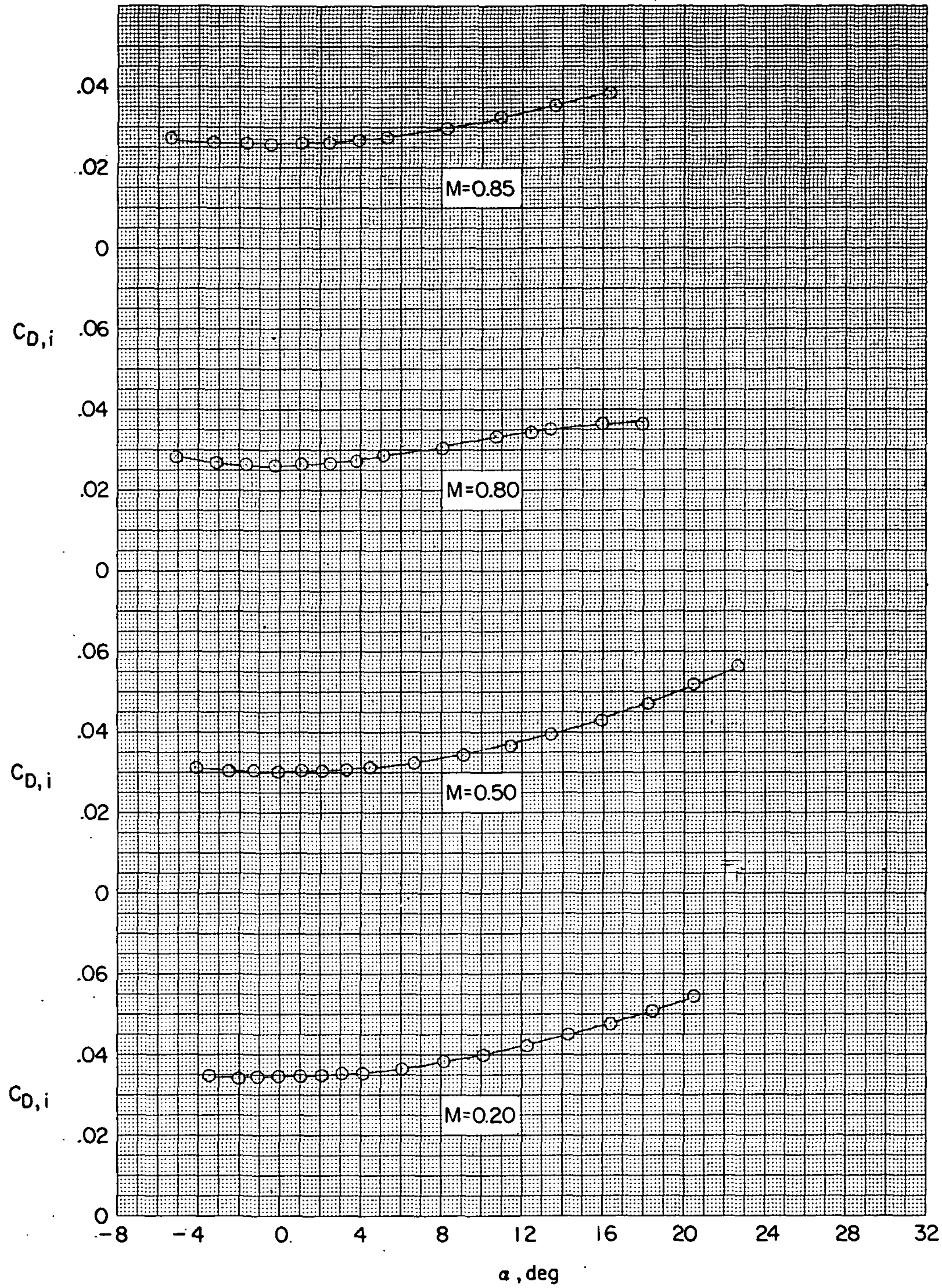

Figure 4.- Internal drag correction.

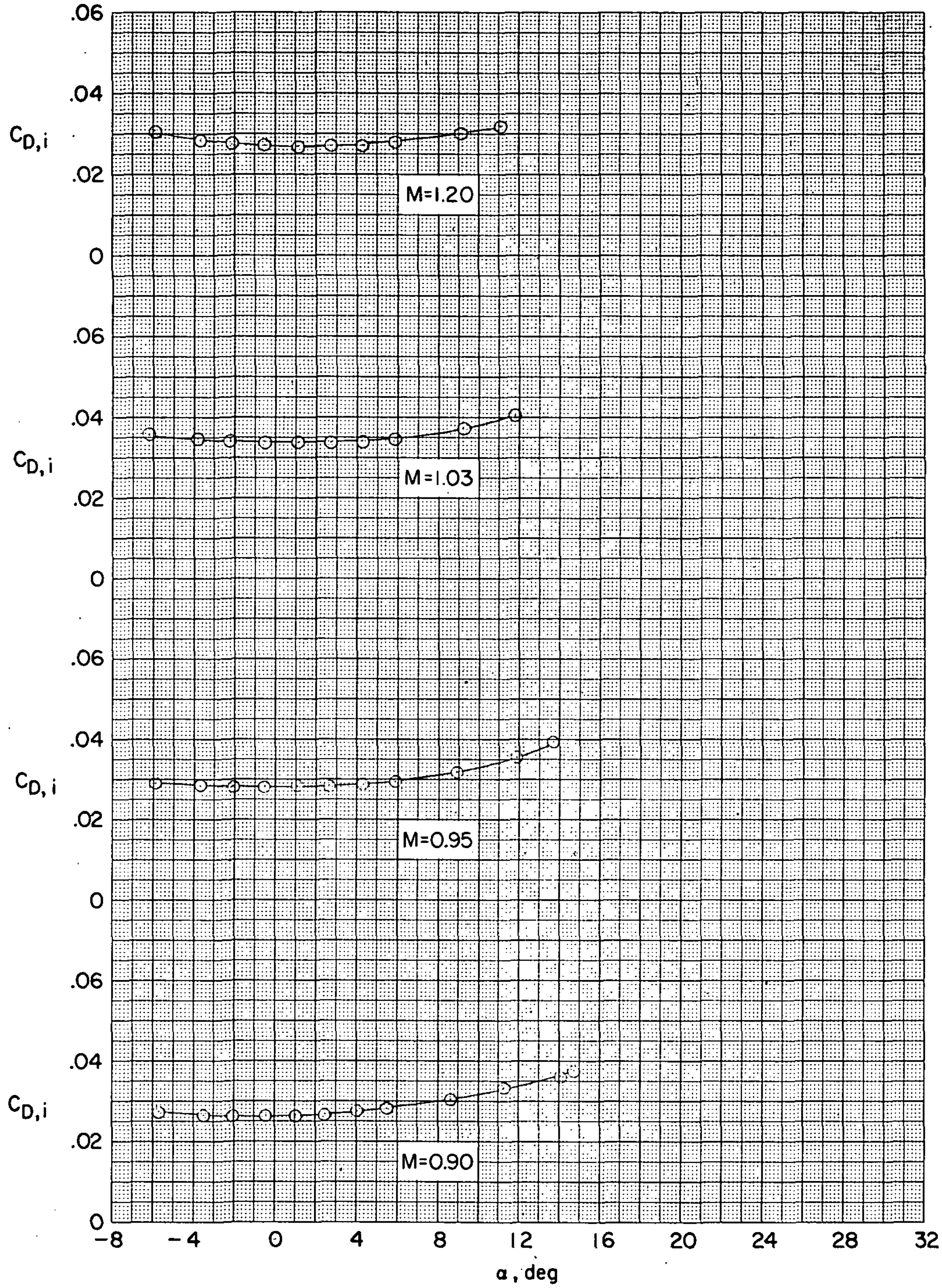

Figure 4.- Continued.

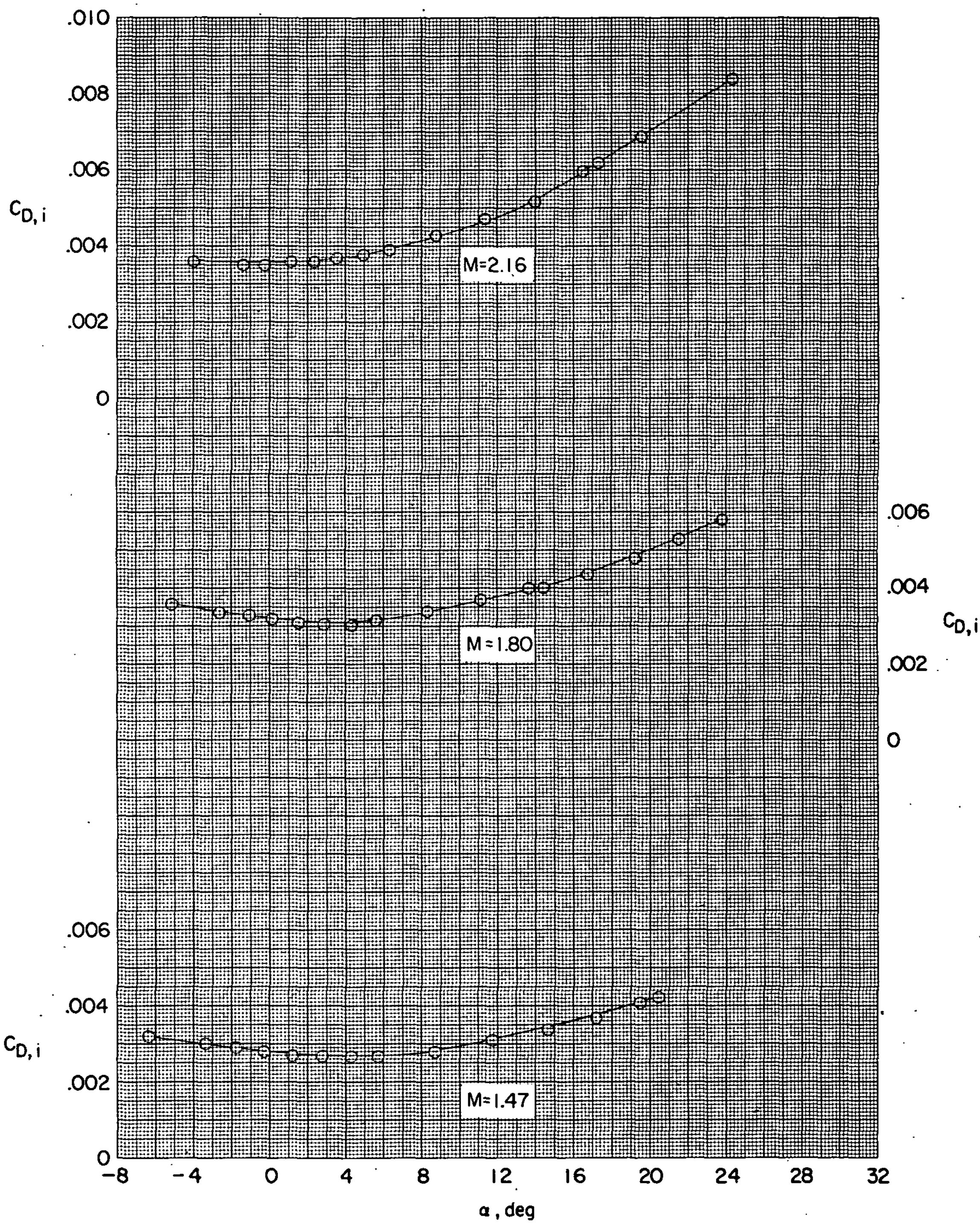

Figure 4.- Concluded.

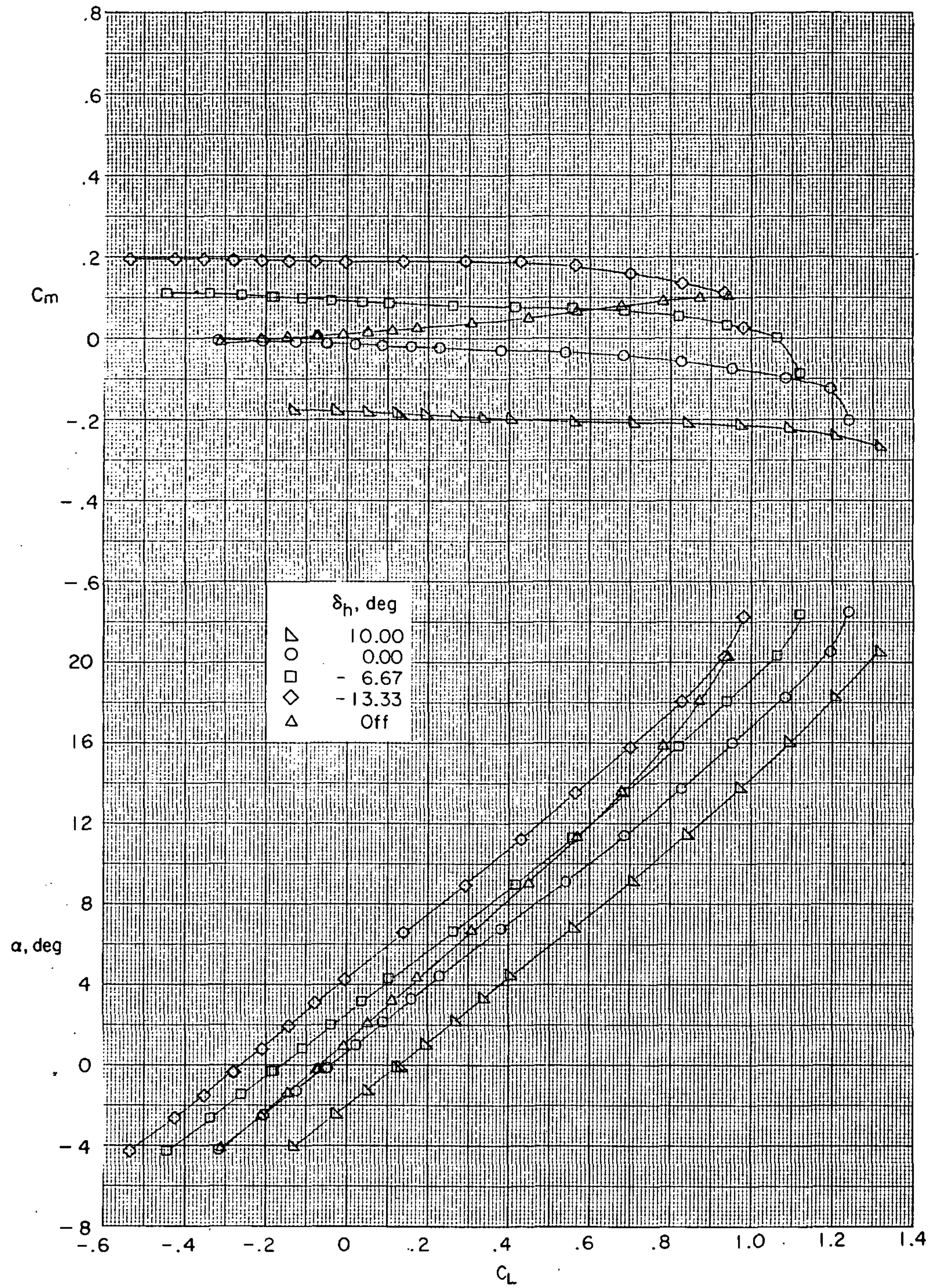

(a) M = 0.50.

Figure 5.- Longitudinal aerodynamic characteristics with the cambered wing.

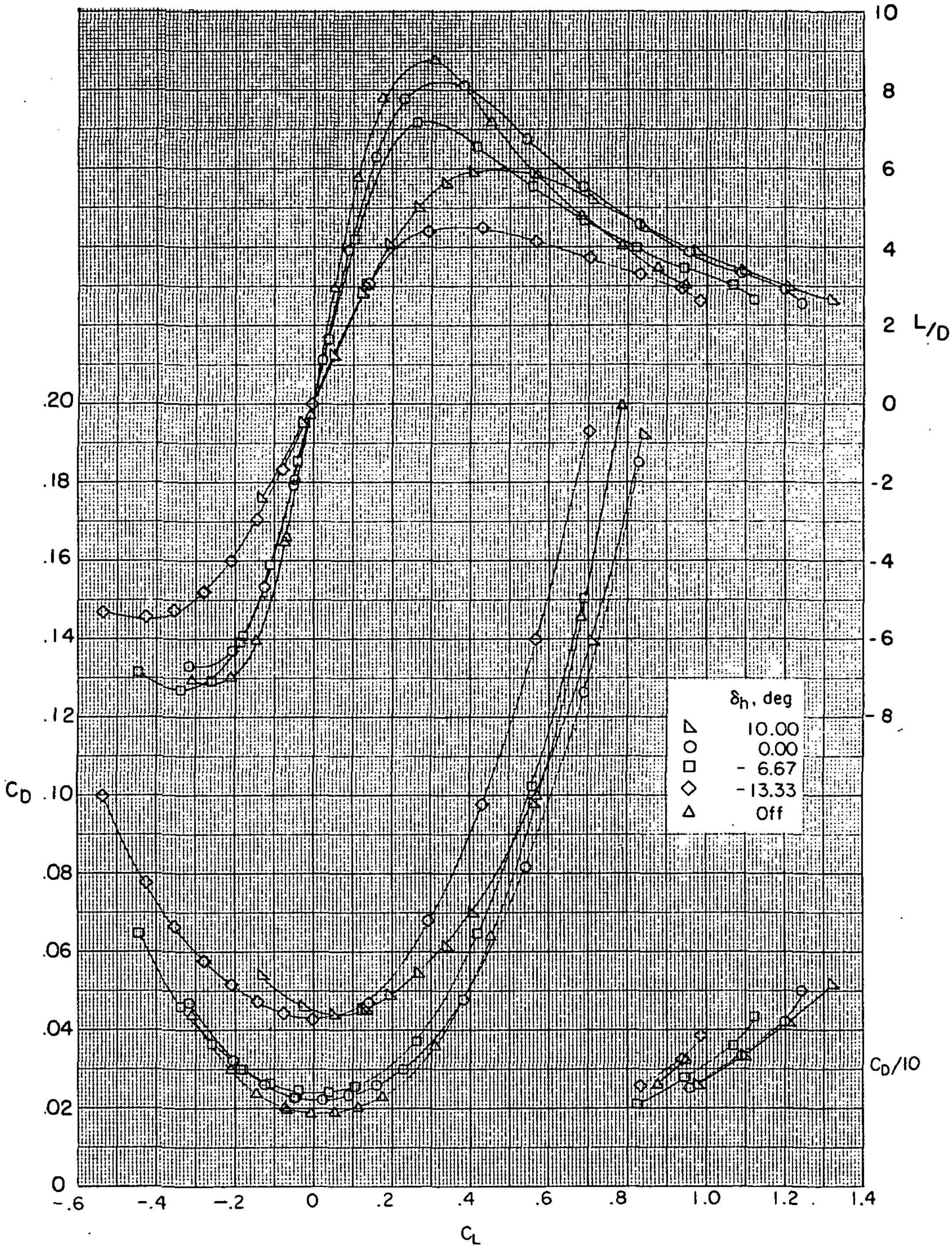

(a) Concluded.

Figure 5.- Continued.

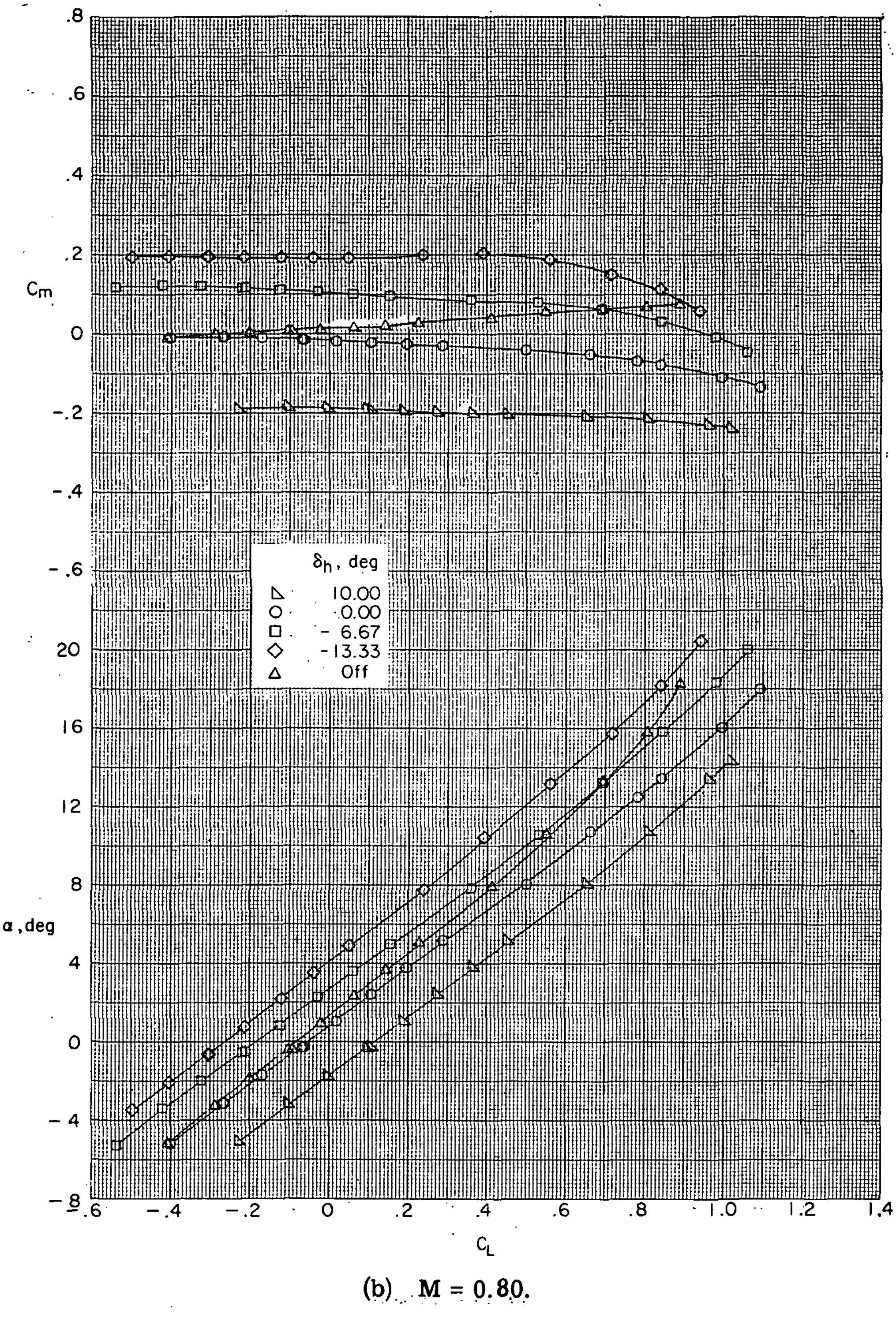

(b) M = 0.80.

Figure 5.- Continued.

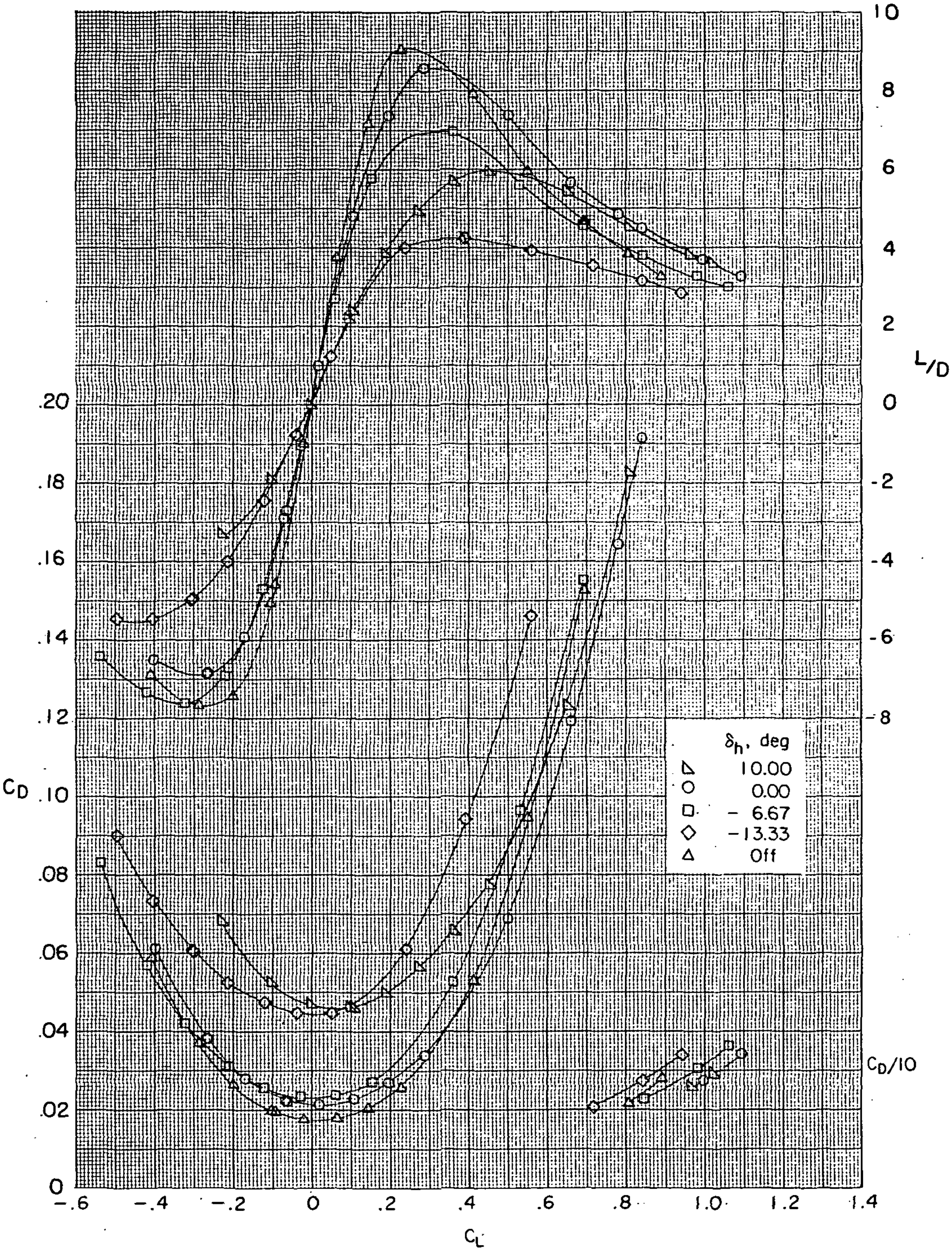

(b) Concluded.

Figure 5.- Continued.

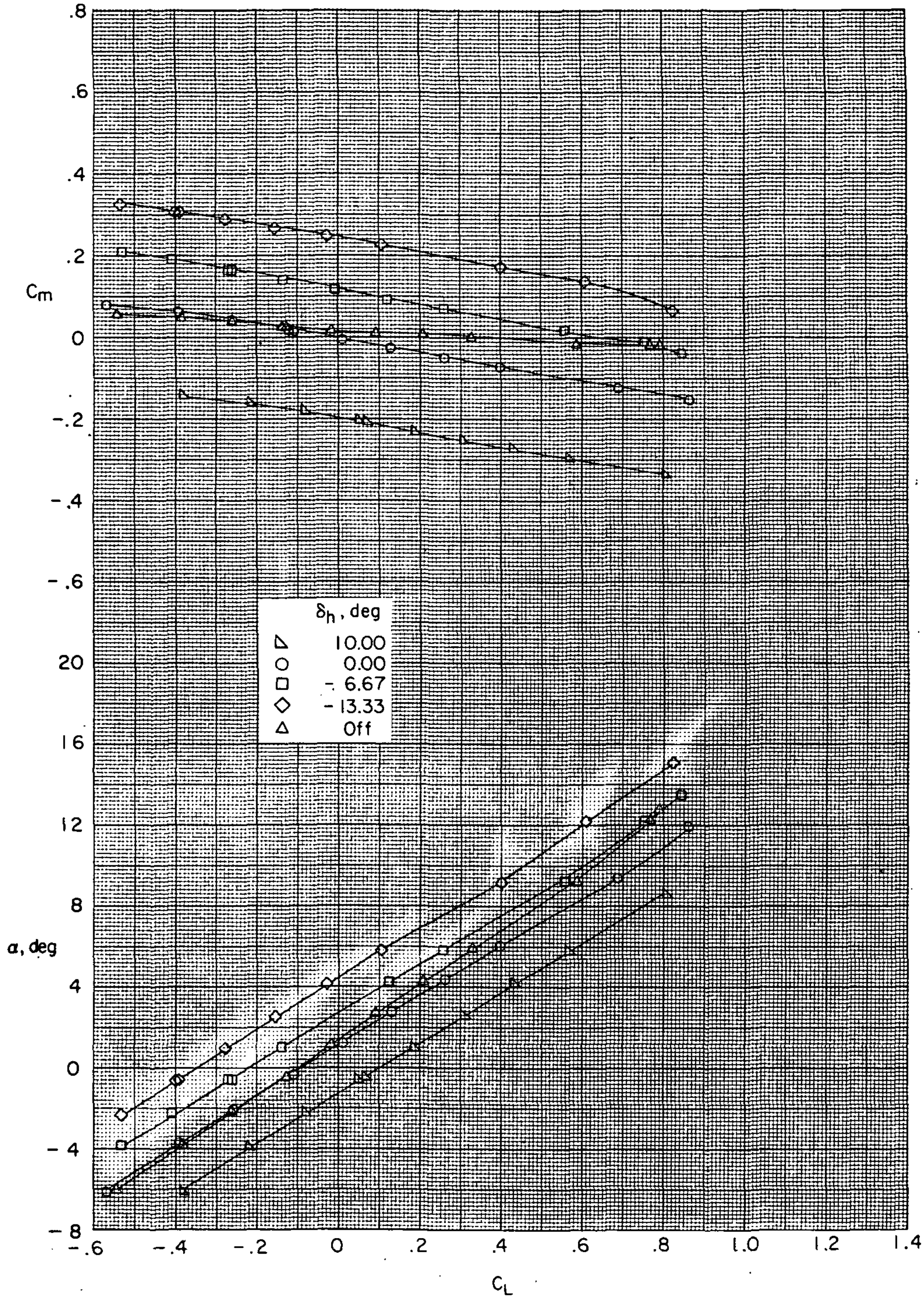

(c) M = 1.03.

Figure 5.- Continued.

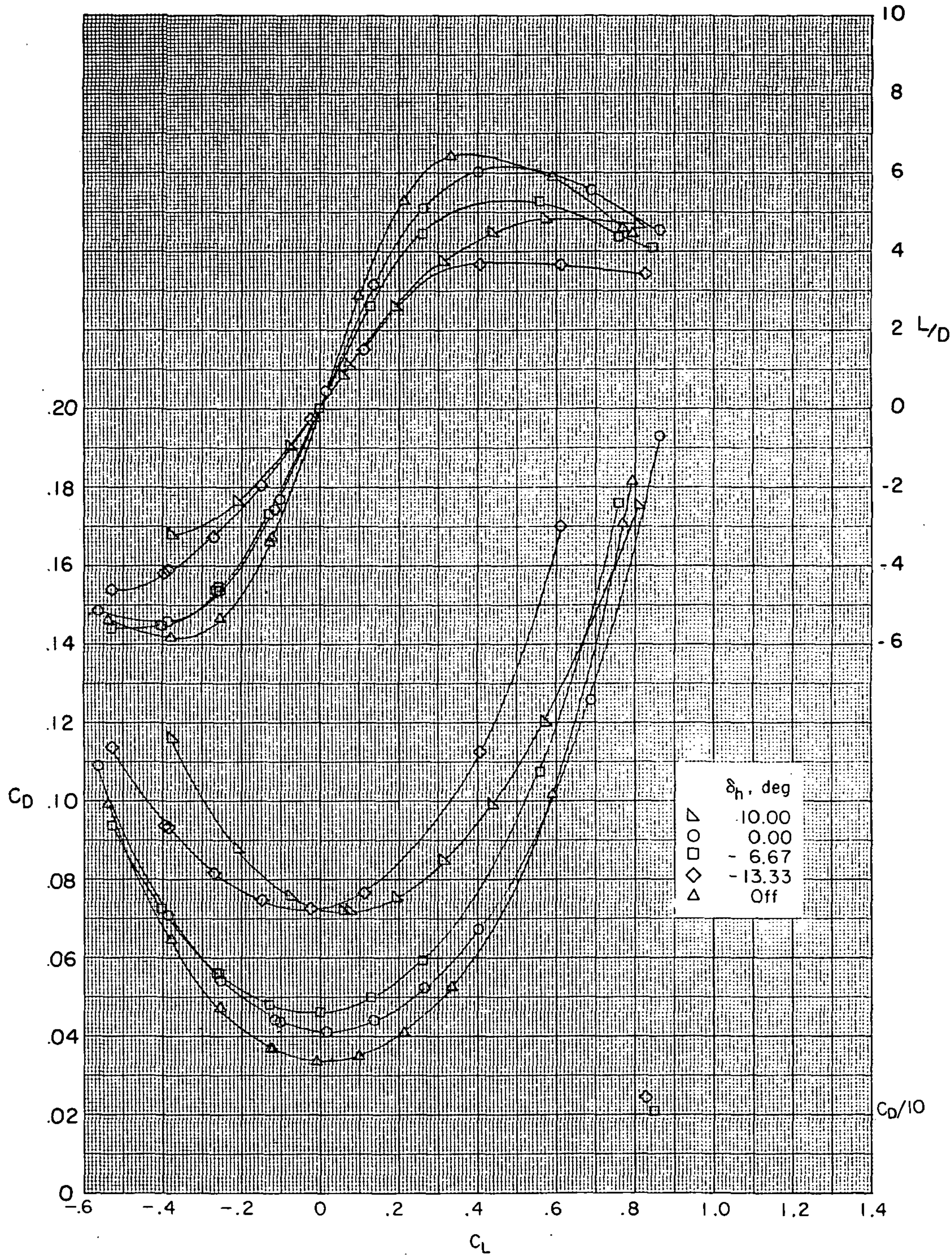

(c) Concluded.

Figure 5.- Continued.

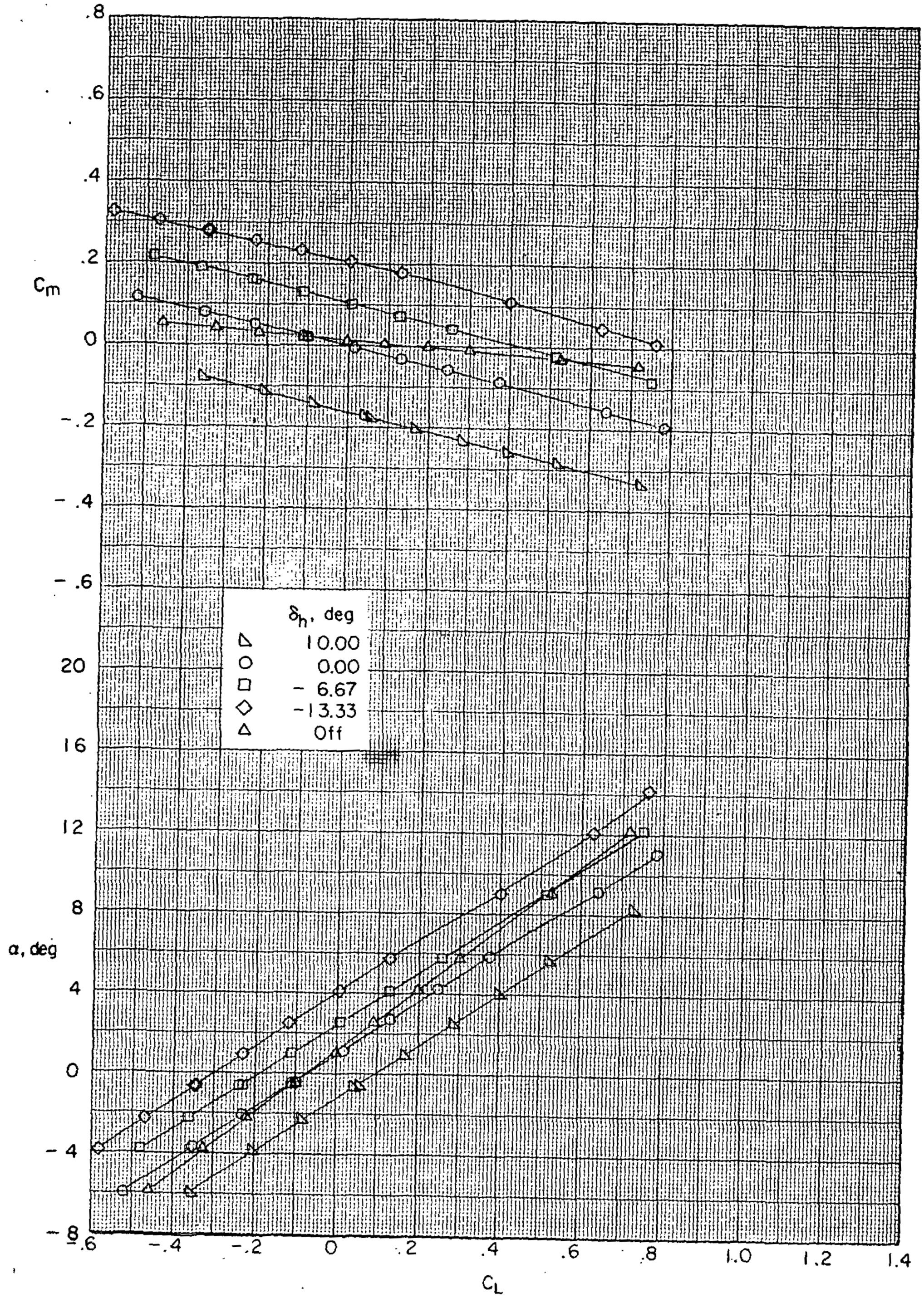

(d) M = 1.20.

Figure 5.- Continued.

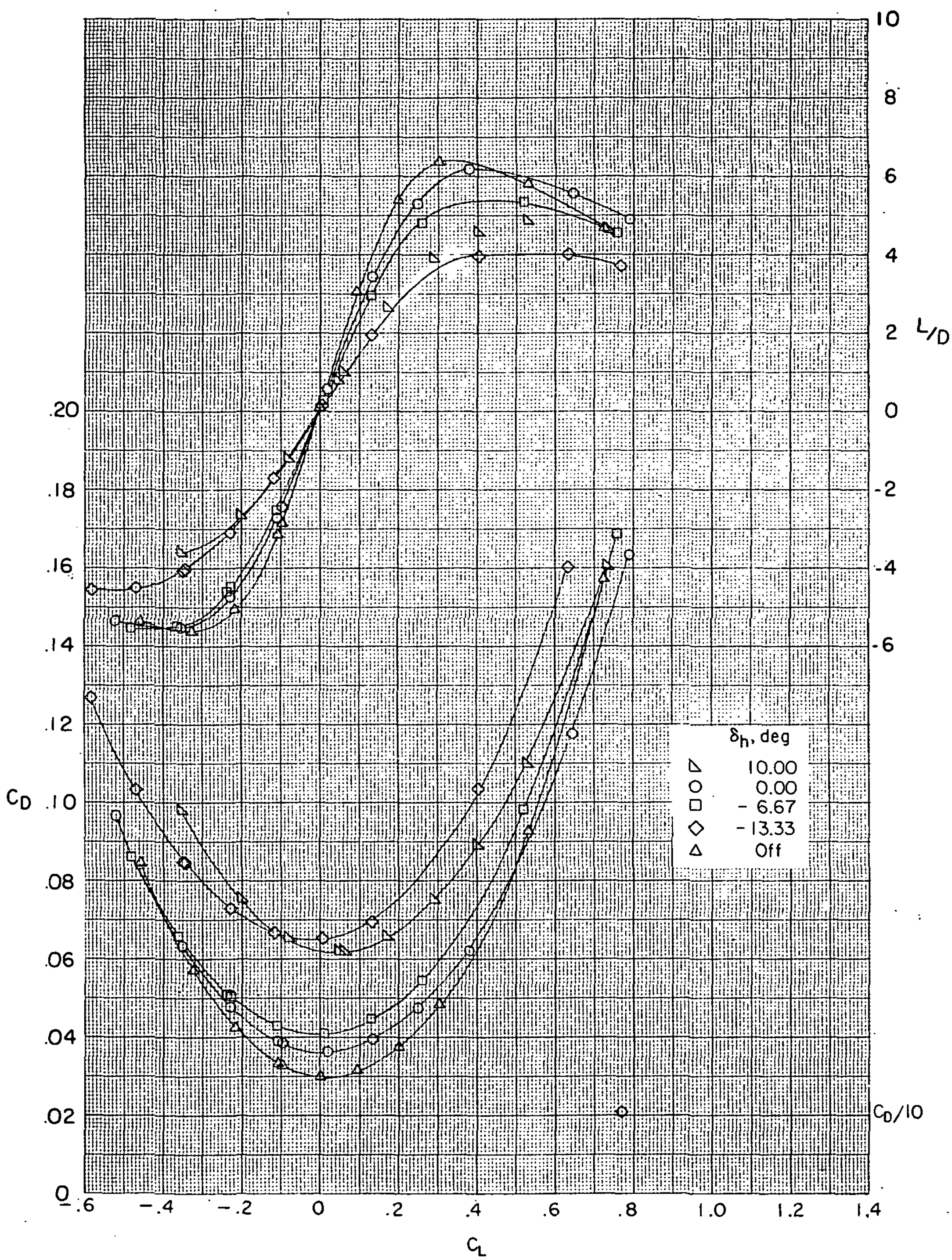

(d) Concluded.

Figure 5.- Continued.

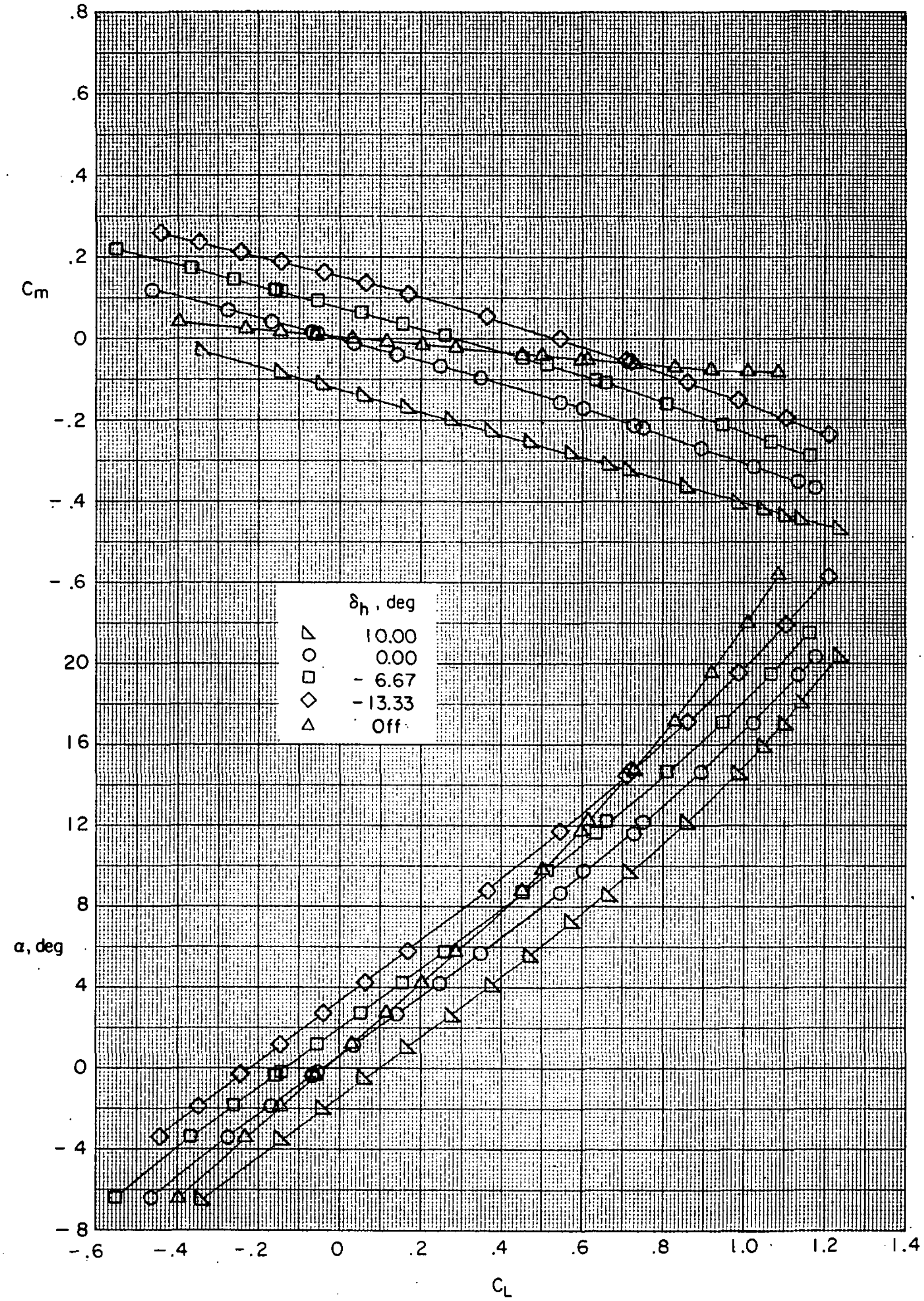

(e) M = 1.47.

Figure 5.- Continued.

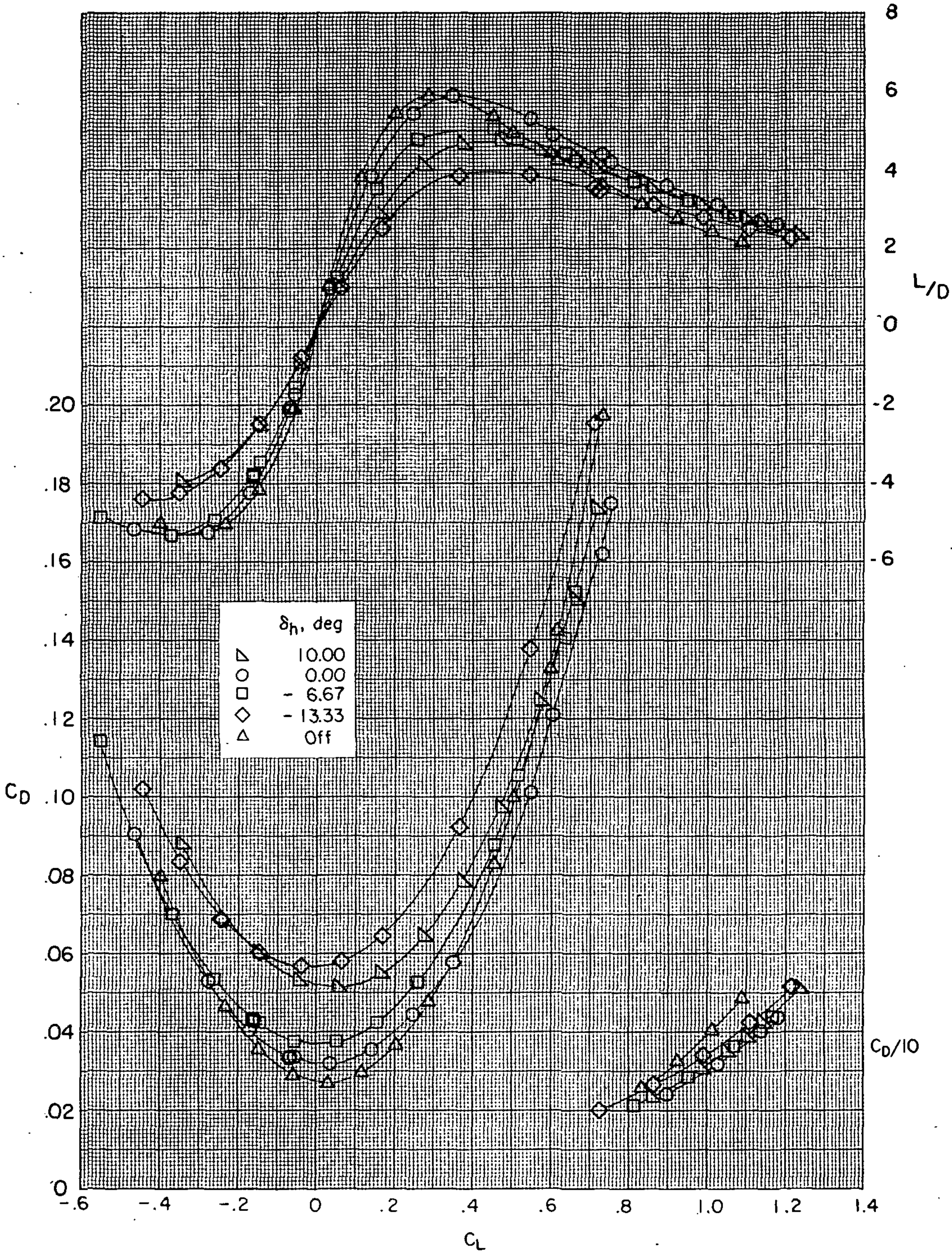

(e) Concluded.

Figure 5.- Continued.

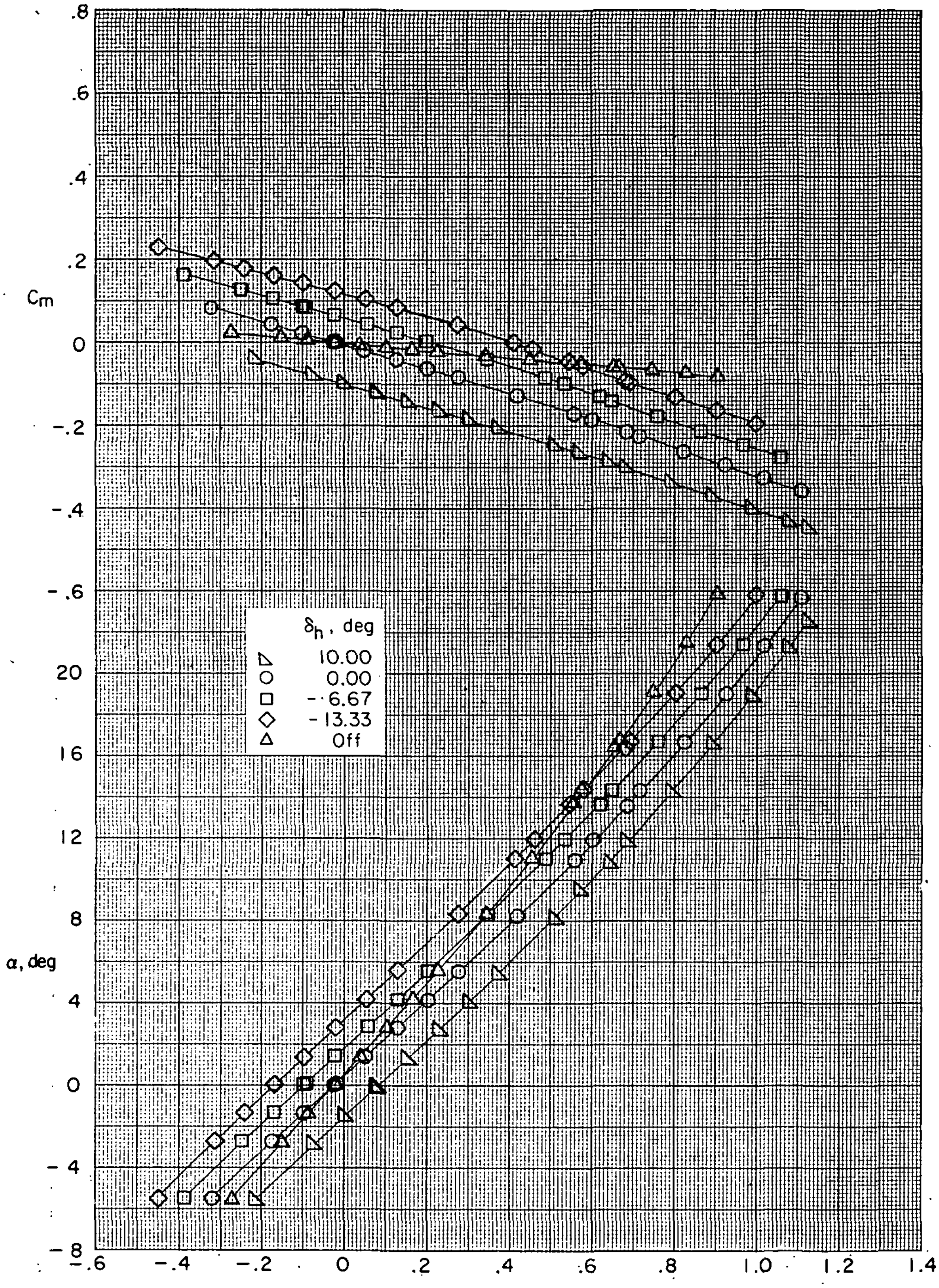

(f) M = 1.80.

Figure 5.- Continued.

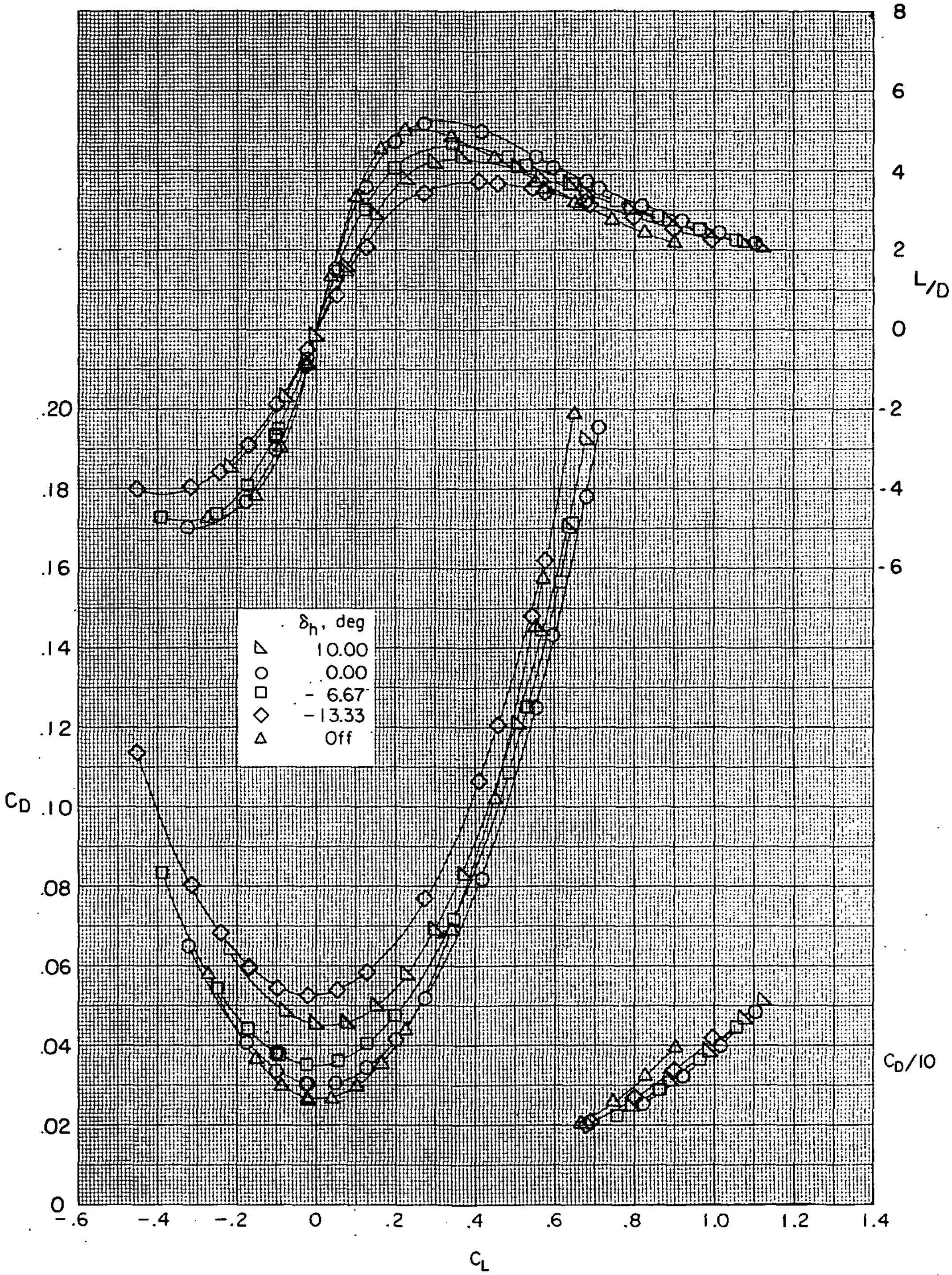

(f) Concluded.

Figure 5.- Continued.

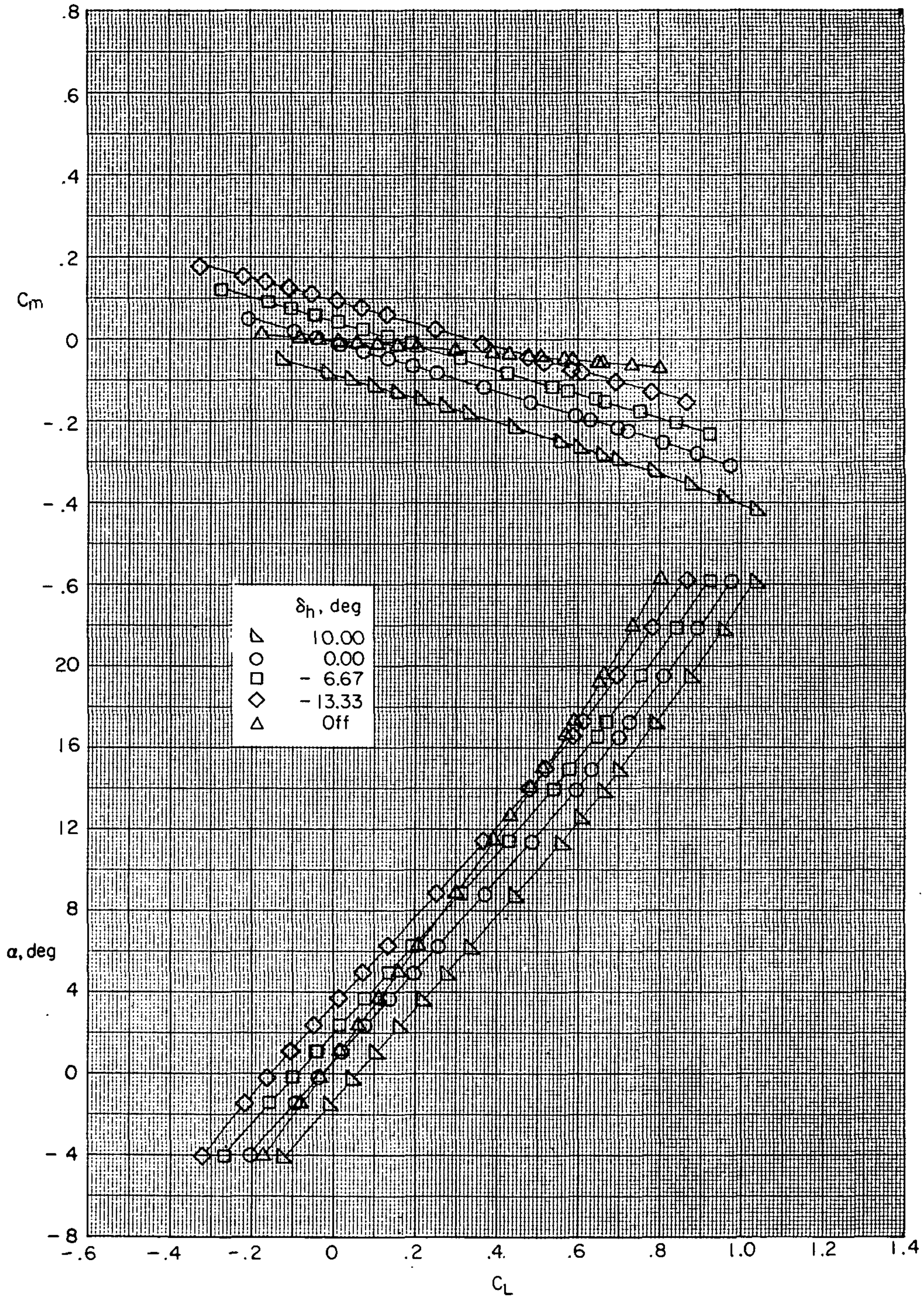

(g) M = 2.16.

Figure 5.- Continued.

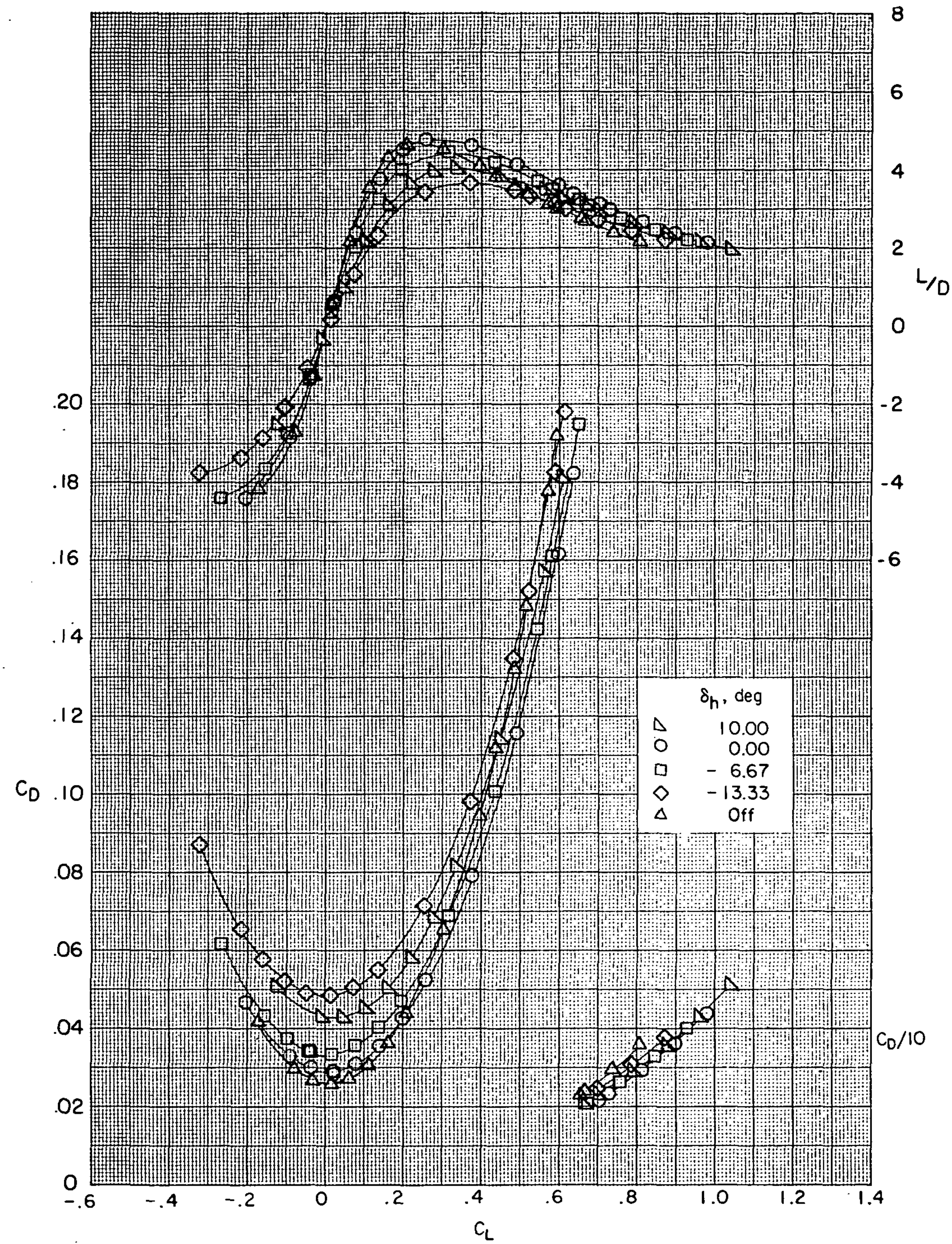

(g) Concluded.

Figure 5.- Concluded.

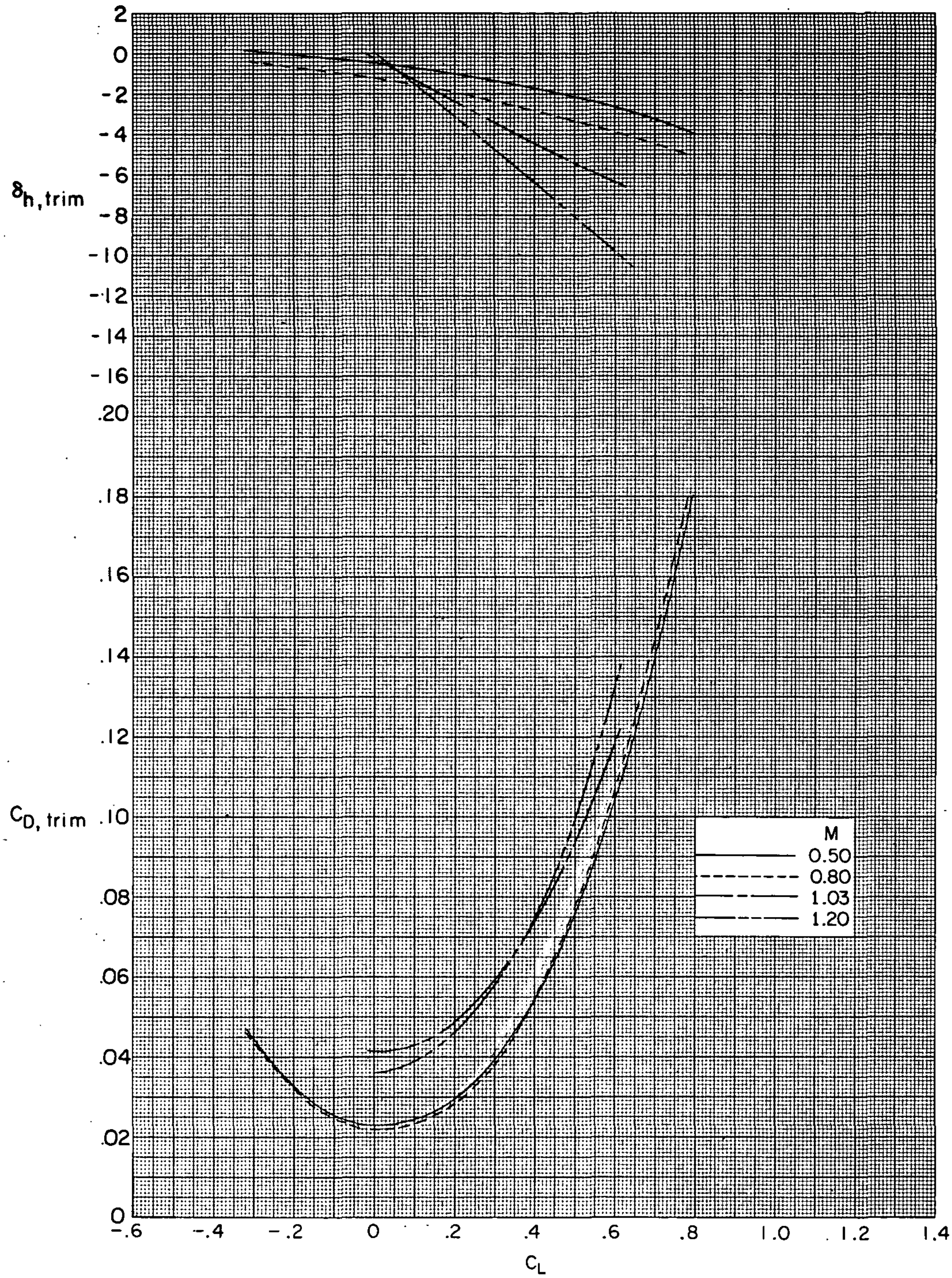

Figure 6.- Longitudinal trim characteristics with the cambered wing.

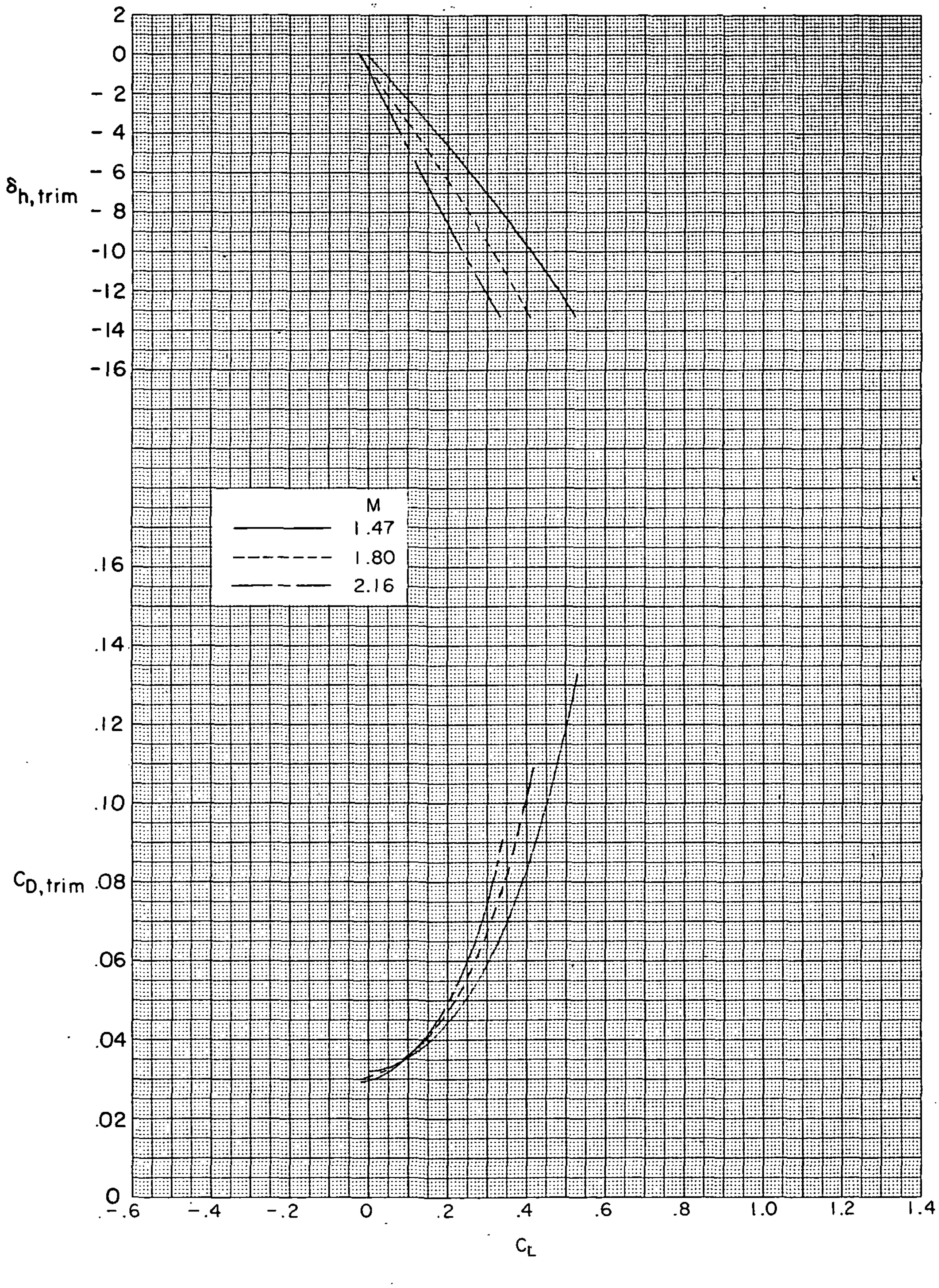

Figure 6.- Concluded.

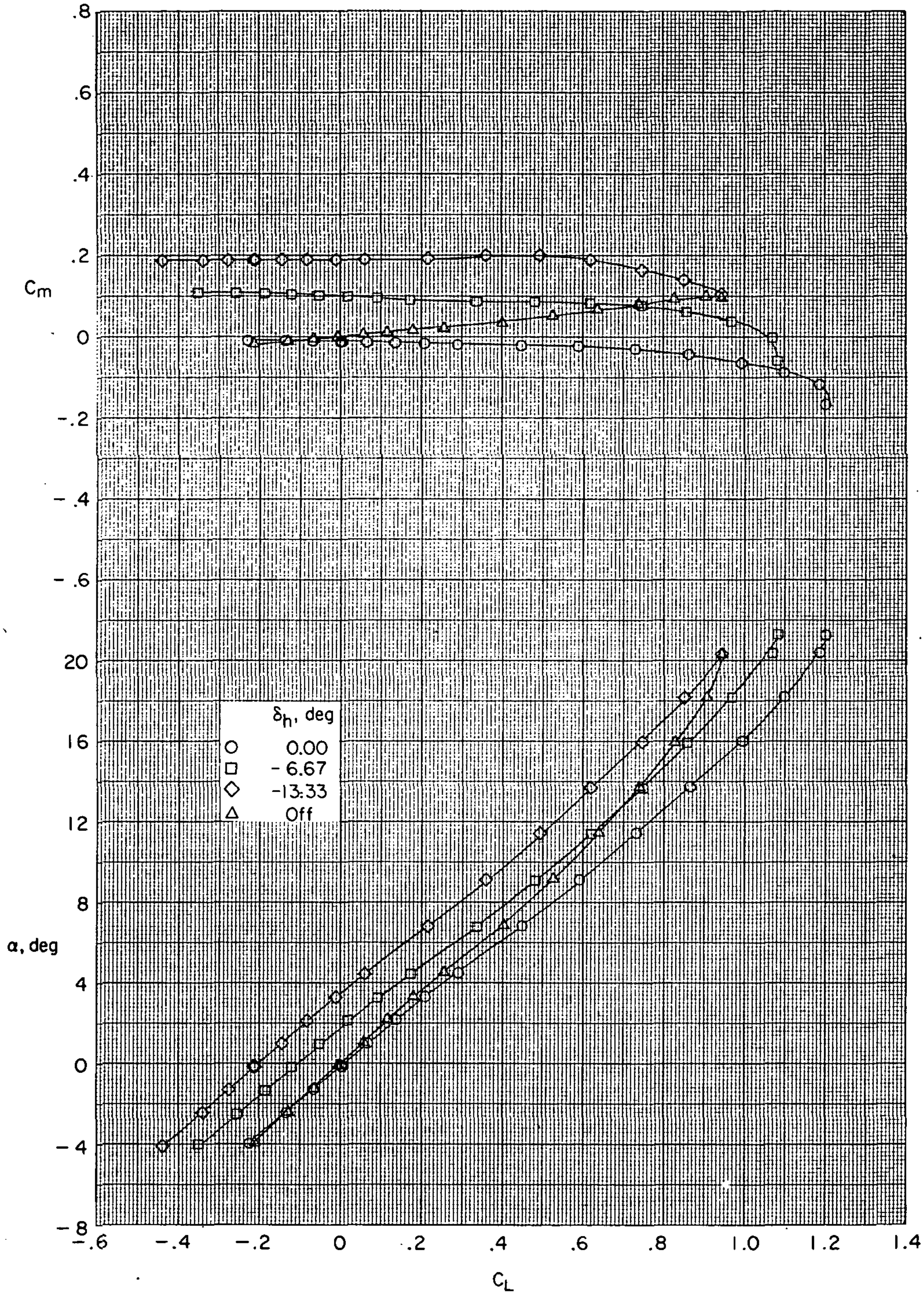

(a) M = 0.50.

Figure 7.- Longitudinal aerodynamic characteristics with the flat wing.

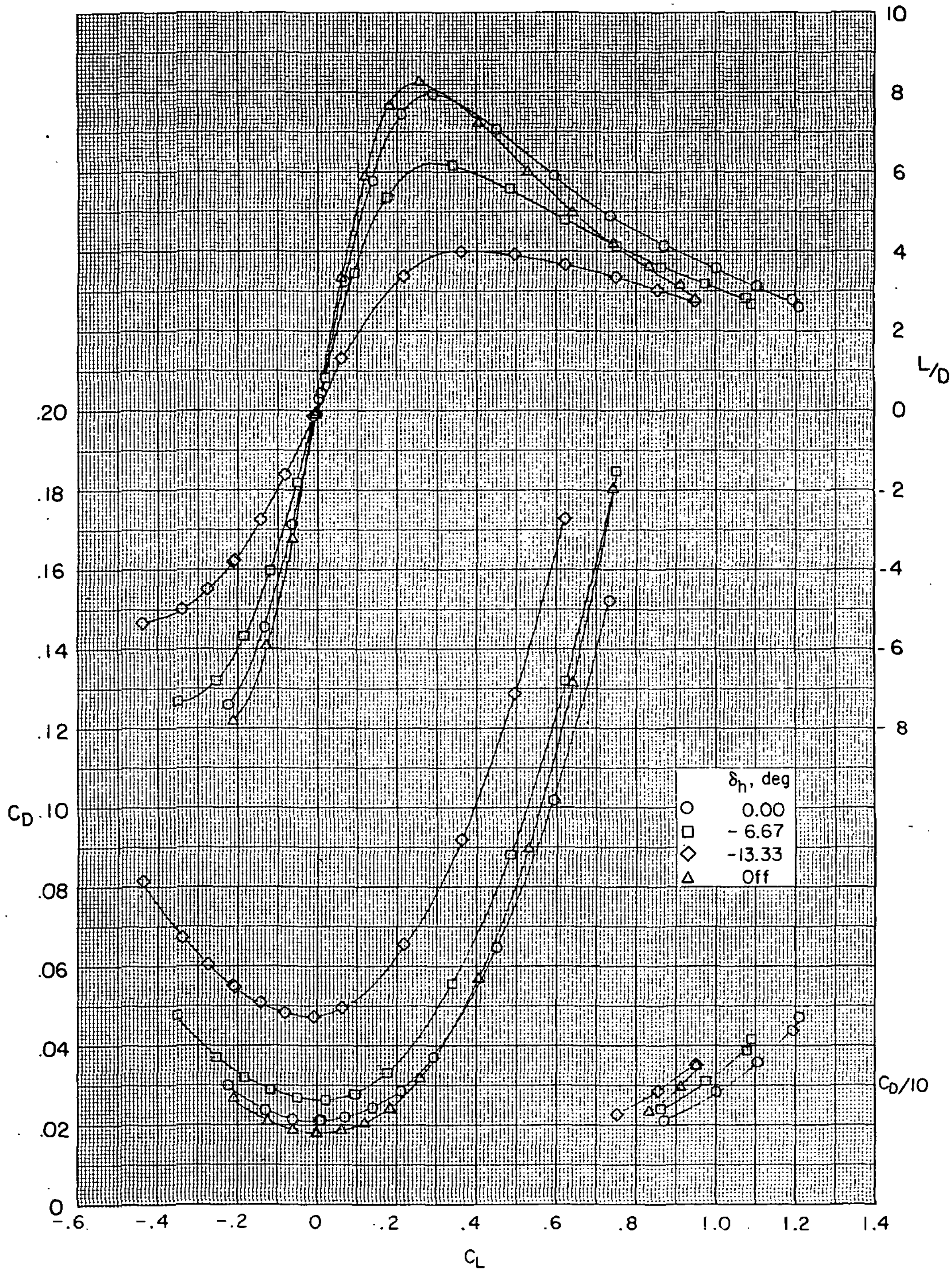

(a) Concluded.

Figure 7.- Continued.

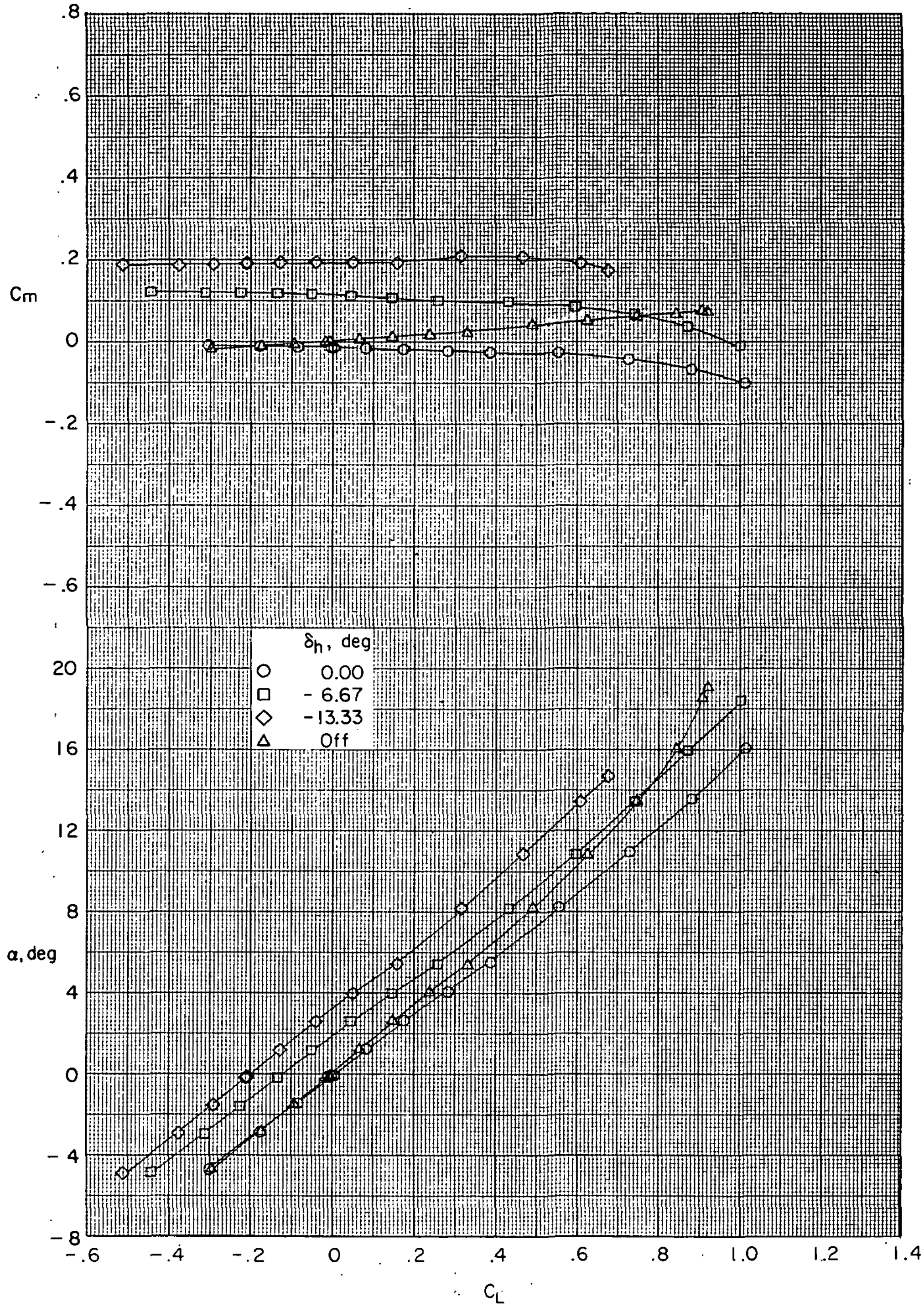

(b) M = 0.80.

Figure 7.- Continued.

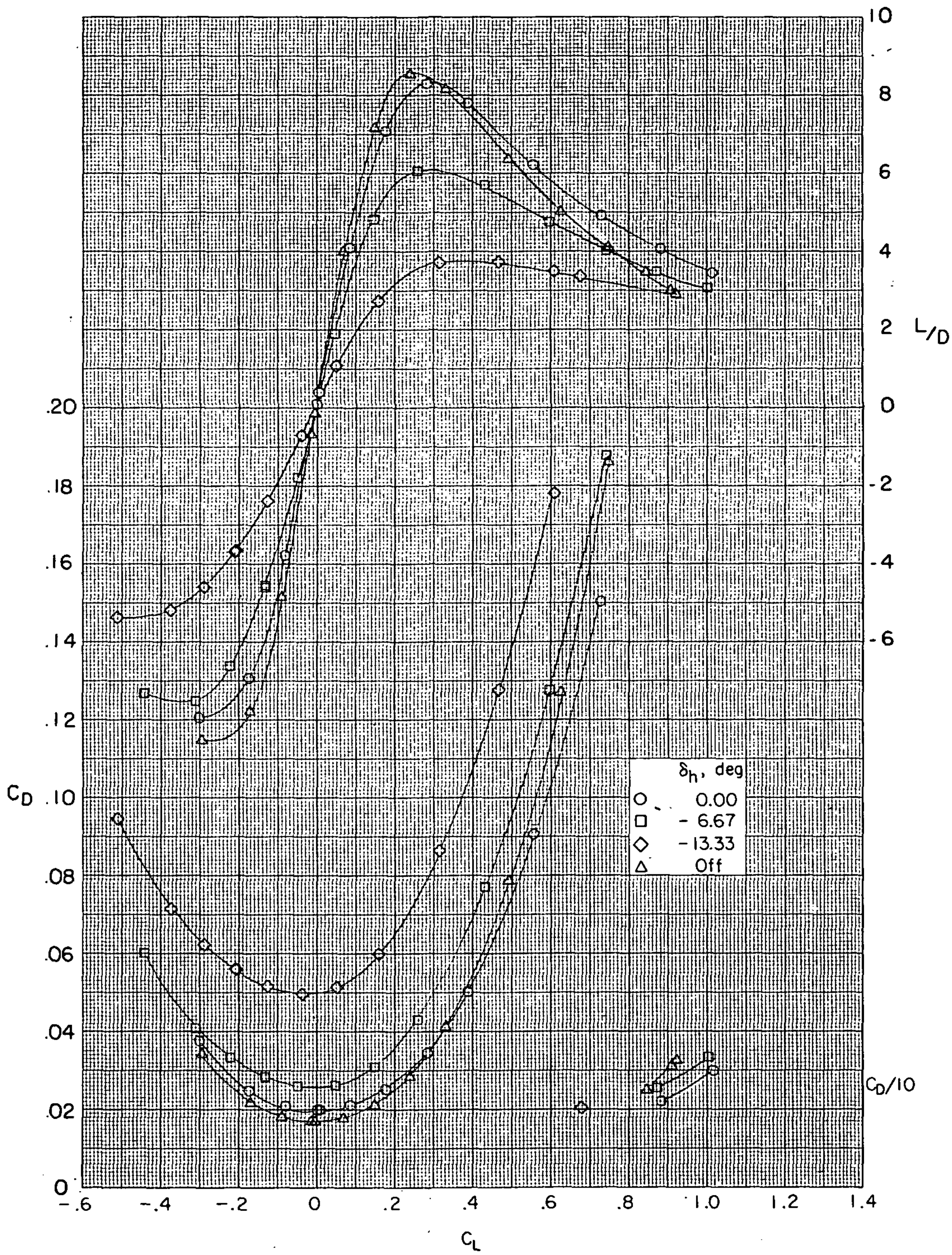

(b) Concluded.

Figure 7.- Continued.

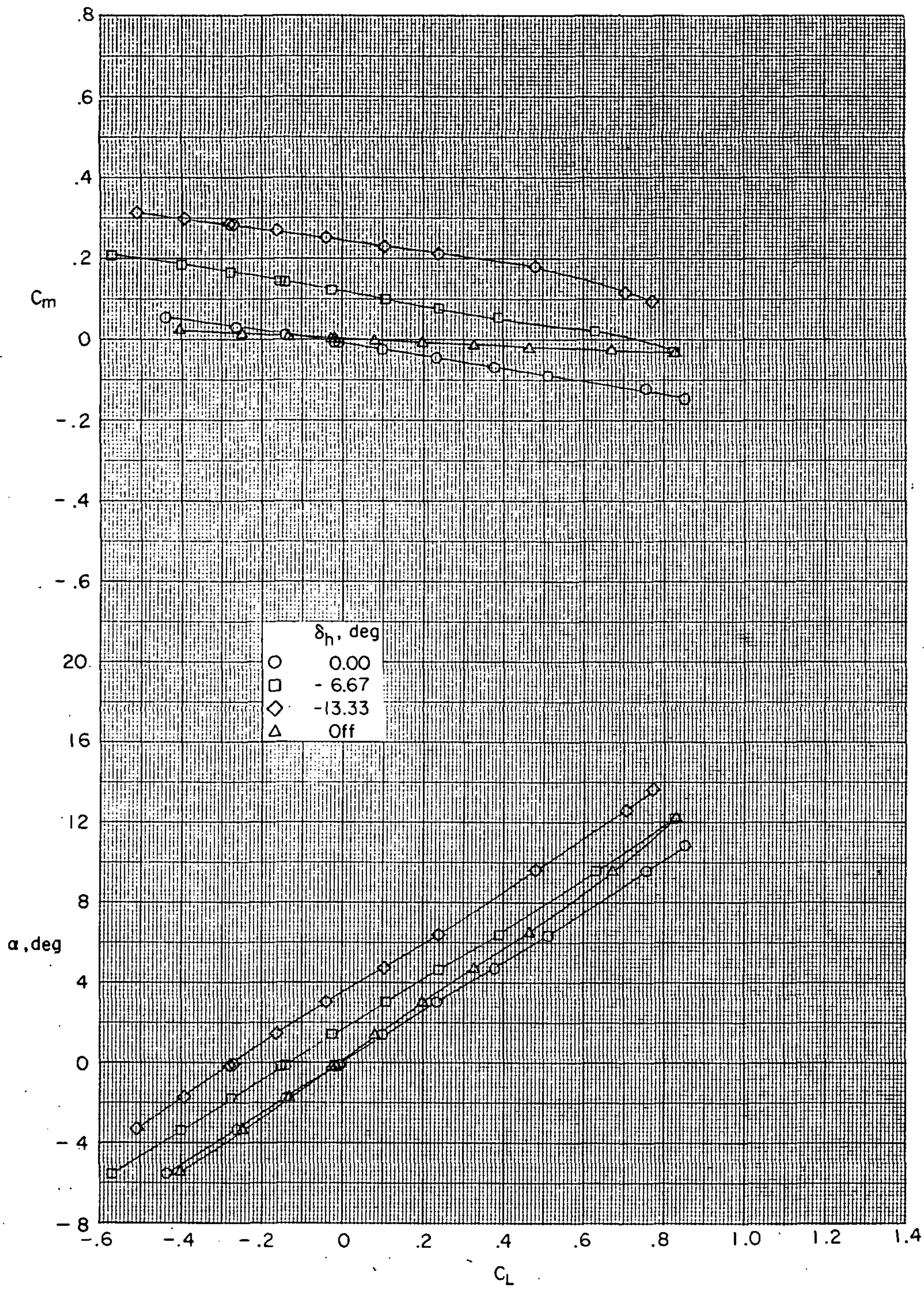

(c) M = 1.03.

Figure 7.- Continued.

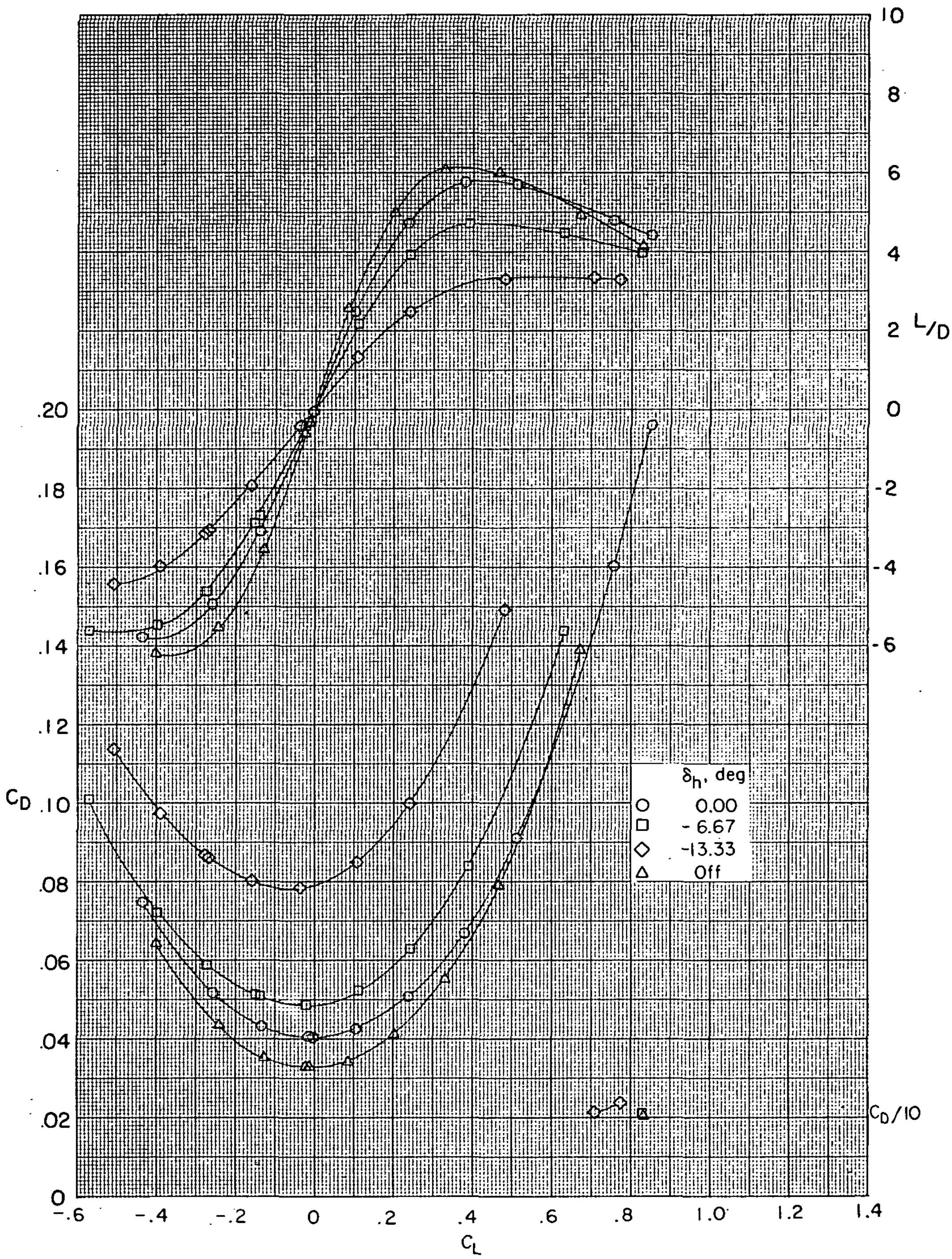

(c) Concluded.

Figure 7.- Continued.

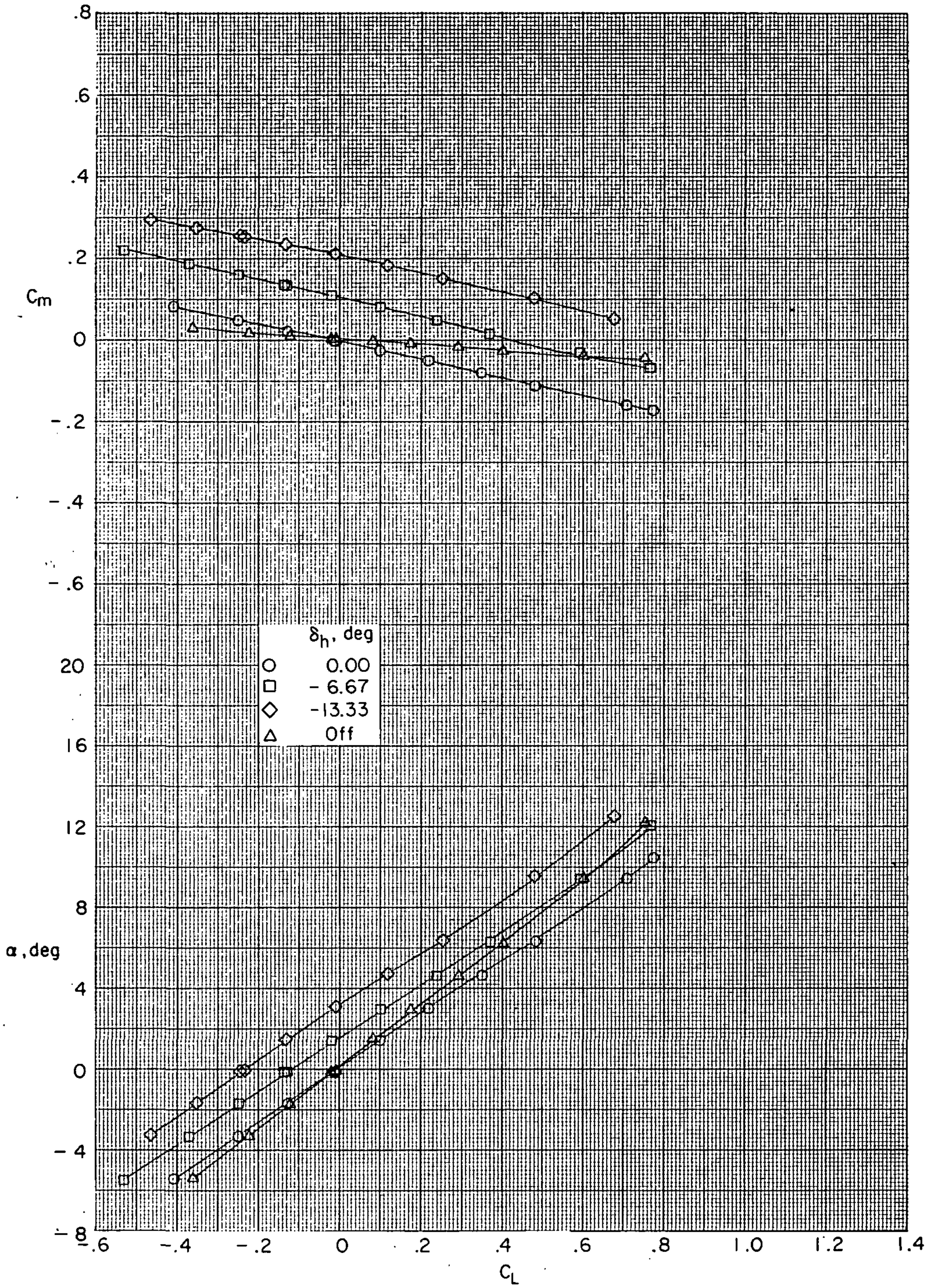

(d) M = 1.20.

Figure 7.- Continued.

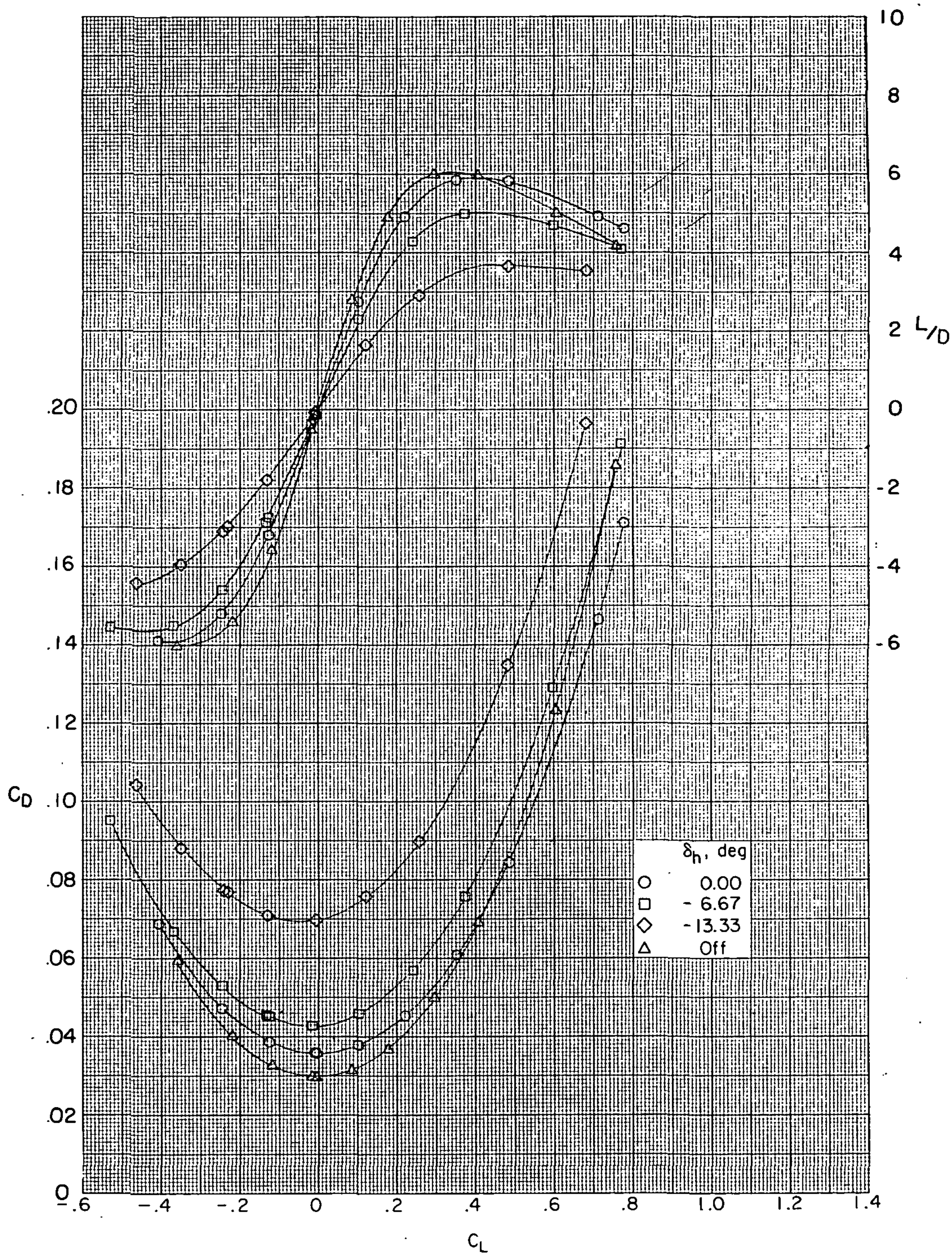

(d) Concluded.

Figure 7.- Continued.

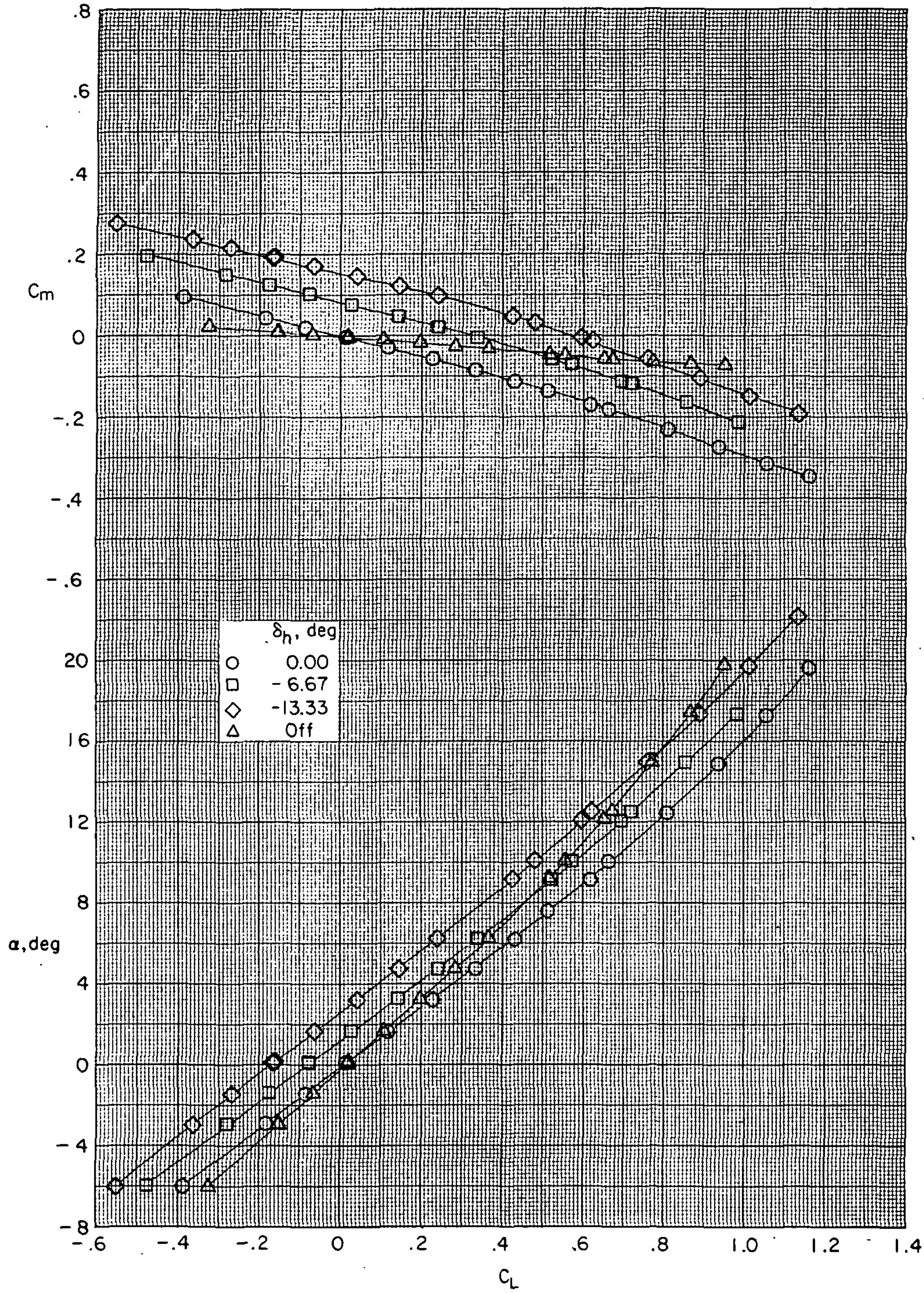

(e) M = 1.47.

Figure 7.- Continued.

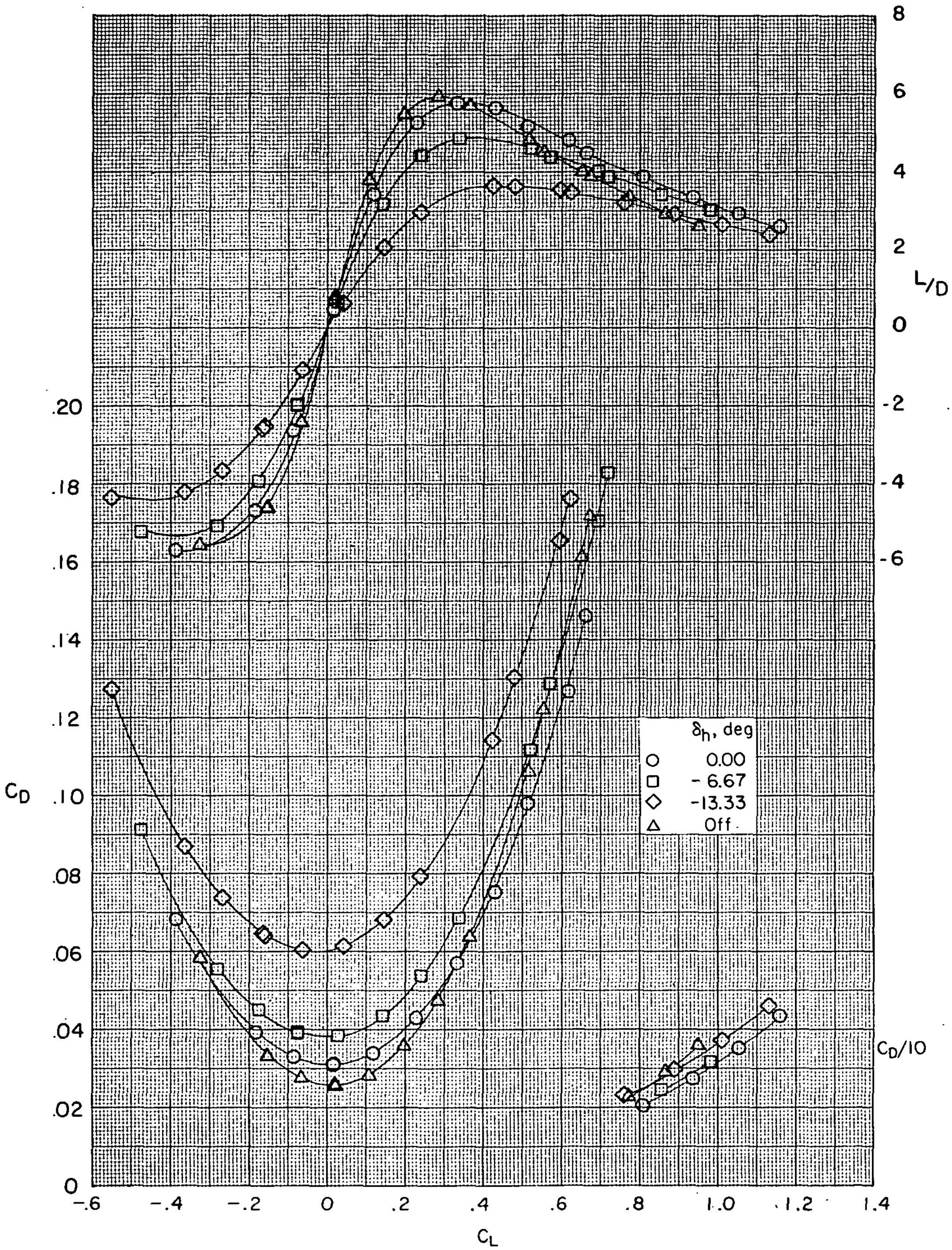

(e) Concluded.

Figure 7.- Continued.

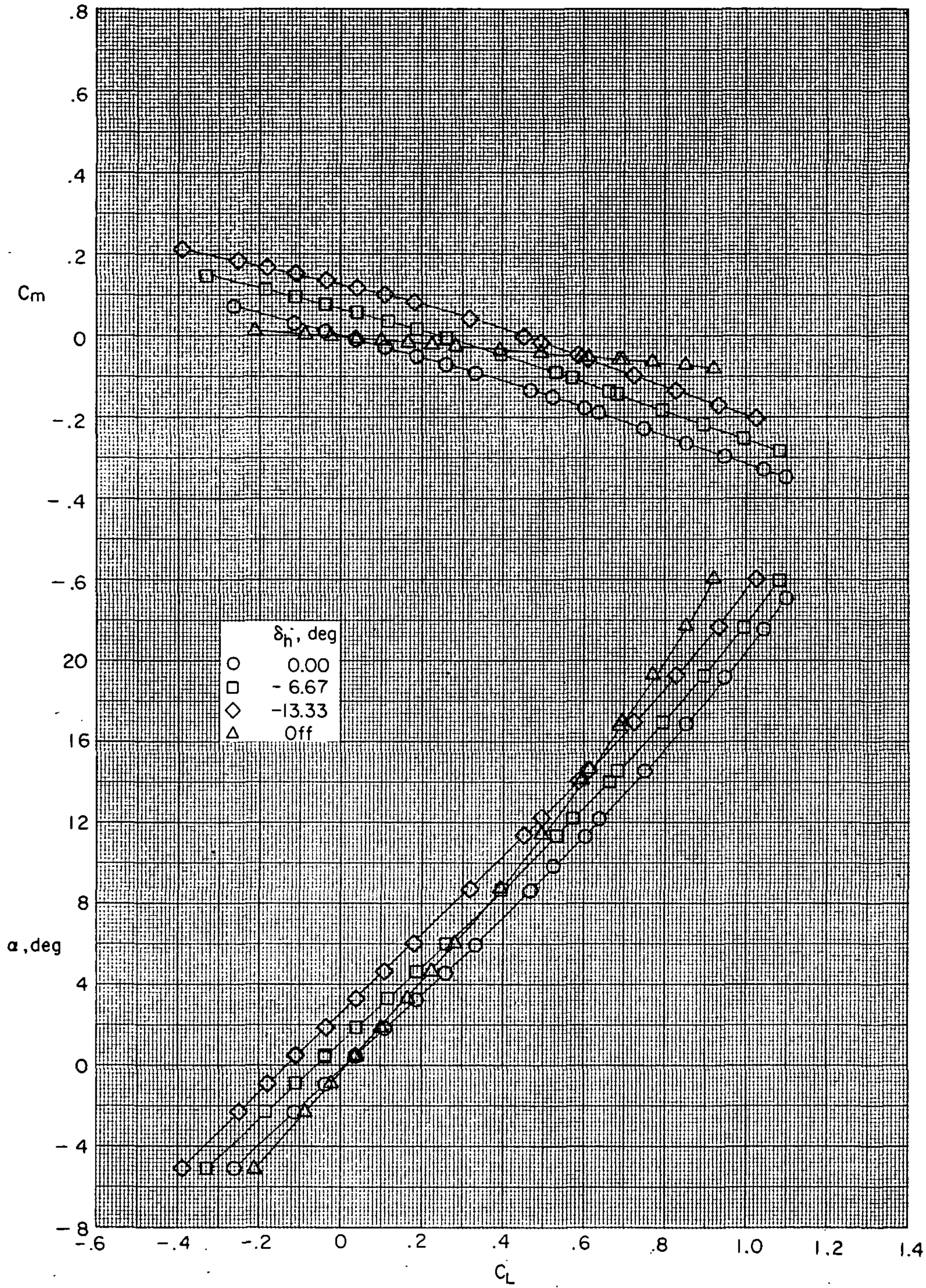

(f) M = 1.80.

Figure 7.- Continued.

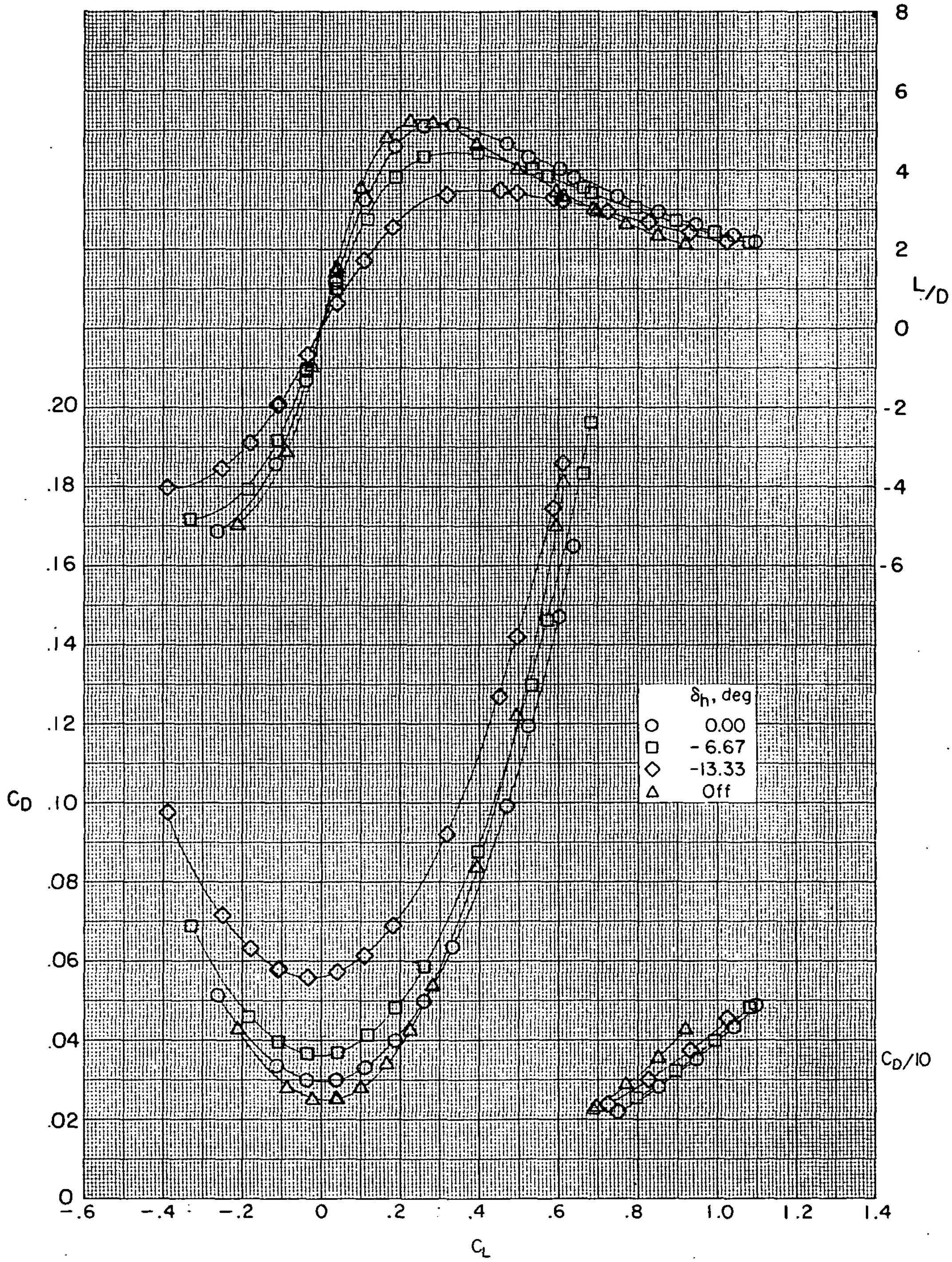

(f) Concluded.

Figure 7.- Continued.

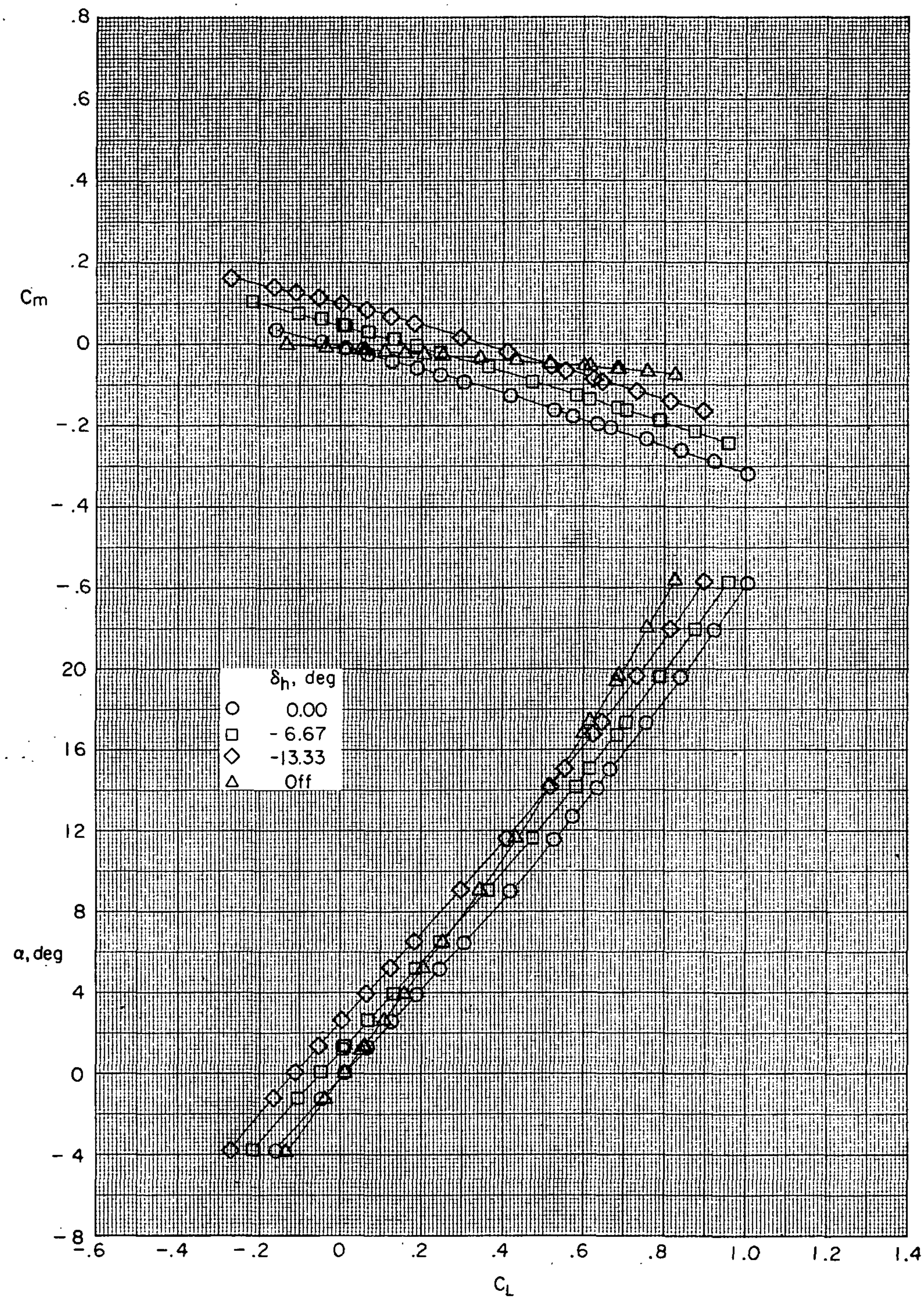

(g) M = 2.16.

Figure 7.- Continued.

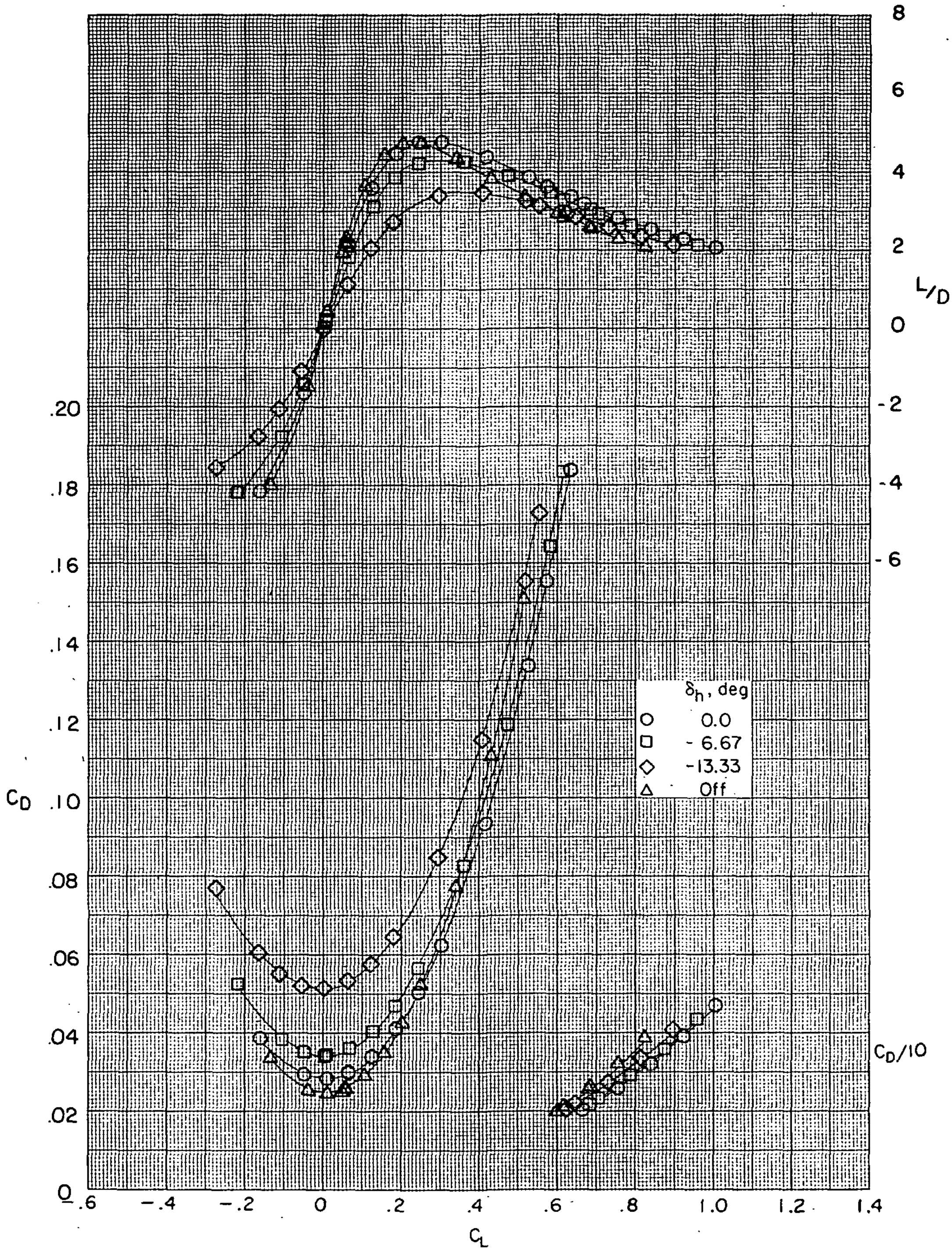

(g) Concluded.

Figure 7.- Concluded.

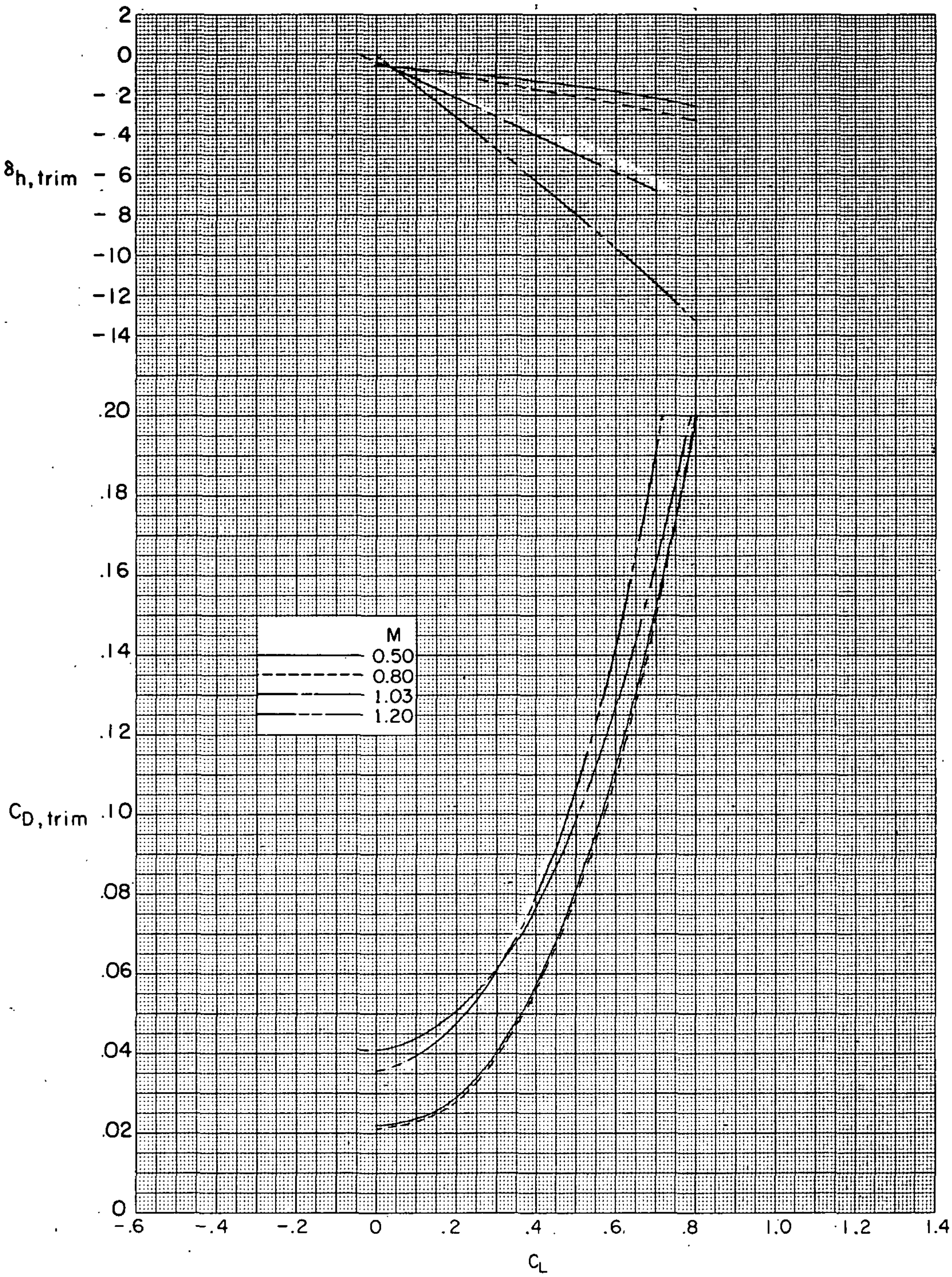

Figure 8.- Longitudinal trim characteristics with the flat wing.

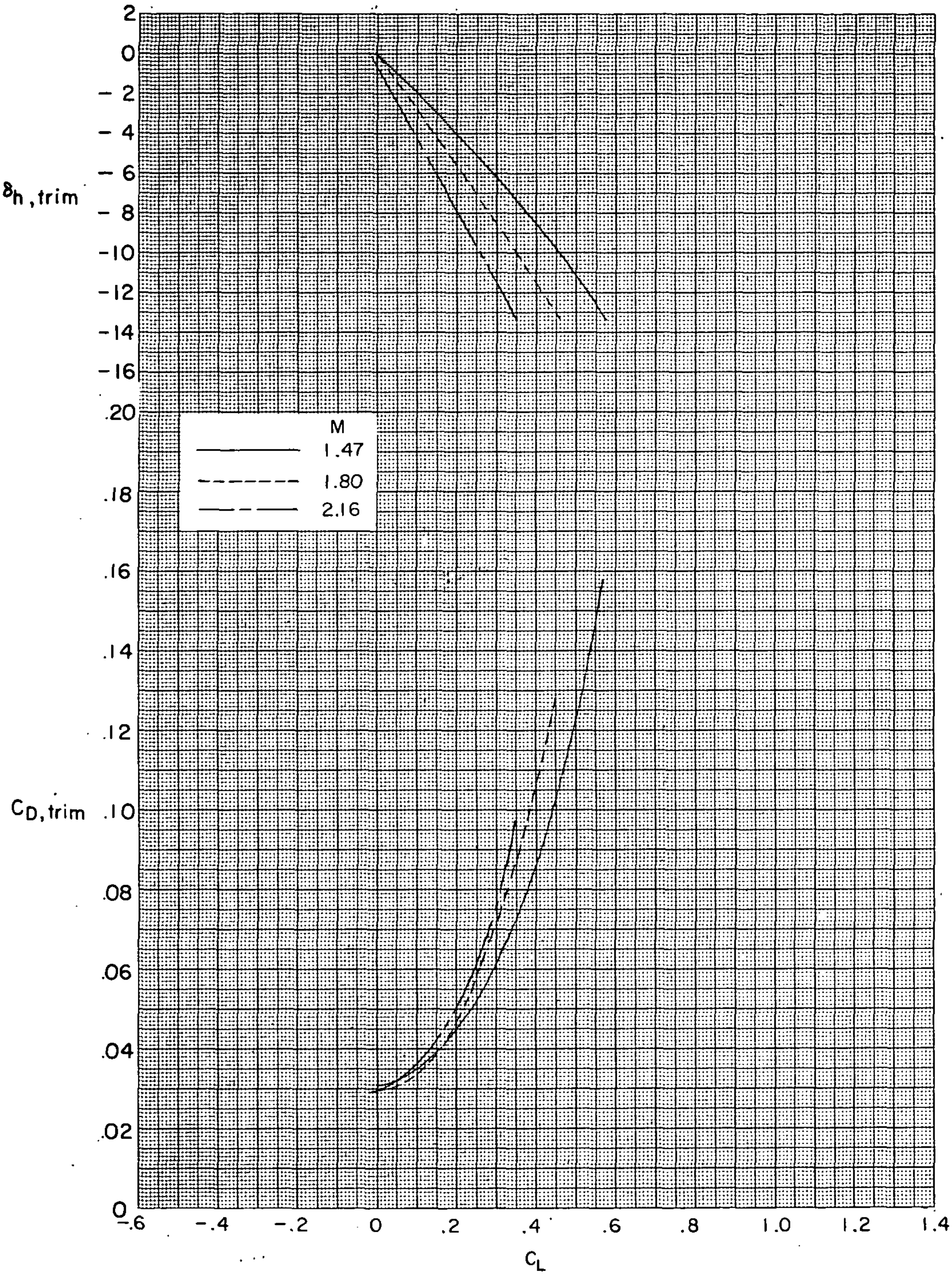

Figure 8.- Concluded.

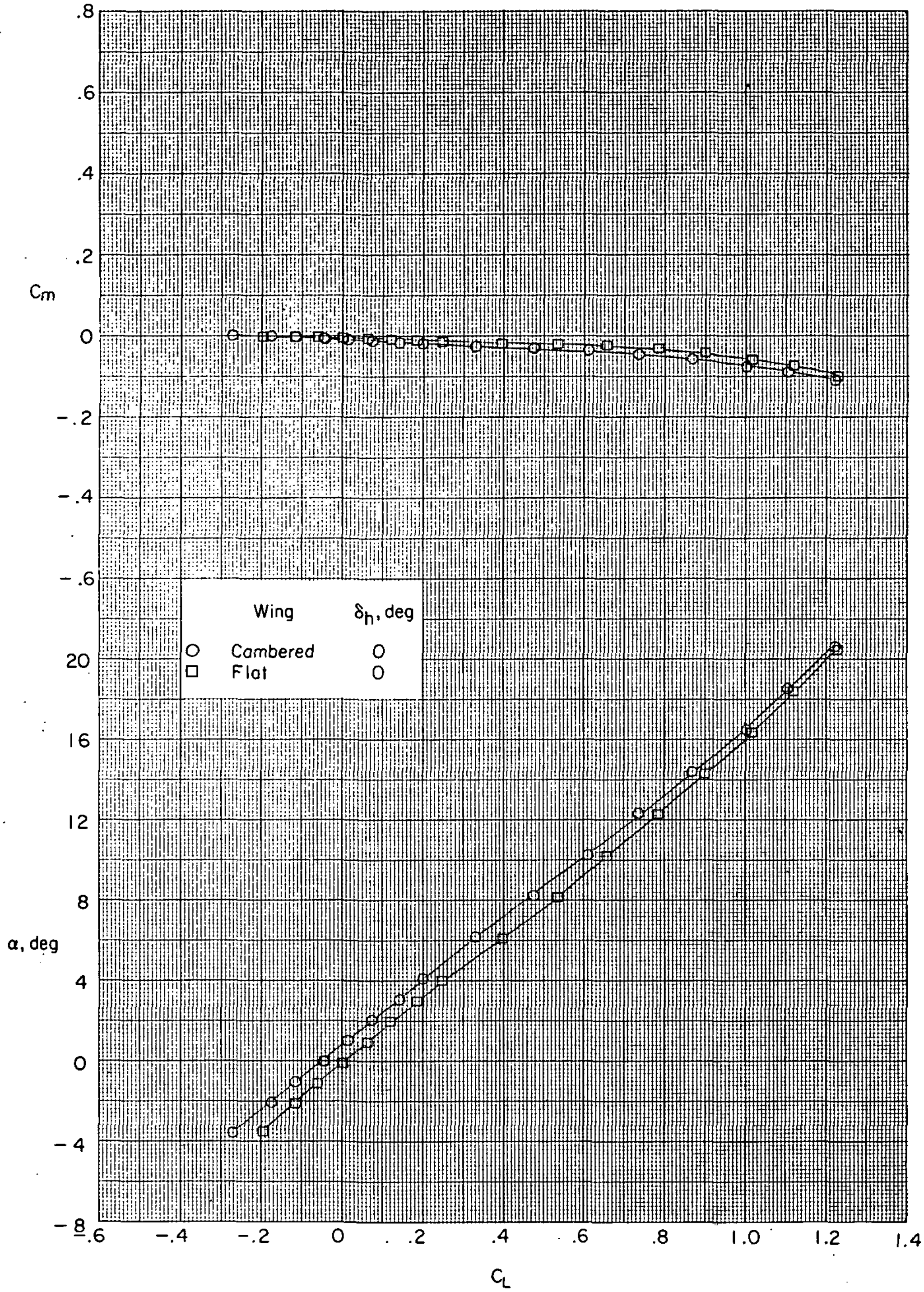

(a) M = 0.20.

Figure 9.- Longitudinal characteristics with the cambered and flat wings.

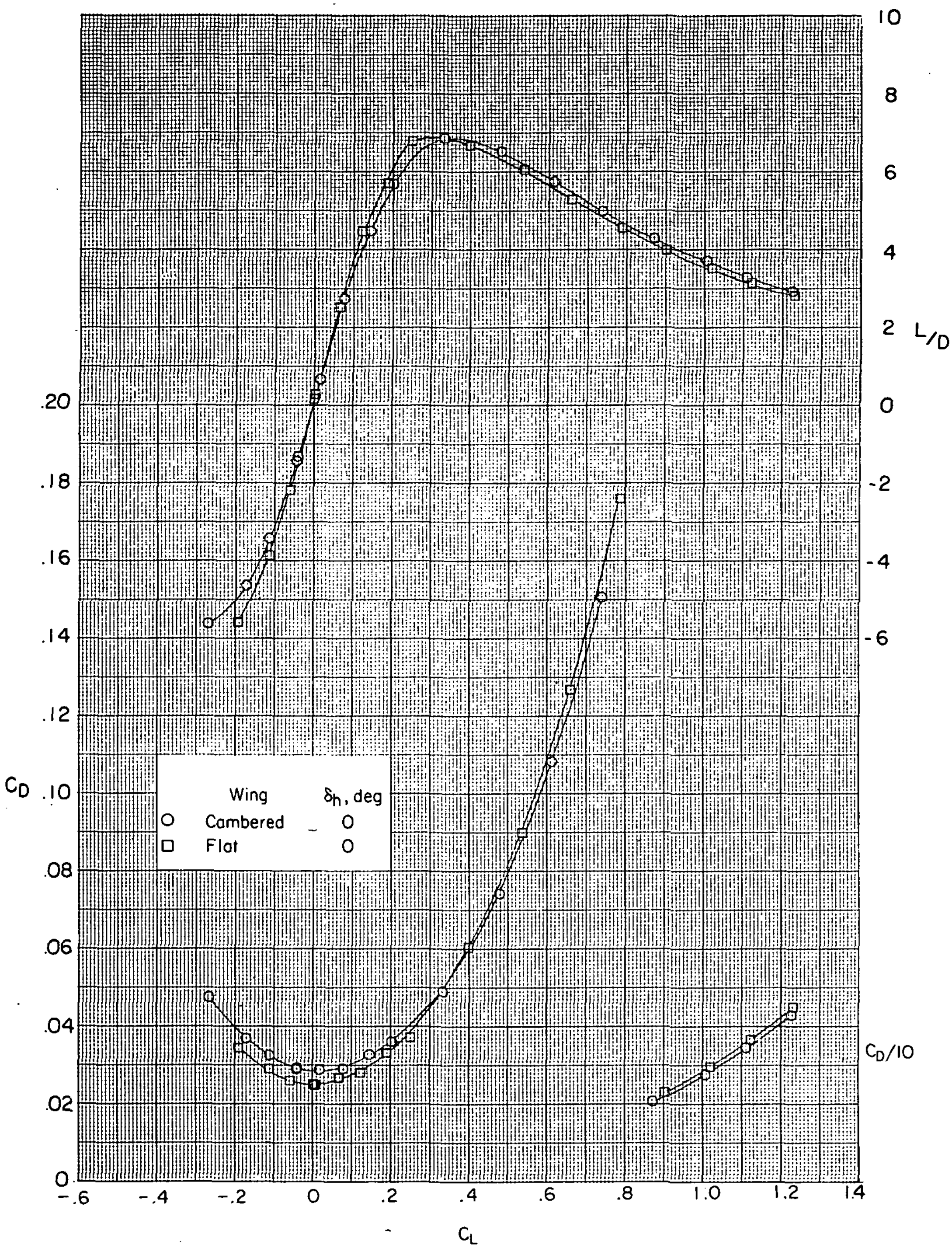

(a) Concluded.

Figure 9.- Continued.

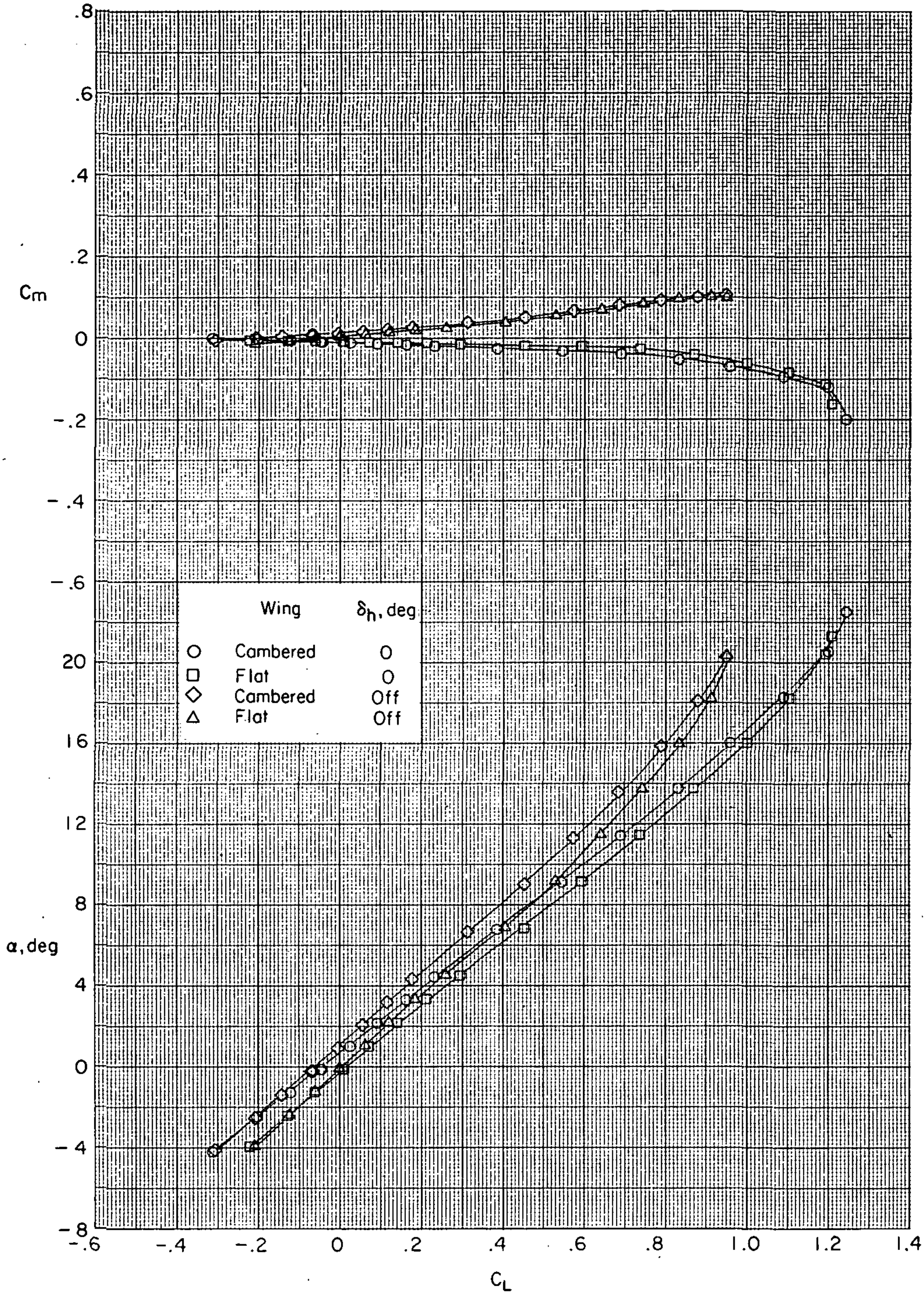

(b) M = 0.50.

Figure 9.- Continued.

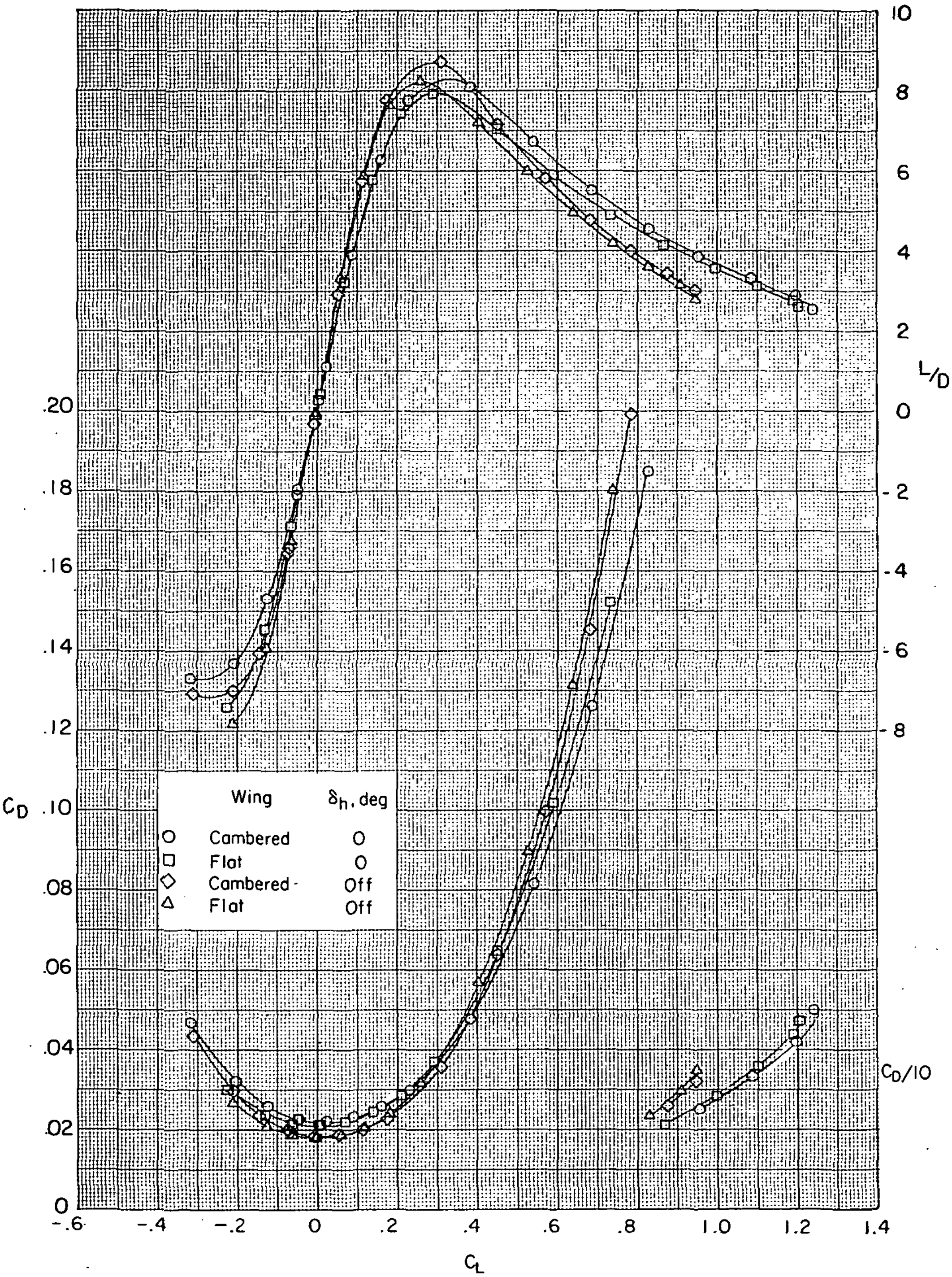

(b) Concluded.

Figure 9.- Continued.

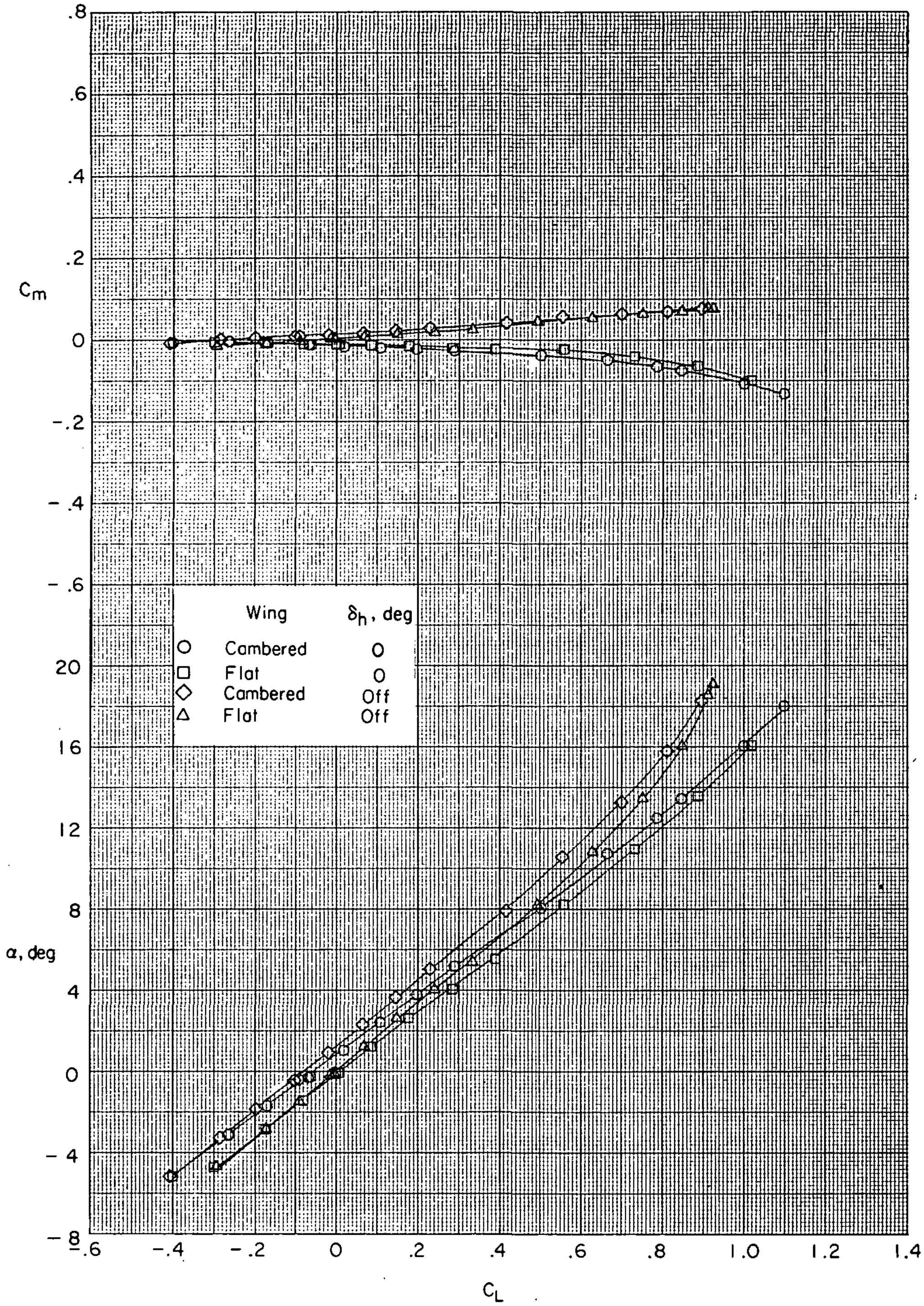

(c) M = 0.80.

Figure 9.- Continued.

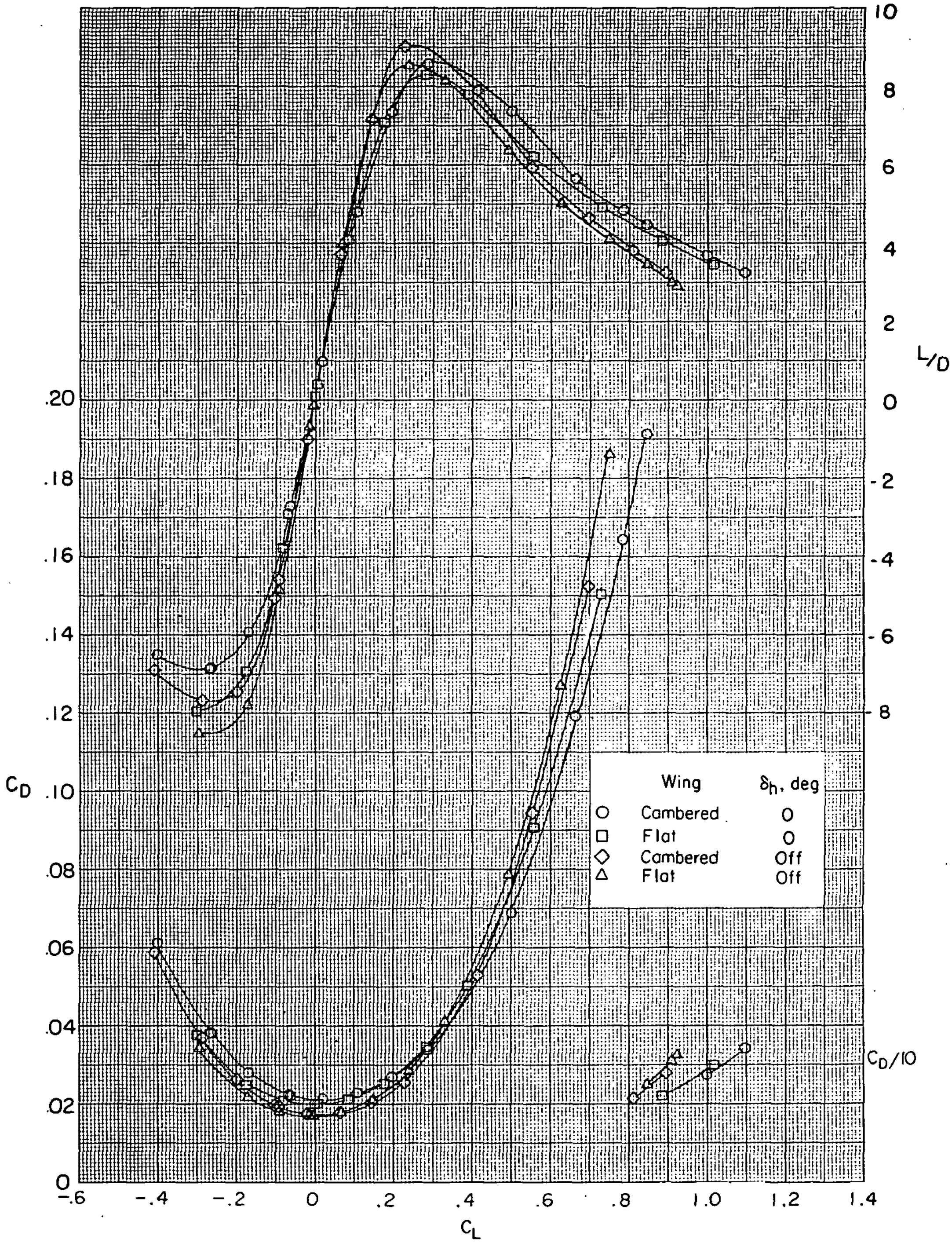

(c) Concluded.

Figure 9.- Continued.

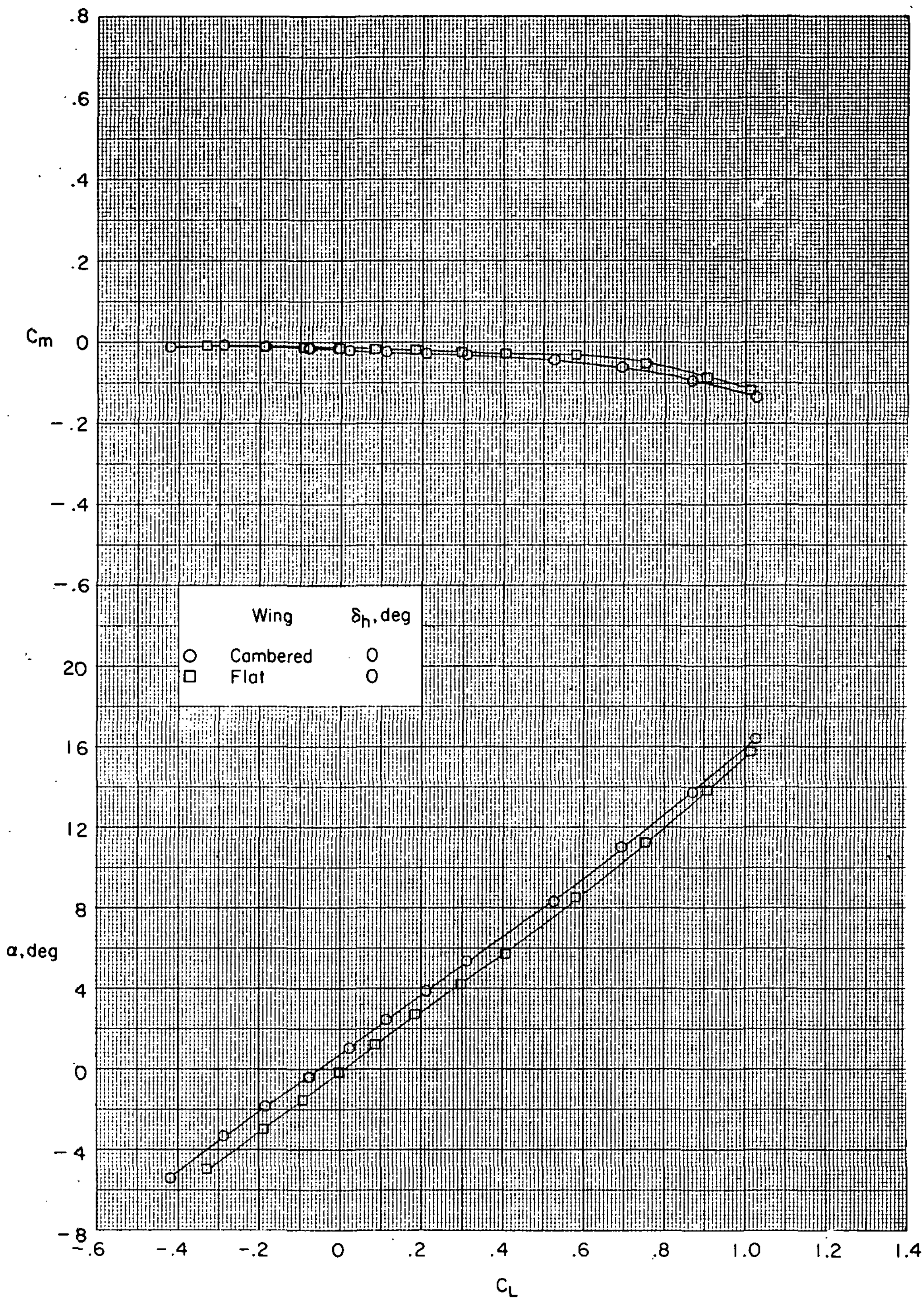

(d) M = 0.85.

Figure 9.- Continued.

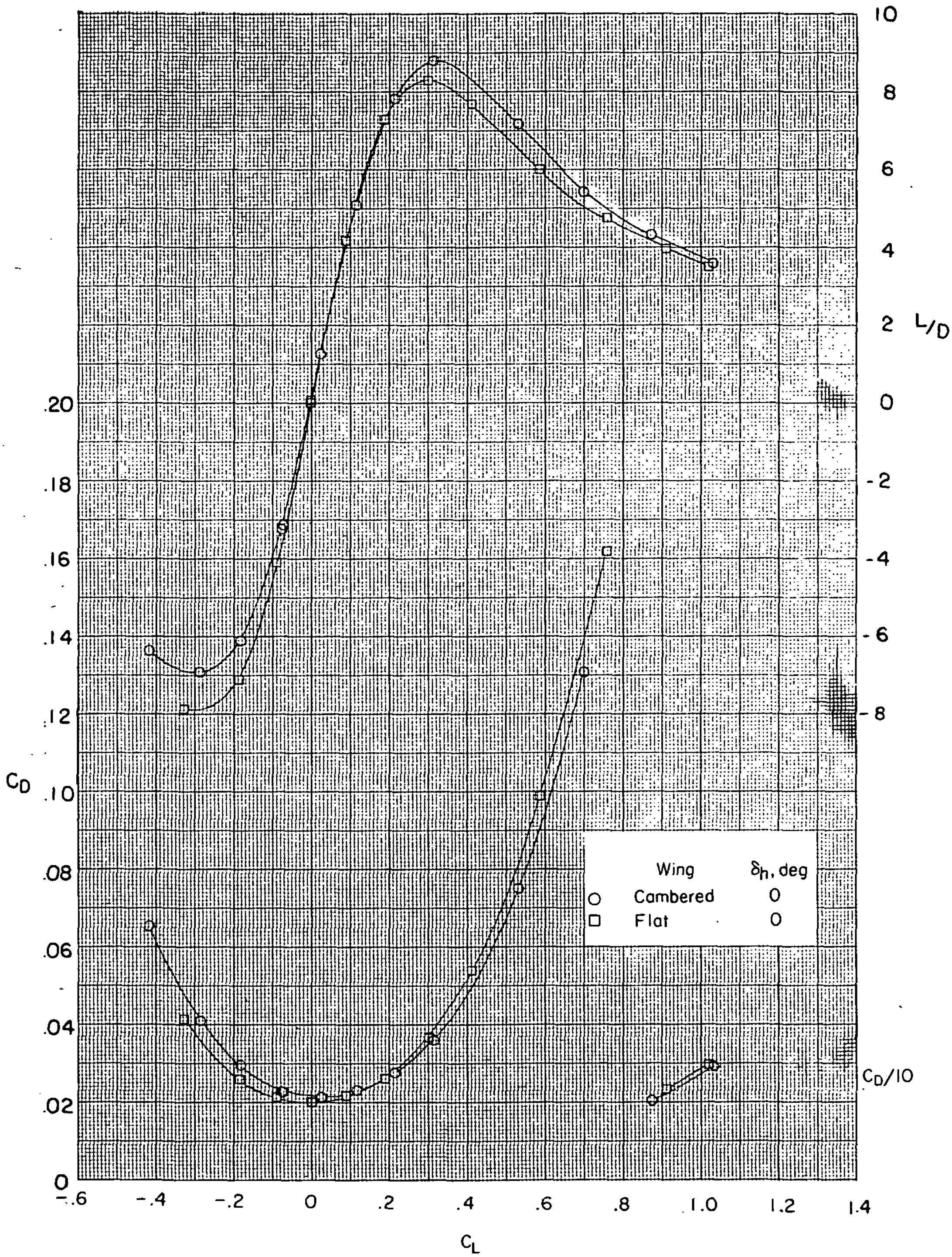

(d) Concluded.

Figure 9.- Continued.

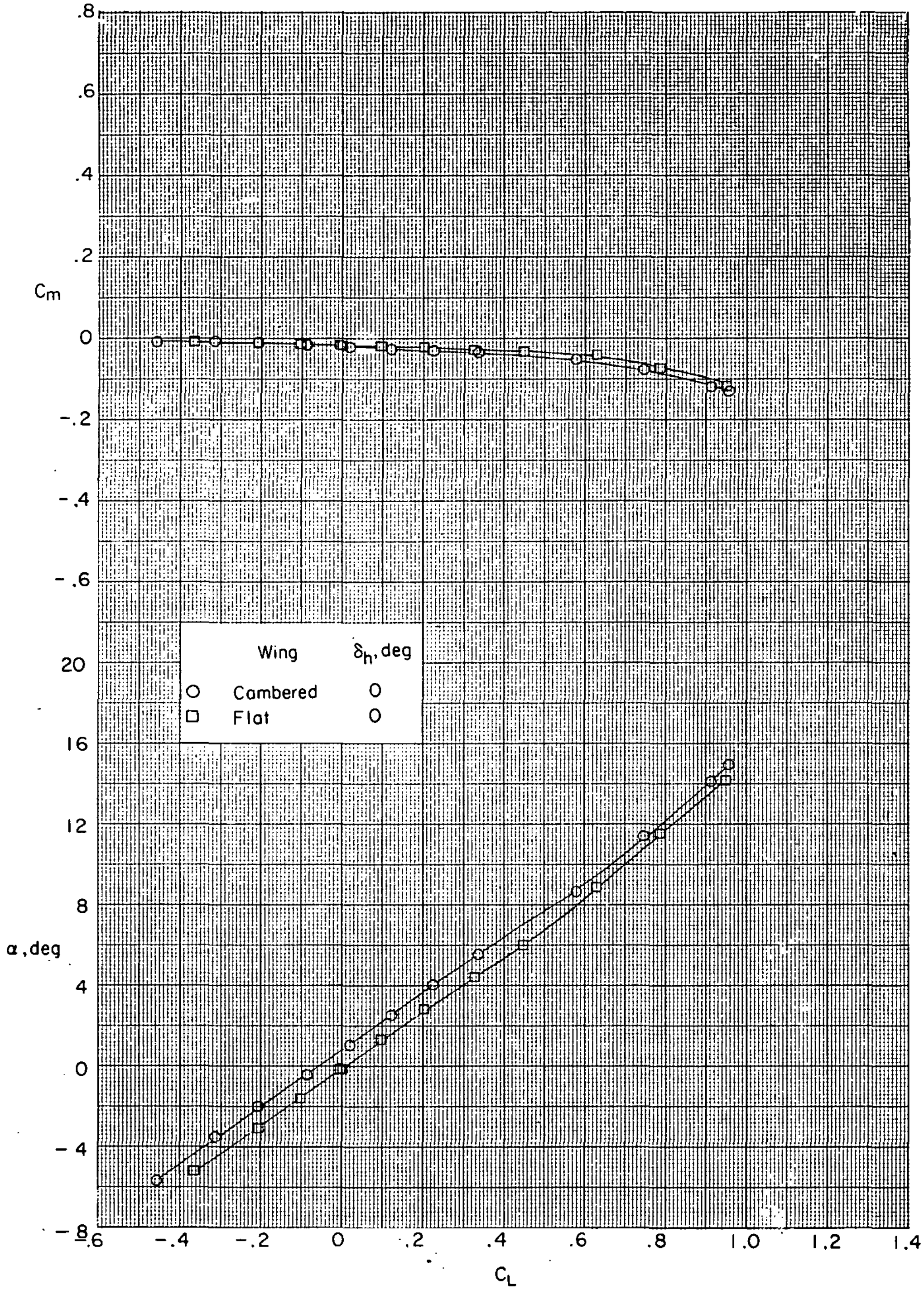

(e) M = 0.90.

Figure 9.- Continued.

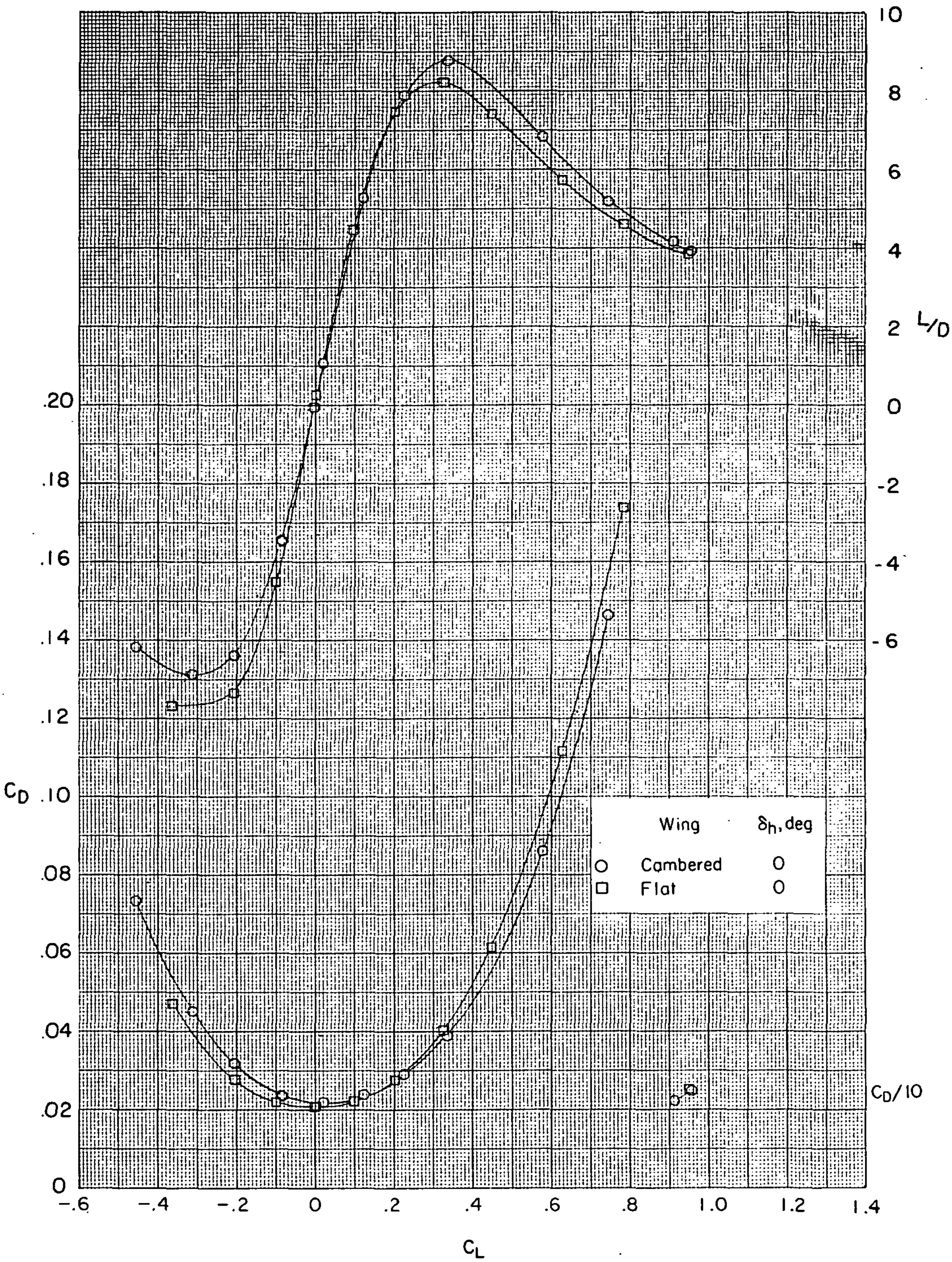

(e) Concluded.

Figure 9.- Continued.

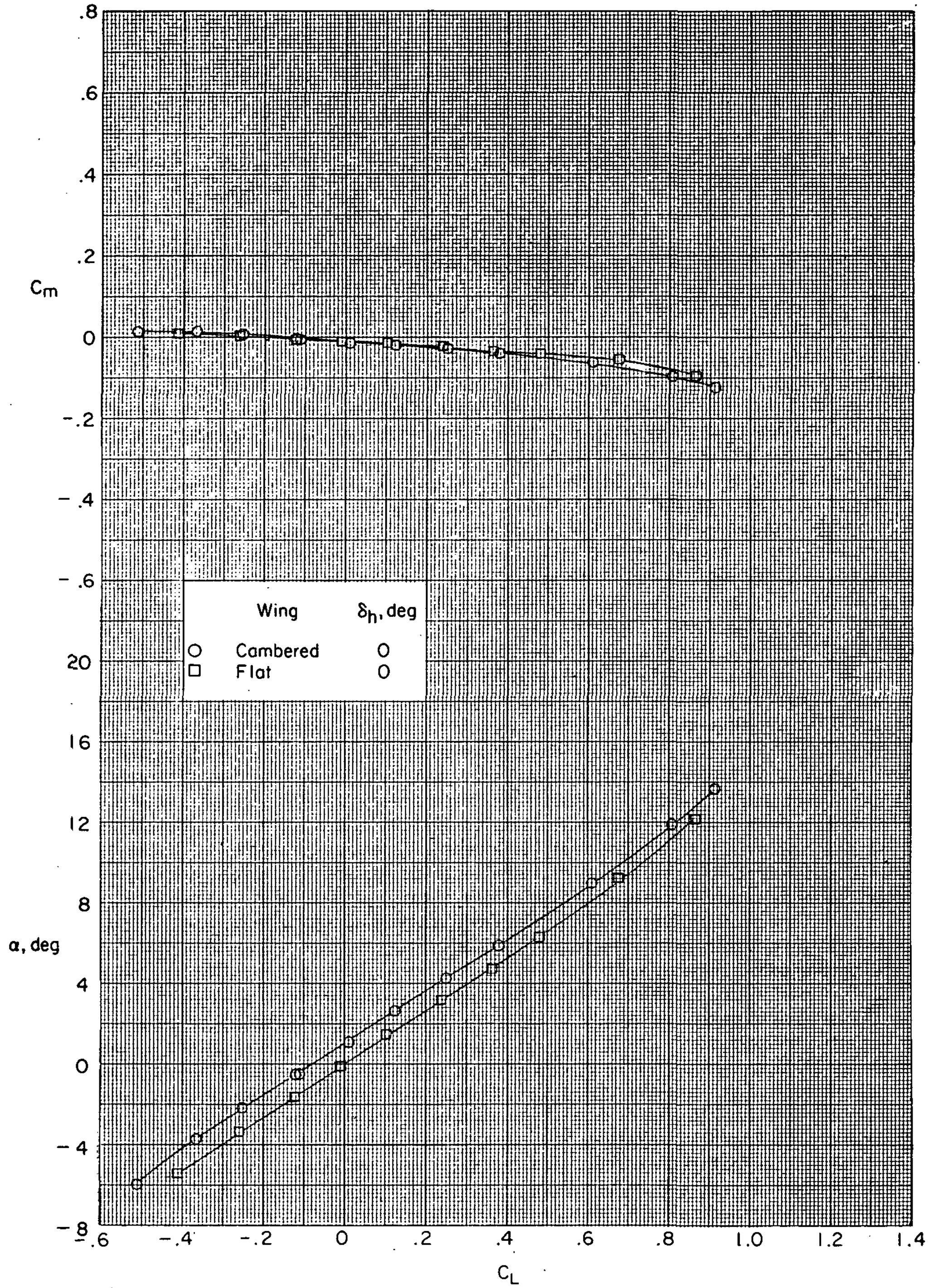

(f) M = 0.95.

Figure 9.- Continued.

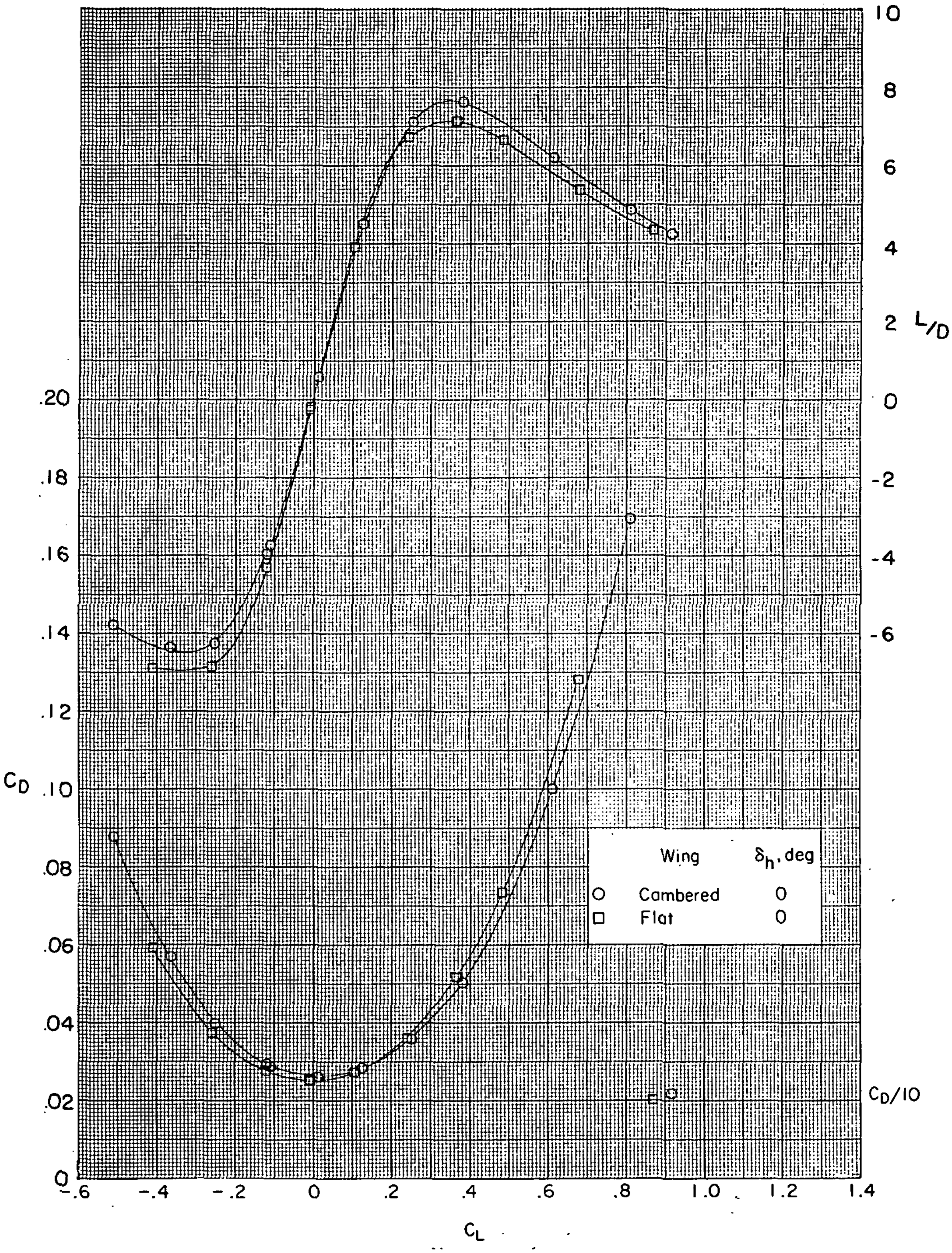

(f) Concluded.

Figure 9.- Continued.

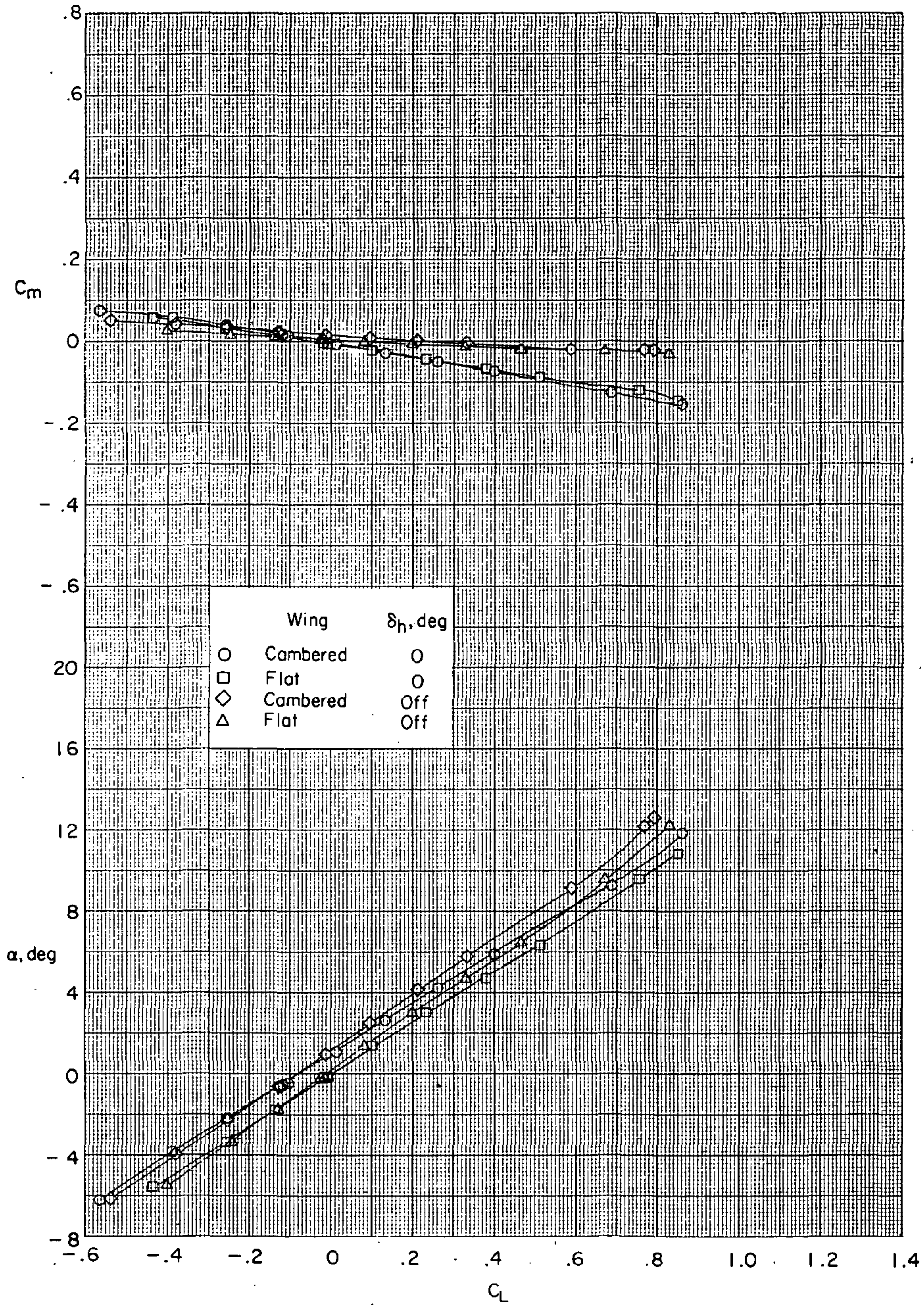

(g) M = 1.03.

Figure 9.- Continued.

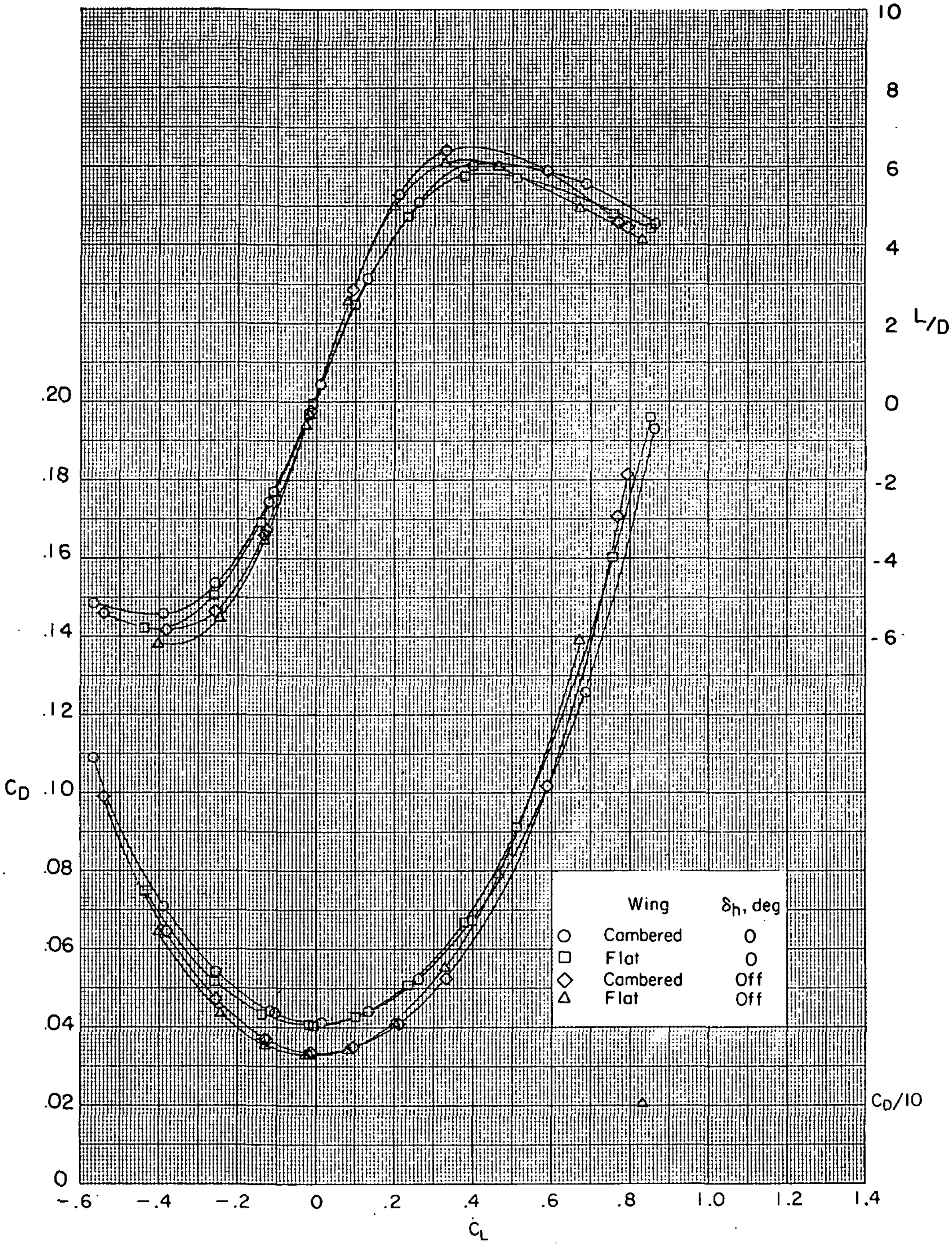

(g) Concluded.

Figure 9.- Continued.

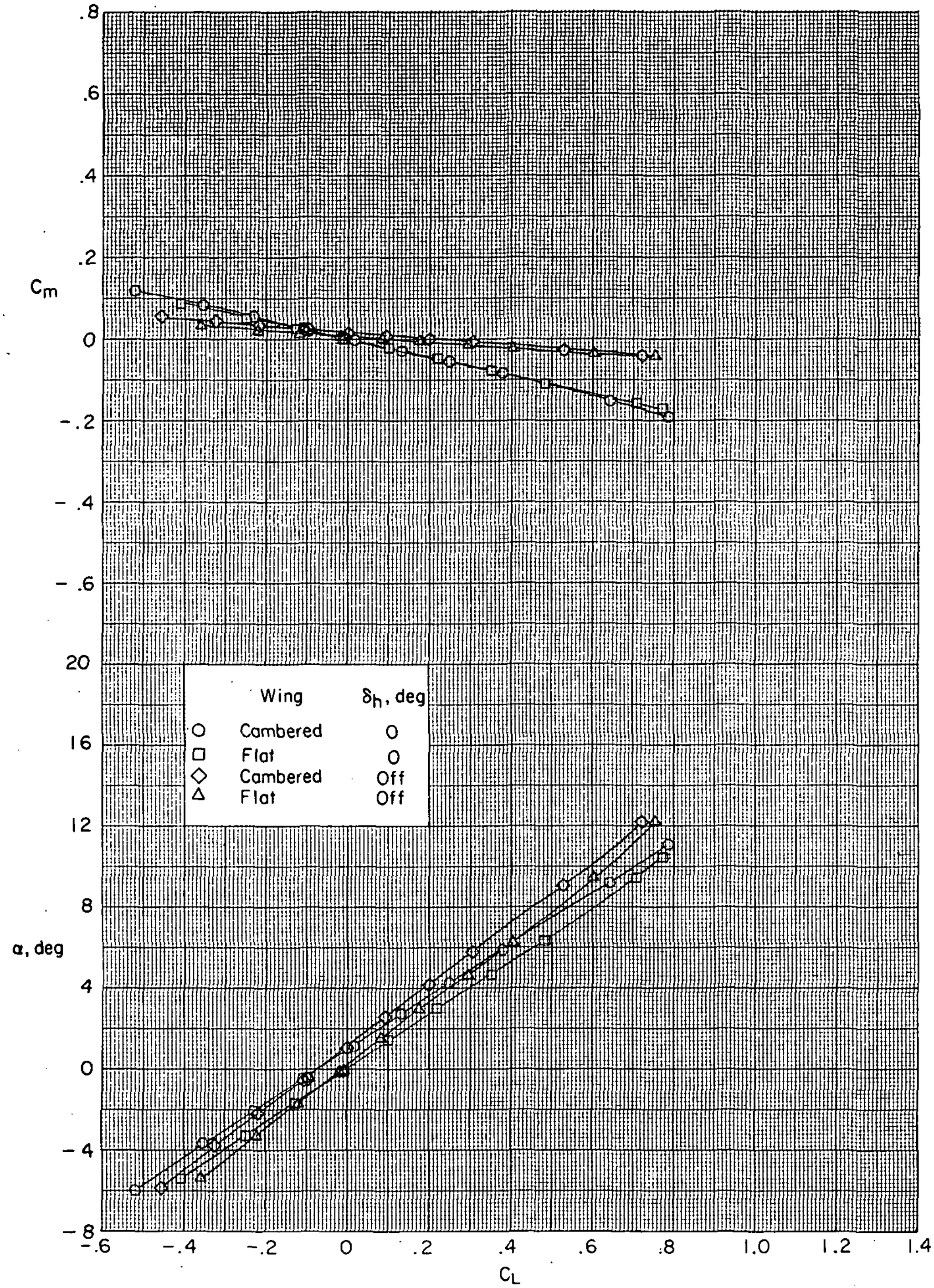

(h) M = 1.20.

Figure 9.- Continued.

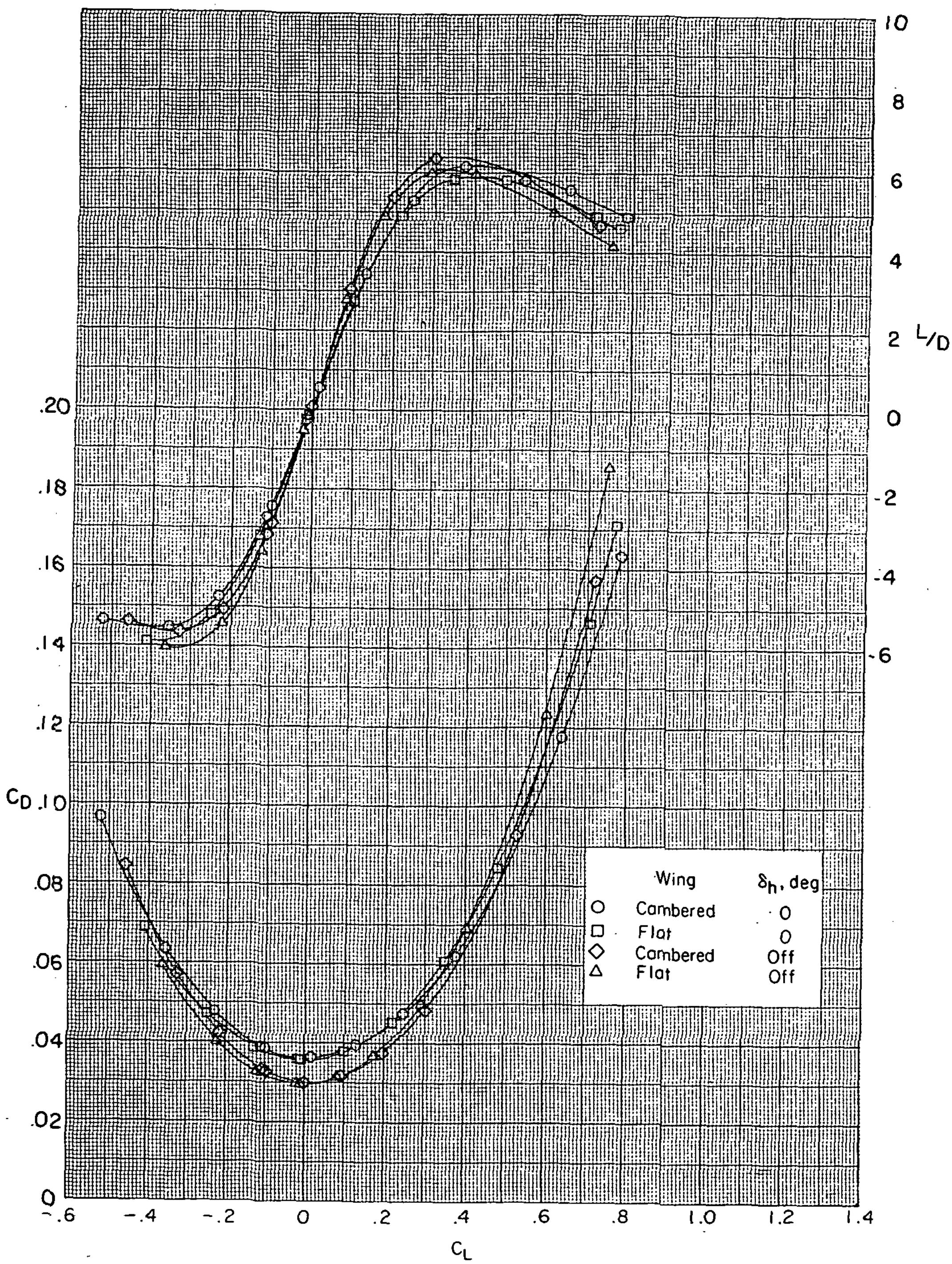

(h) Concluded.

Figure 9.- Continued.

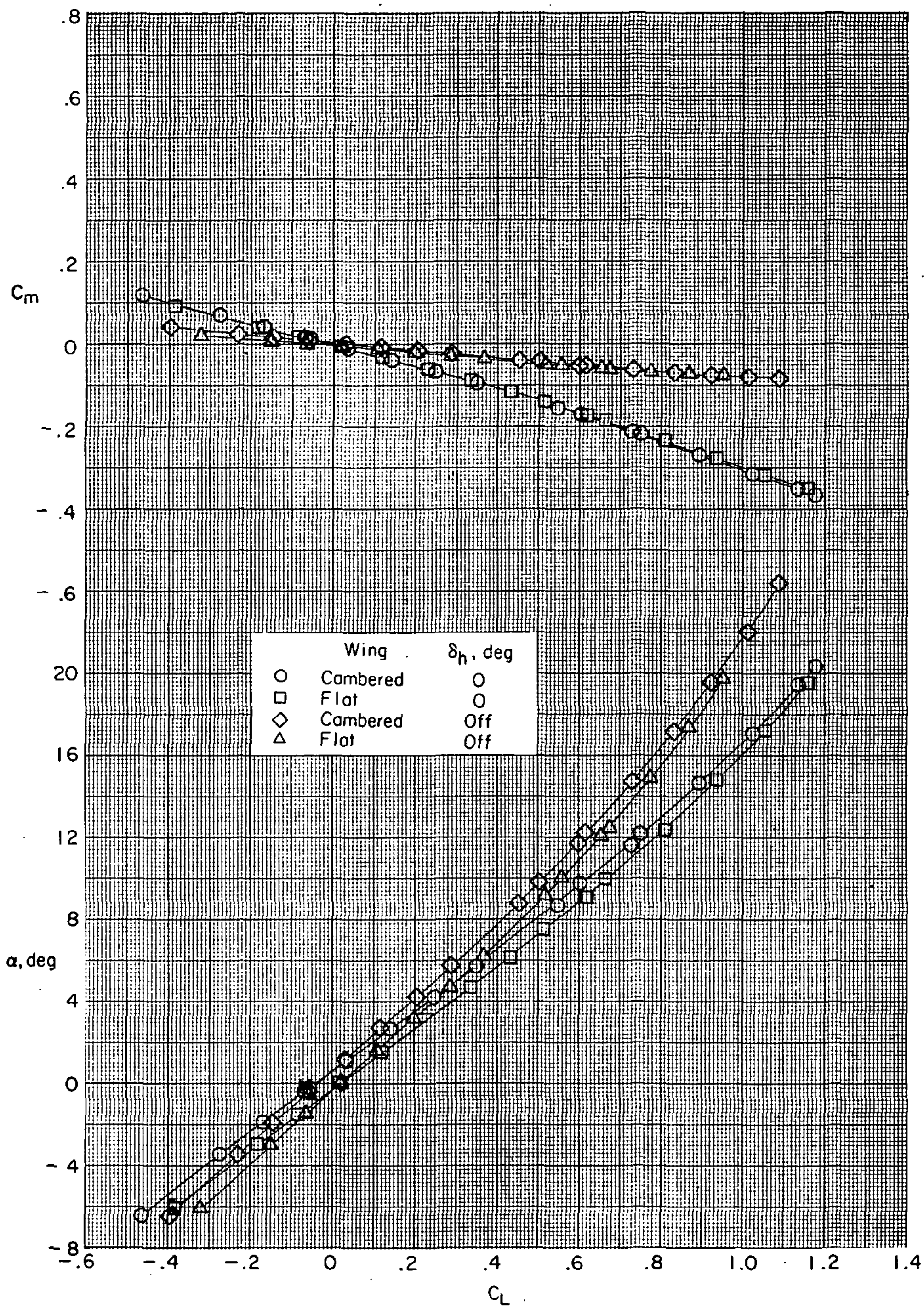

(i) M = 1.47.

Figure 9.- Continued.

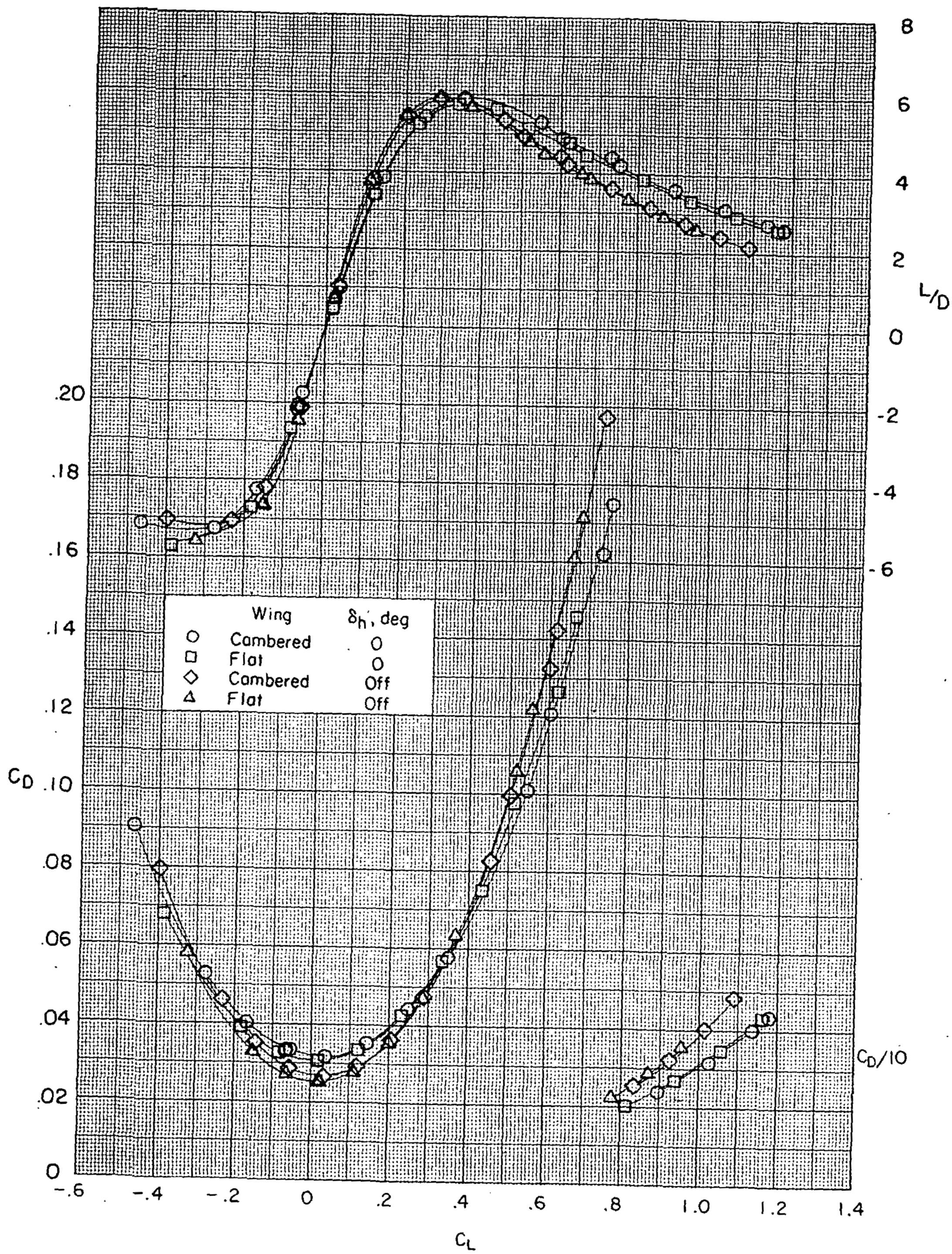

(i) Concluded.

Figure 9.- Continued.

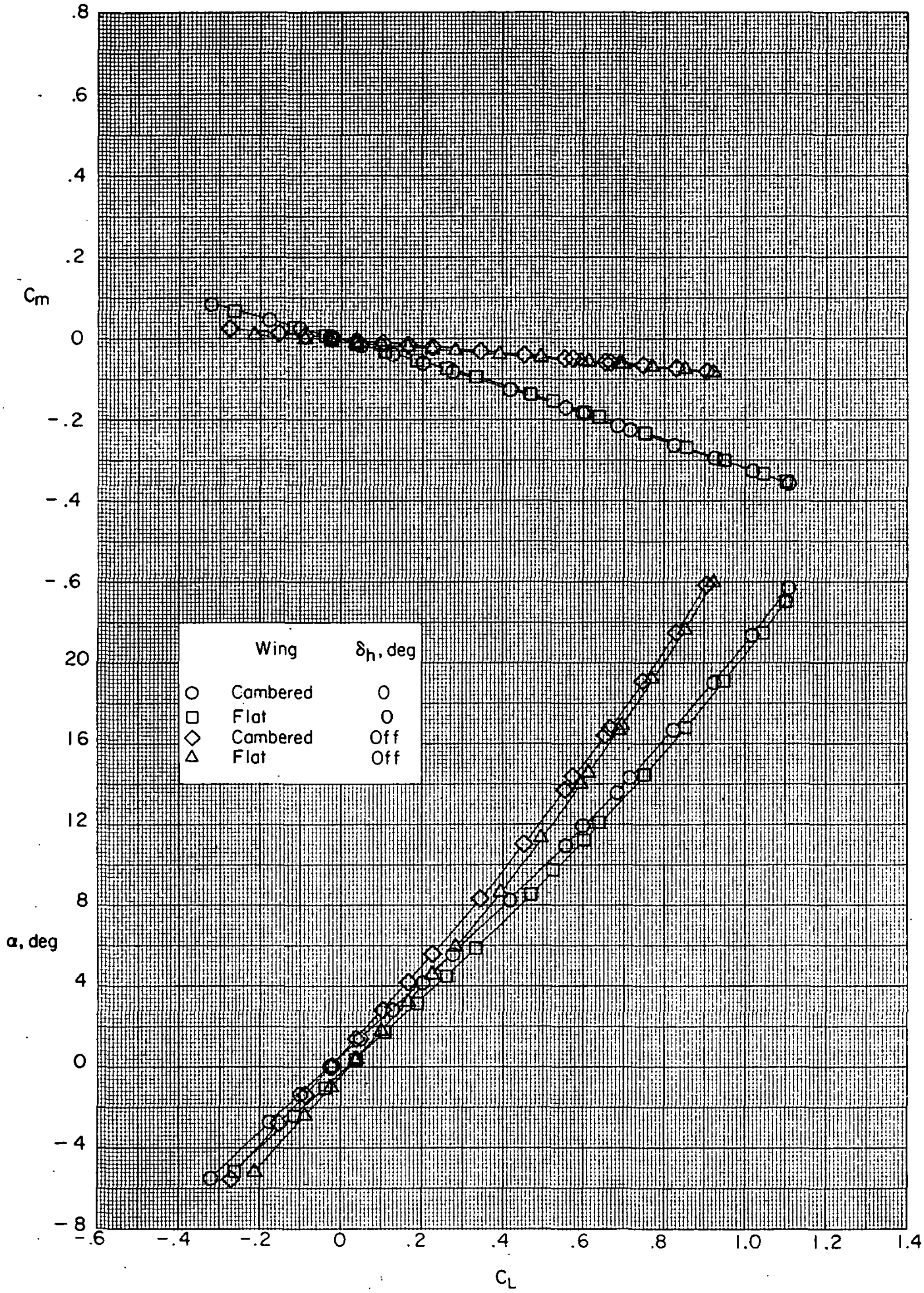

(j) M = 1.80.

Figure 9.- Continued.

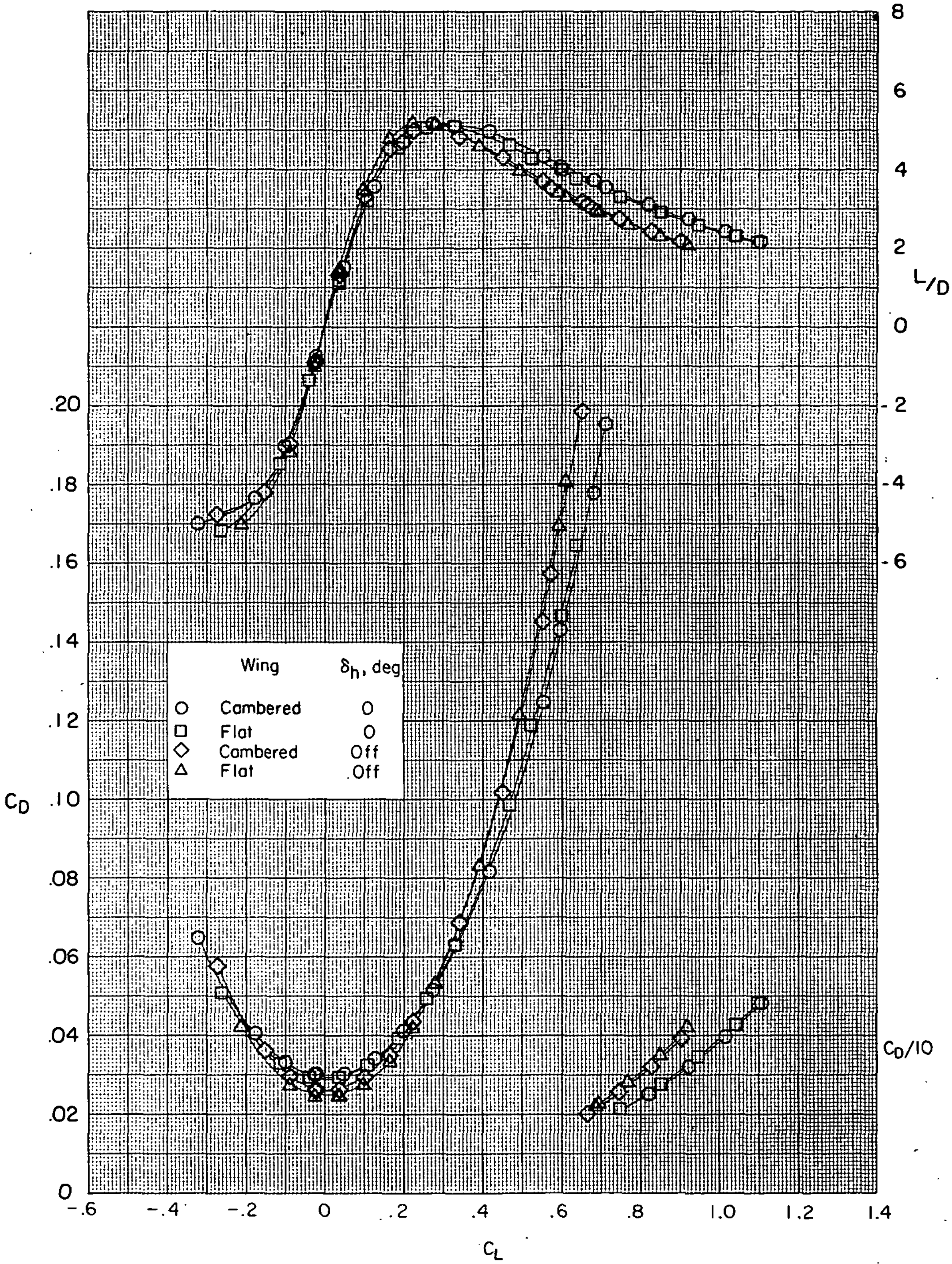

(j) Concluded.

Figure 9.- Continued.

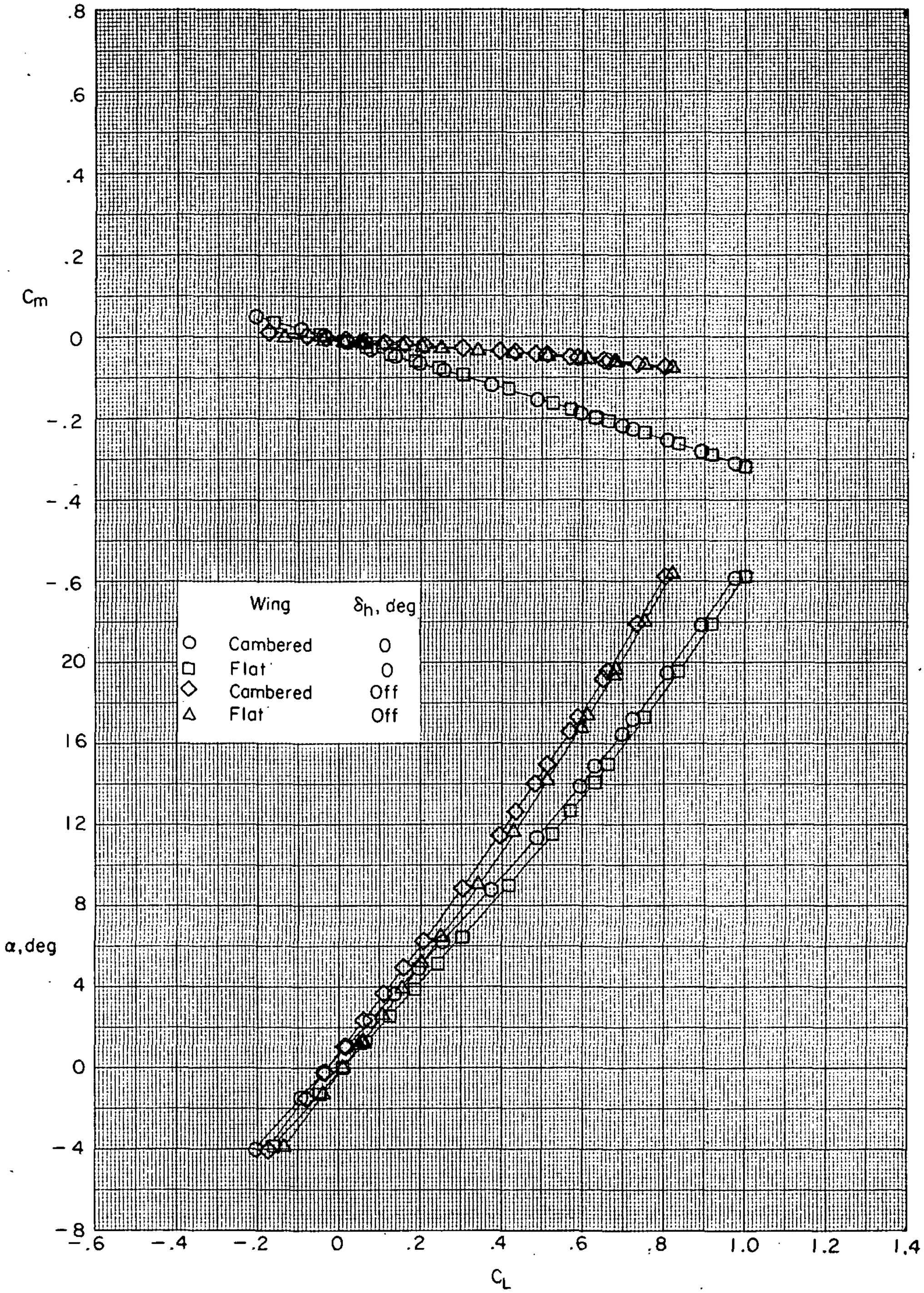

(k) M = 2.16.

Figure 9.- Continued.

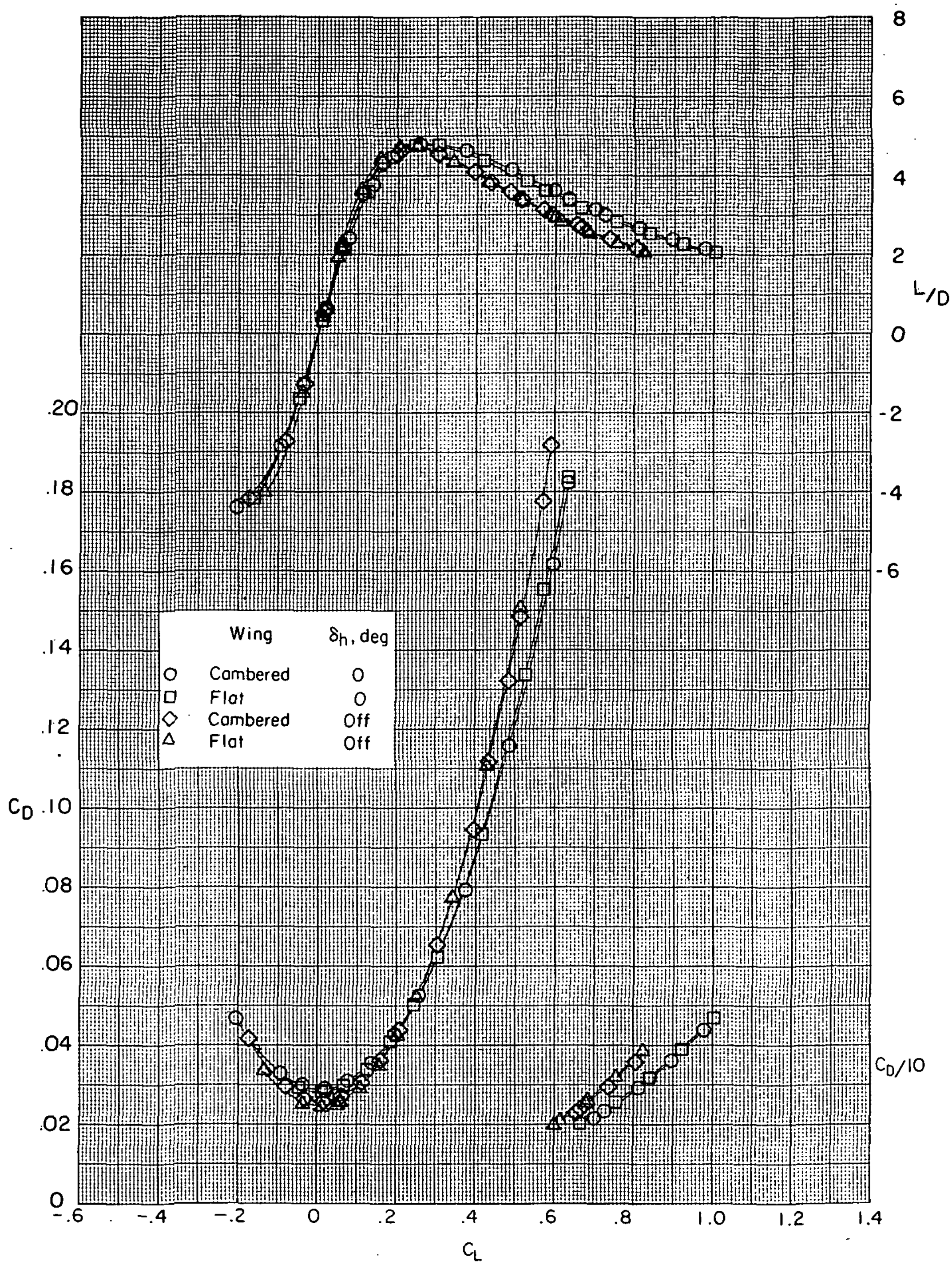

(k) Concluded.

Figure 9.- Concluded.

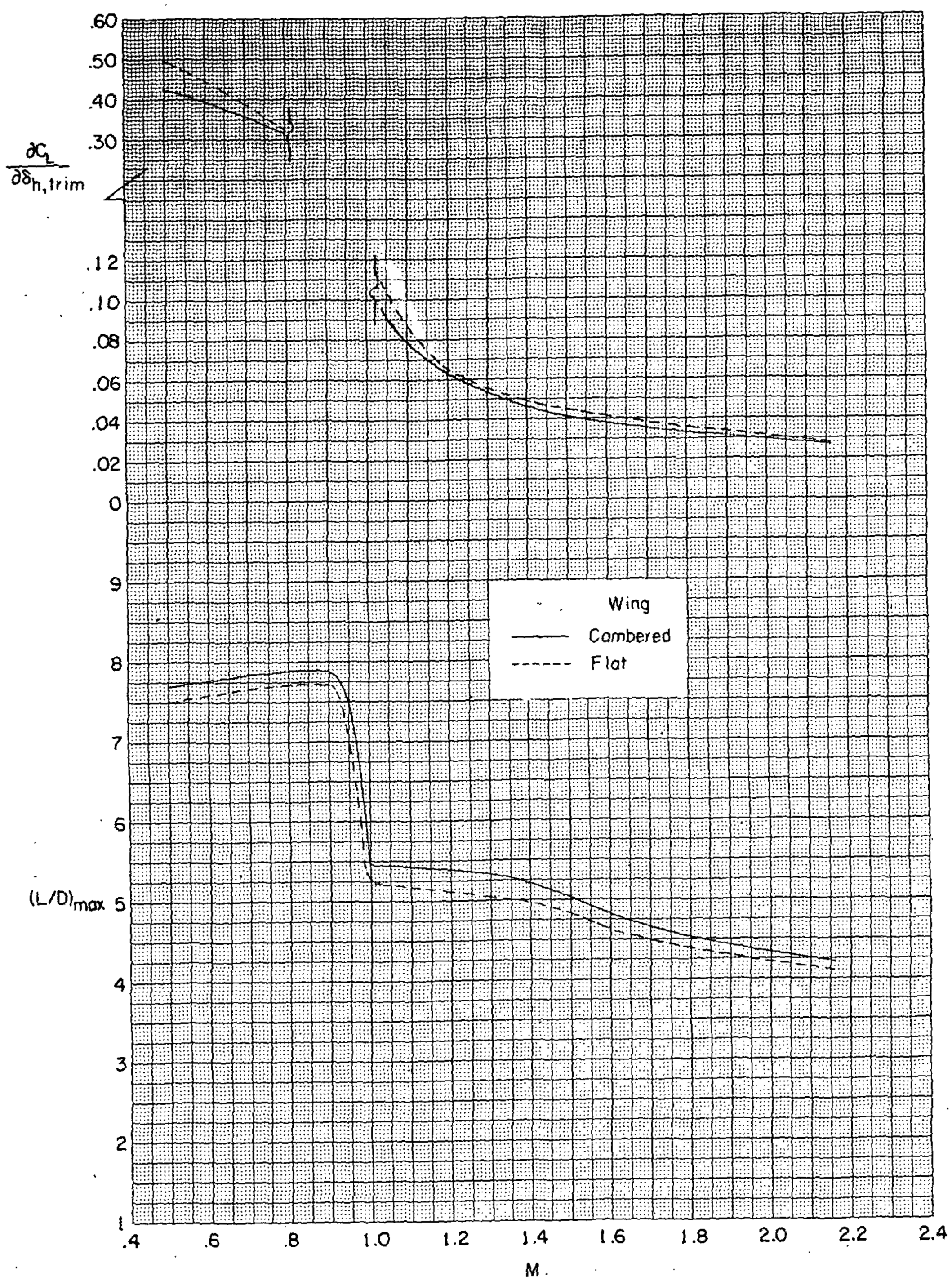

Figure 10.- Trimmed $(L/D)_{max}$ and tail control effectiveness plotted against Mach number.

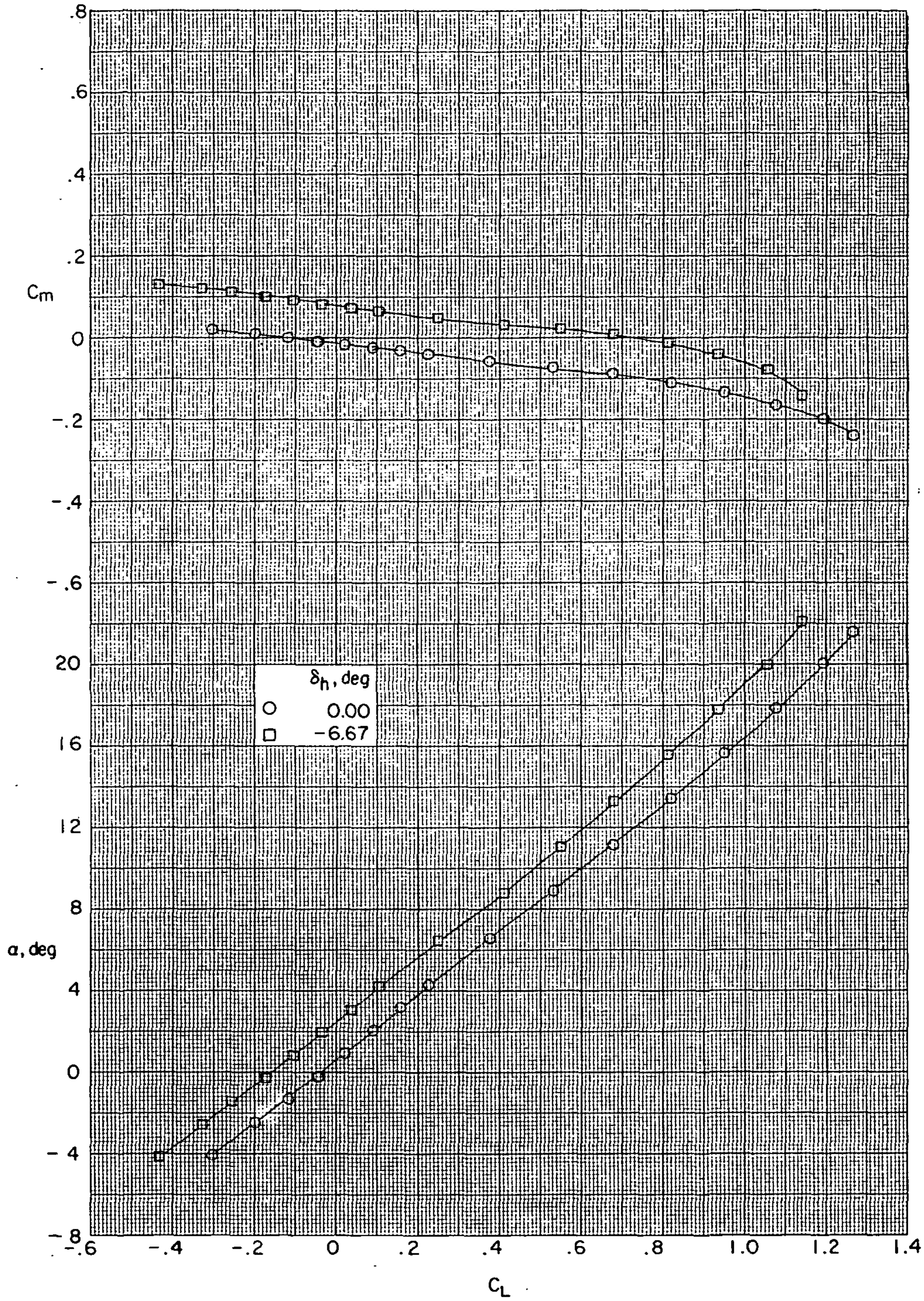

(a) M = 0.50.

Figure 11.- Longitudinal aerodynamic characteristics with cambered wing moved rearward.

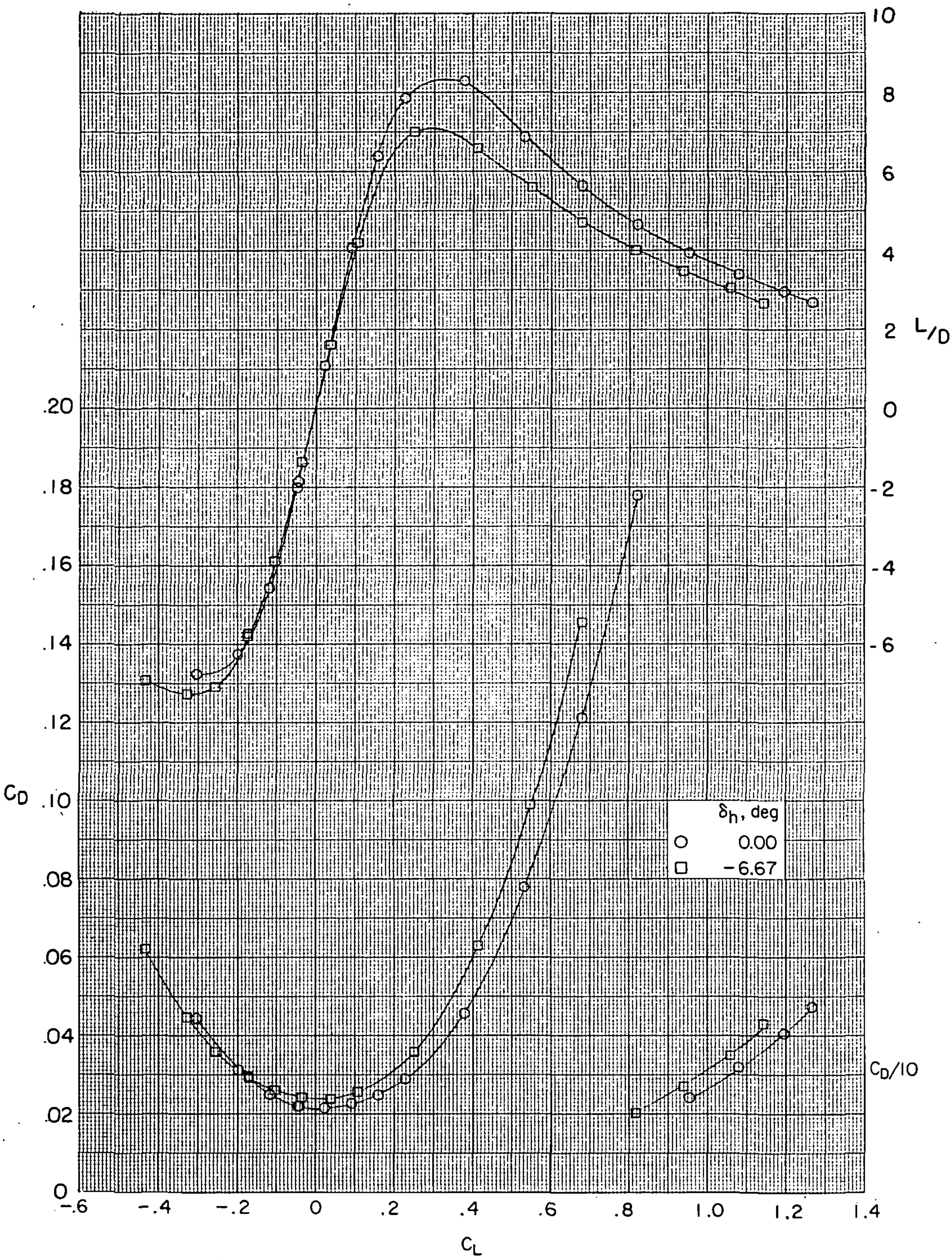

(a) Concluded.

Figure 11.- Continued.

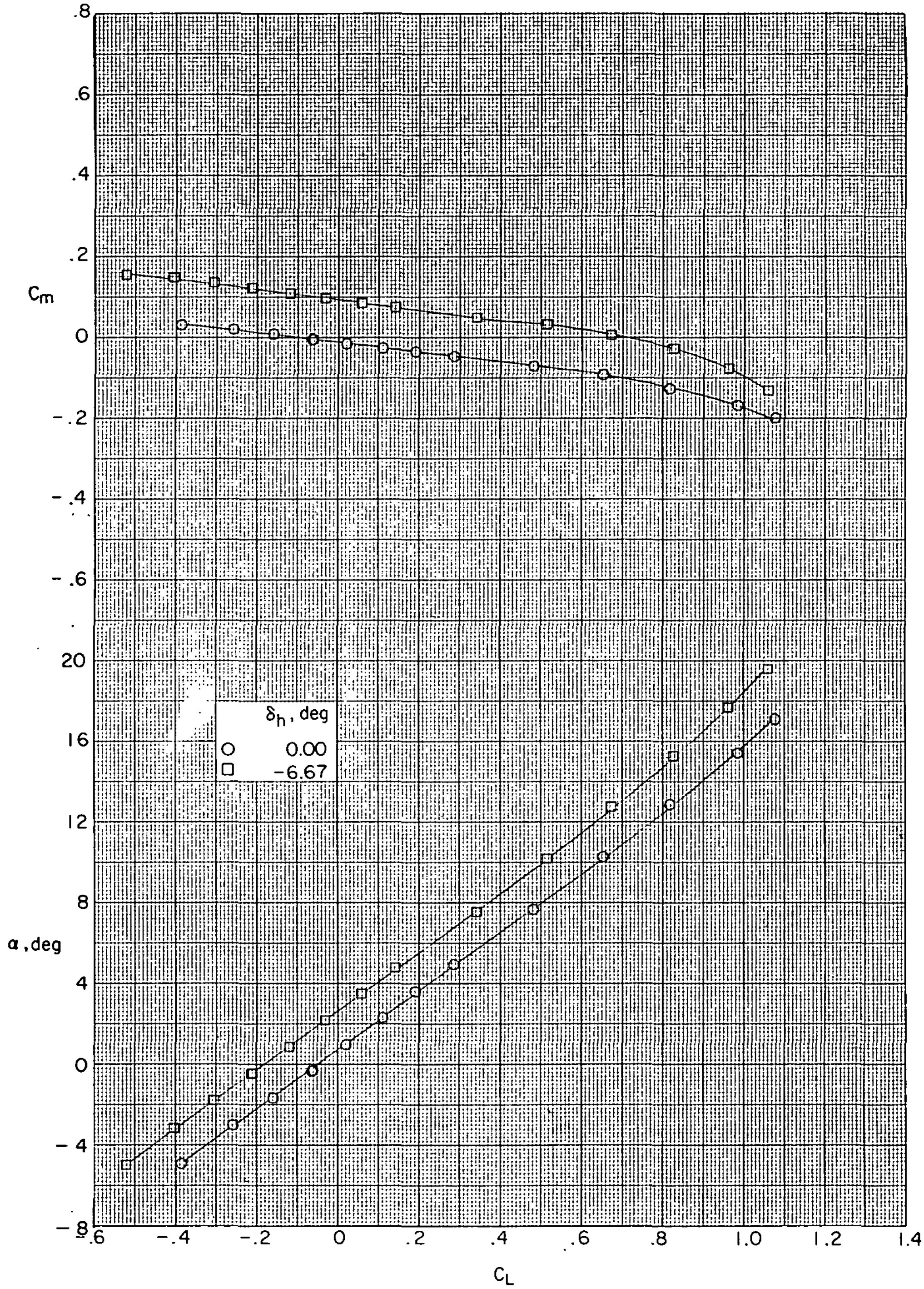

(b) M = 0.80.

Figure 11.- Continued.

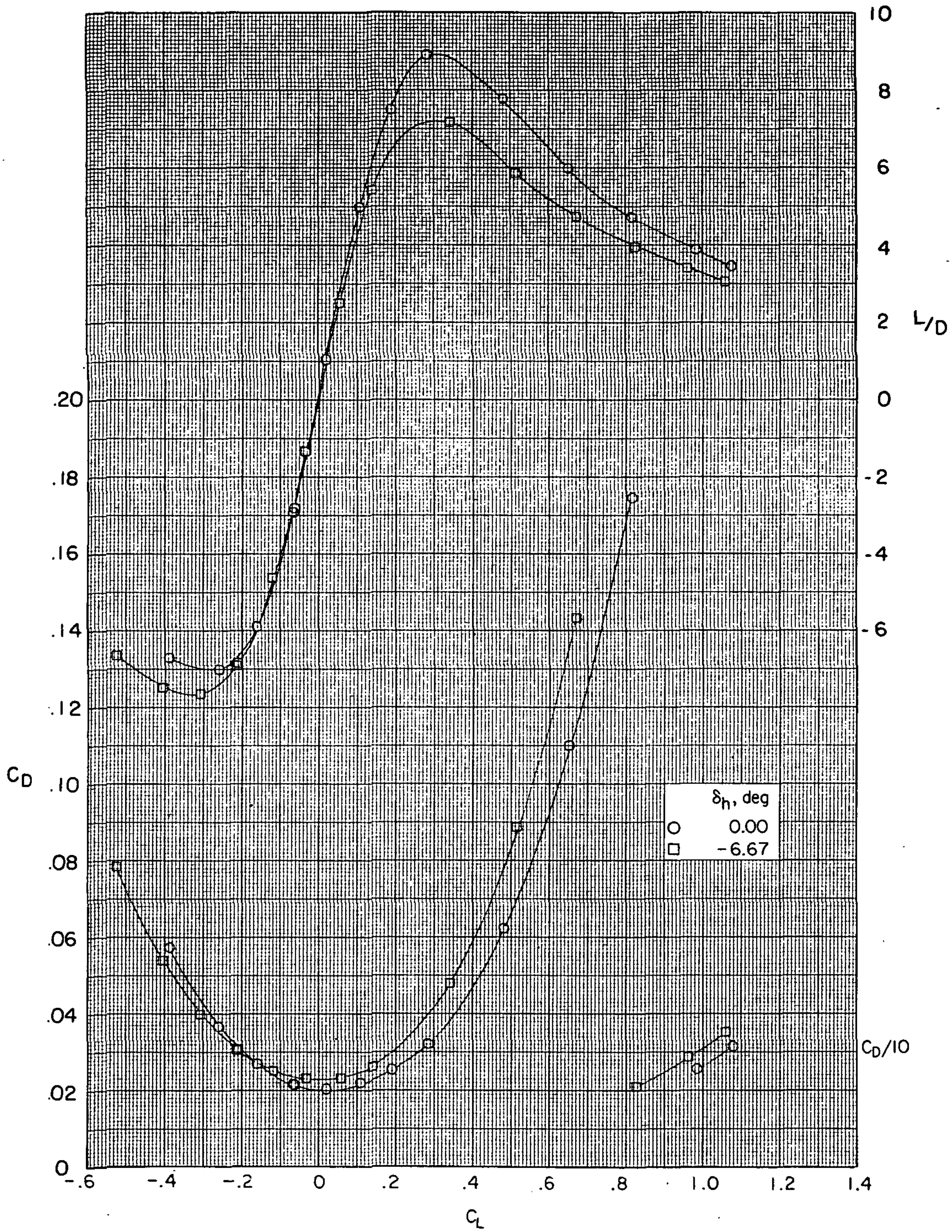

(b) Concluded.

Figure 11.- Continued.

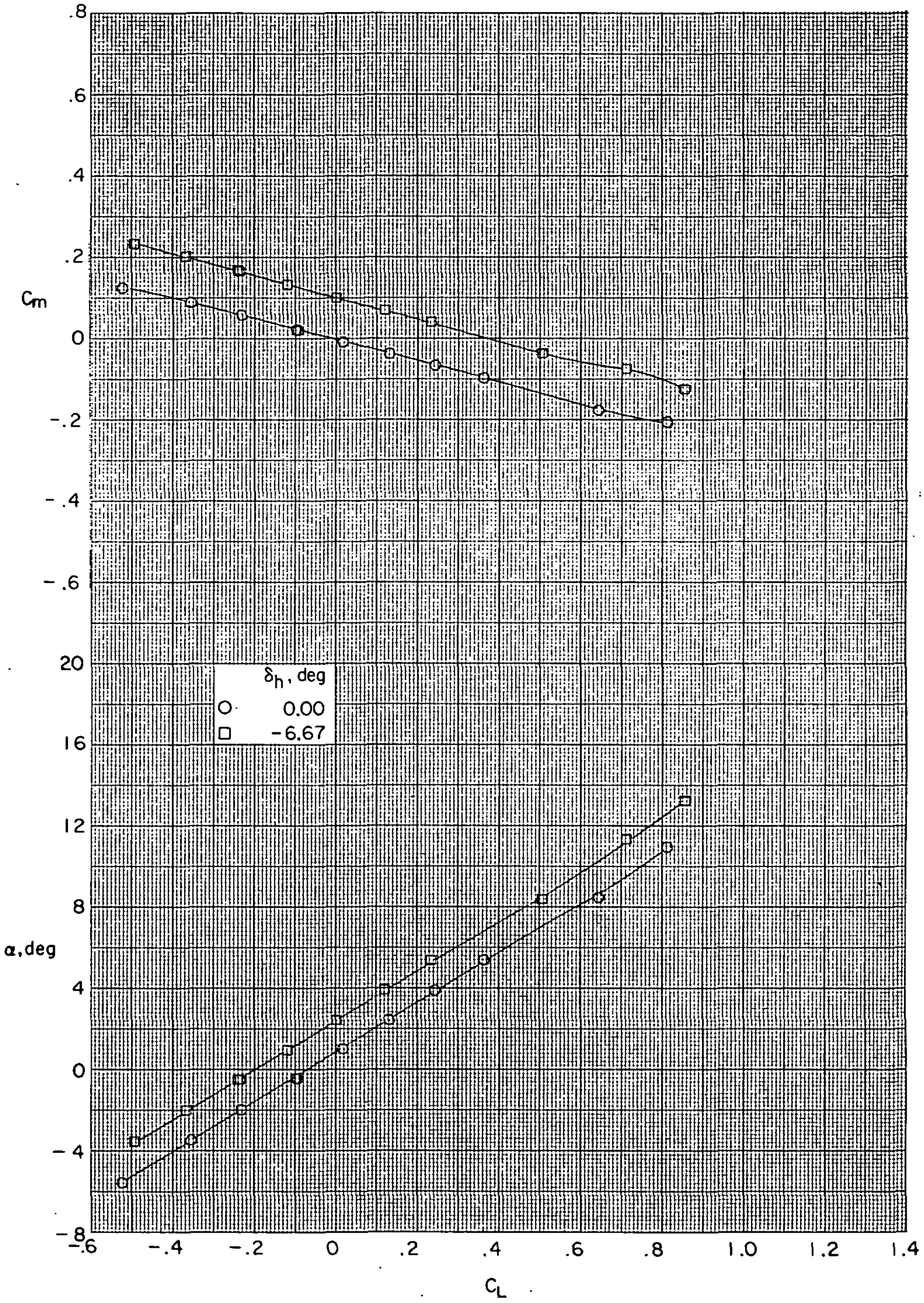

(c) M = 1.03.

Figure 11.- Continued.

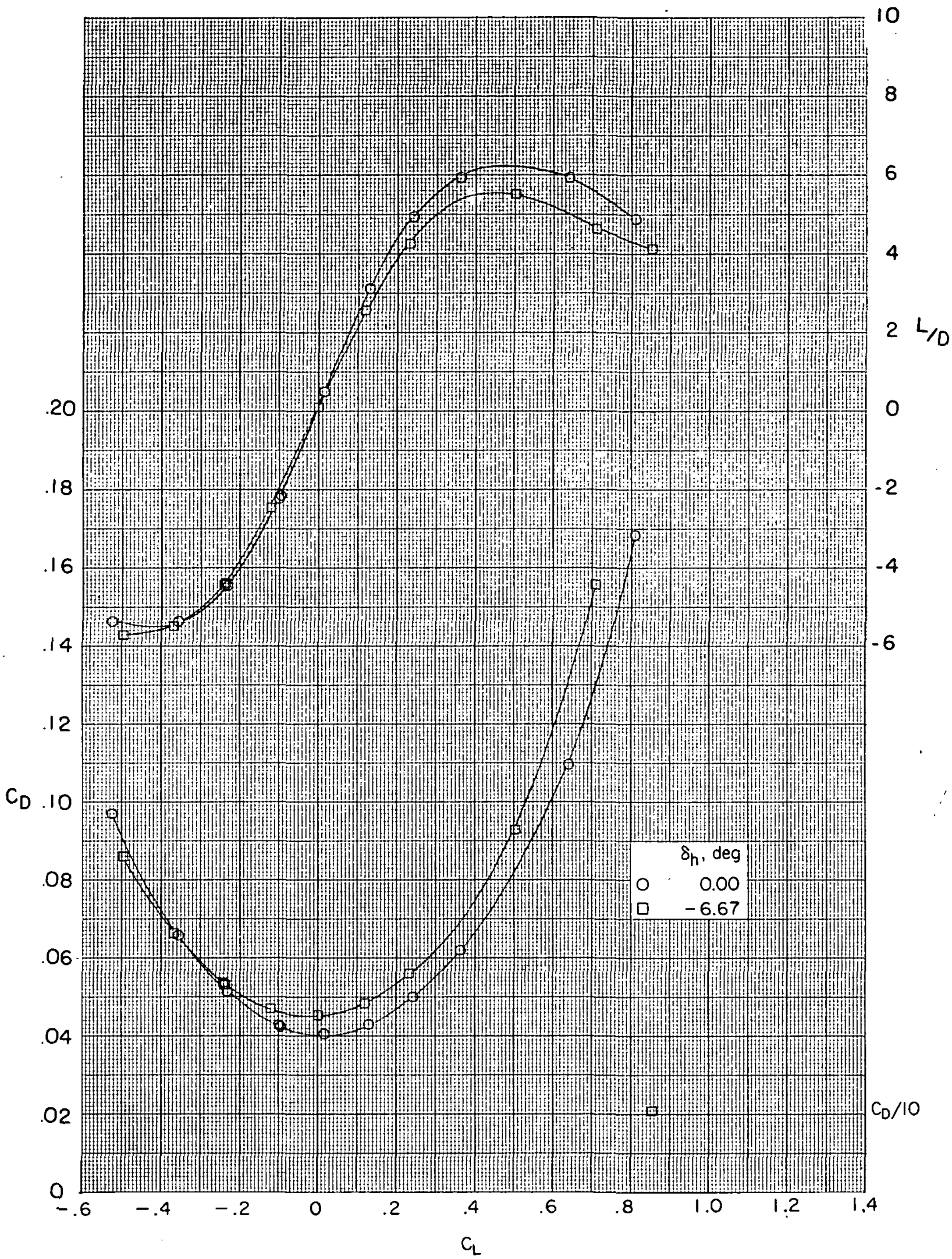

(c) Concluded.

Figure 11.- Continued.

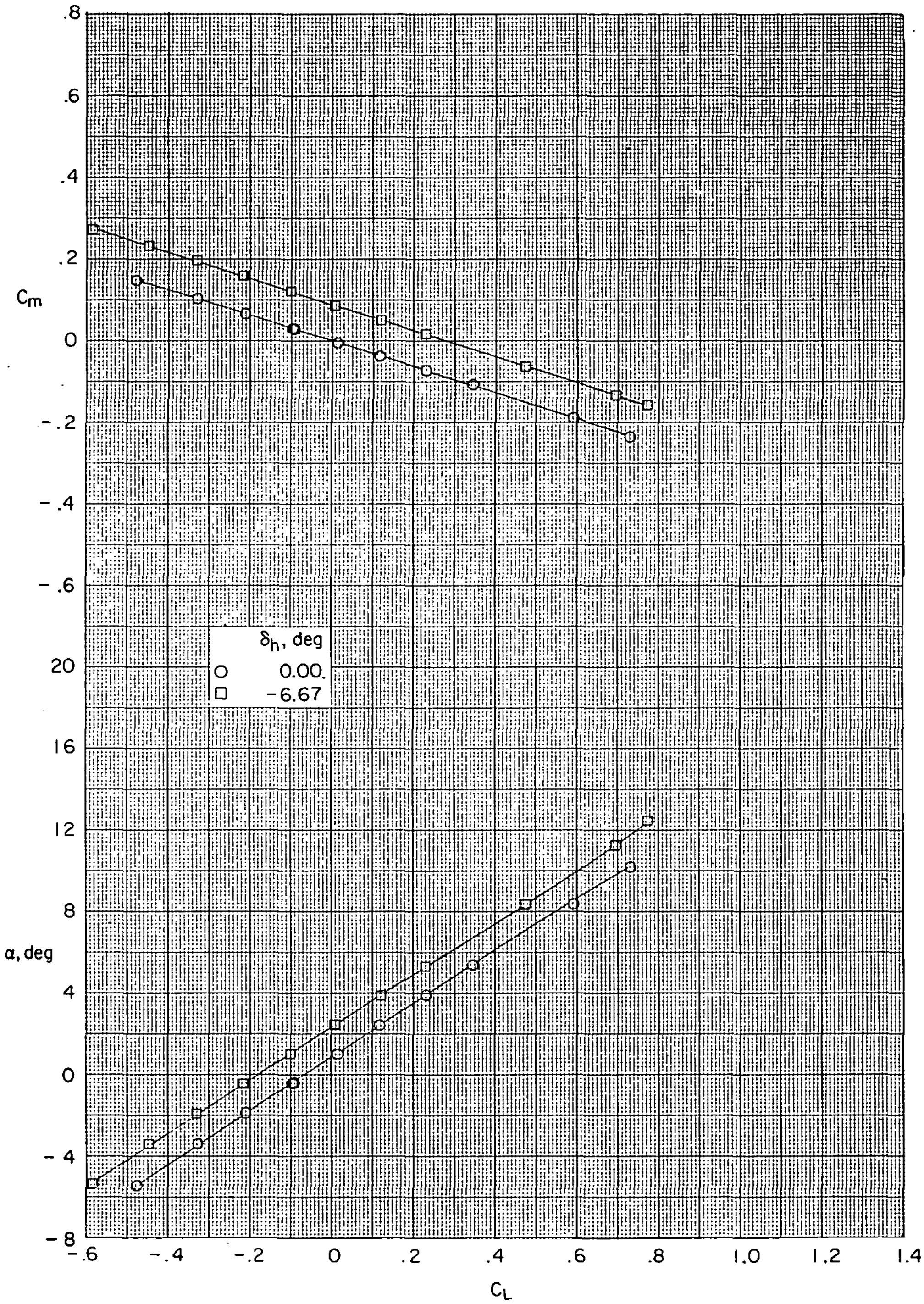

(d) M = 1.20.

Figure 11.- Continued.

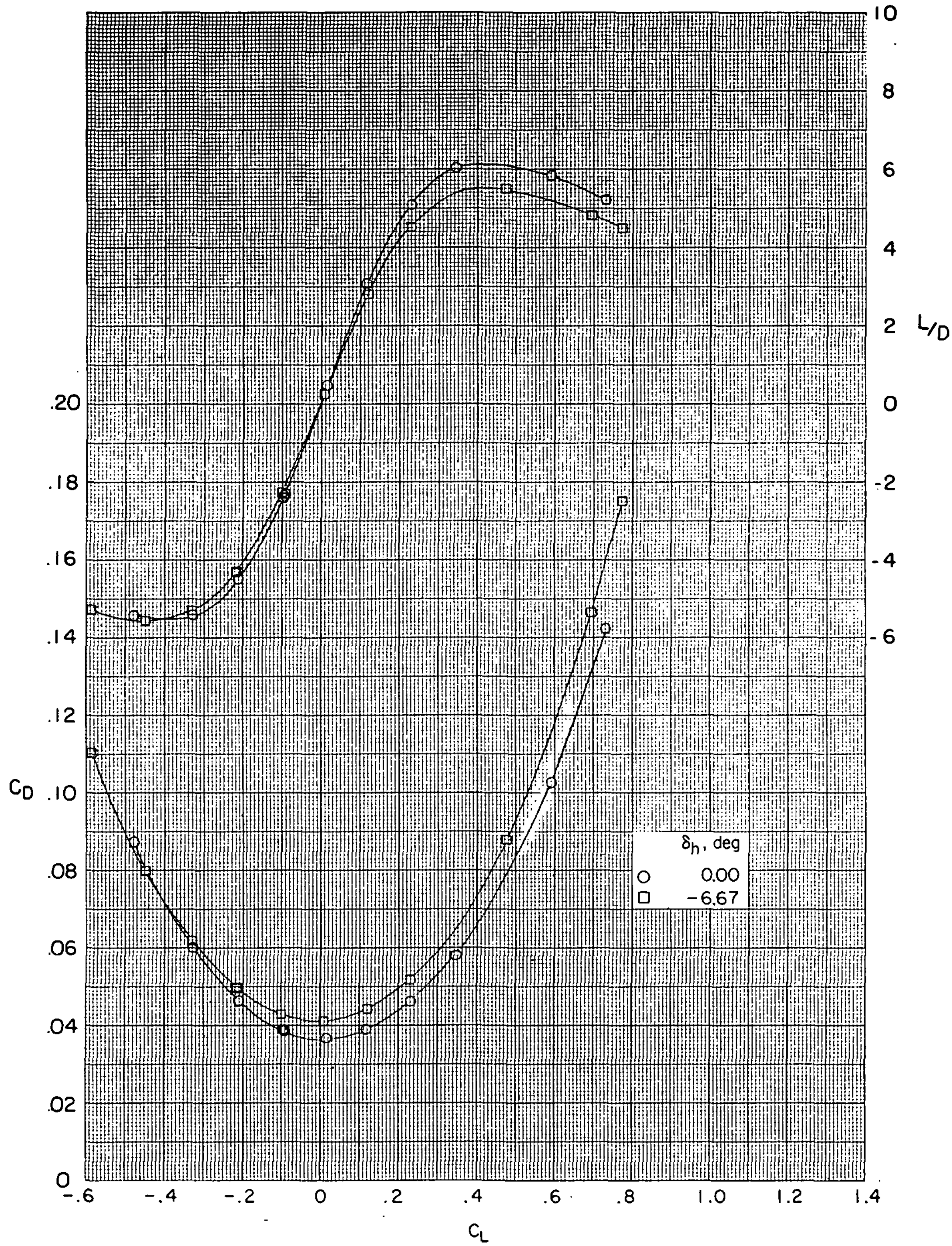

(d) Concluded.

Figure 11.- Continued.

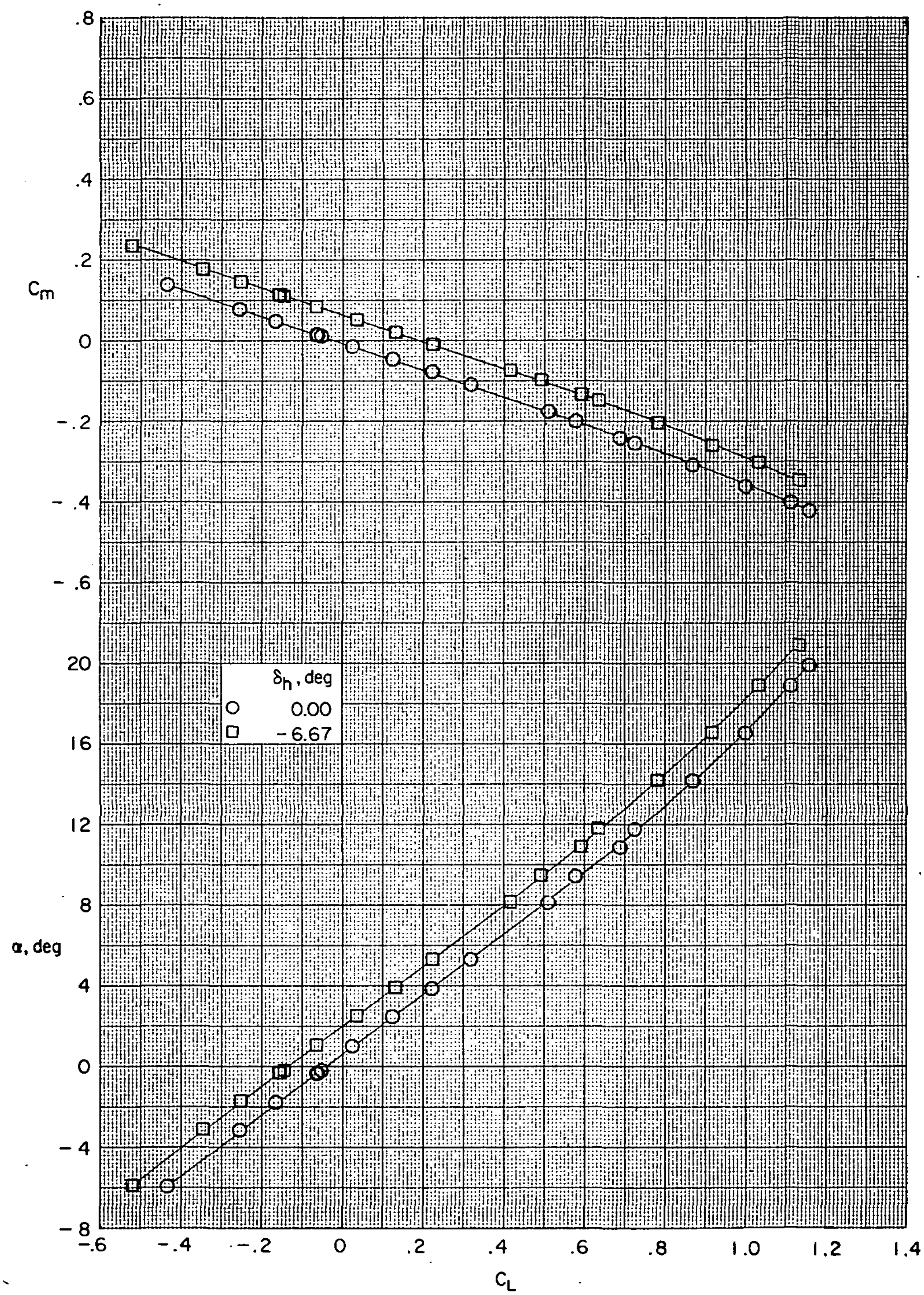

(e) M = 1.47.

Figure 11.- Continued.

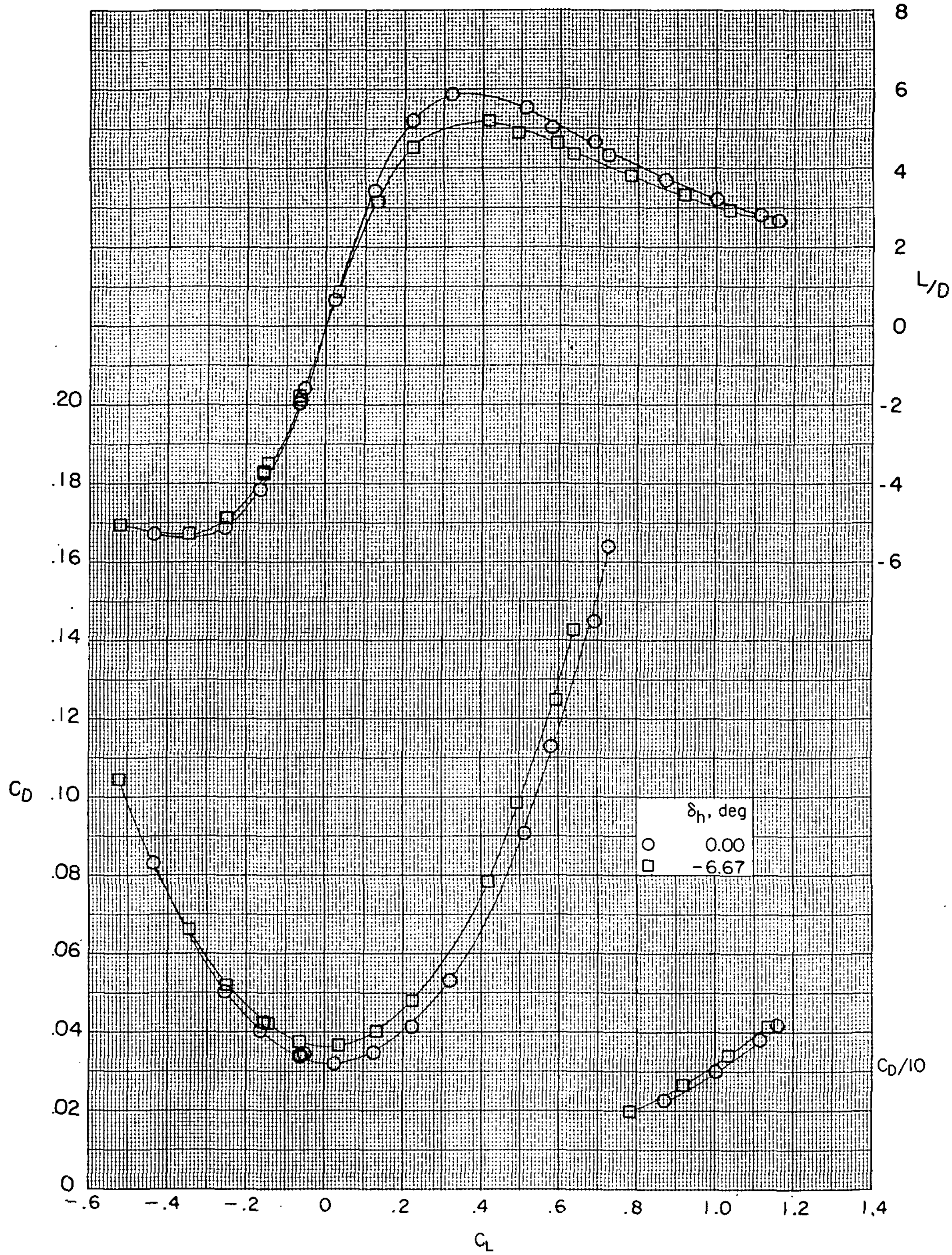

(e) Concluded.

Figure 11.- Continued.

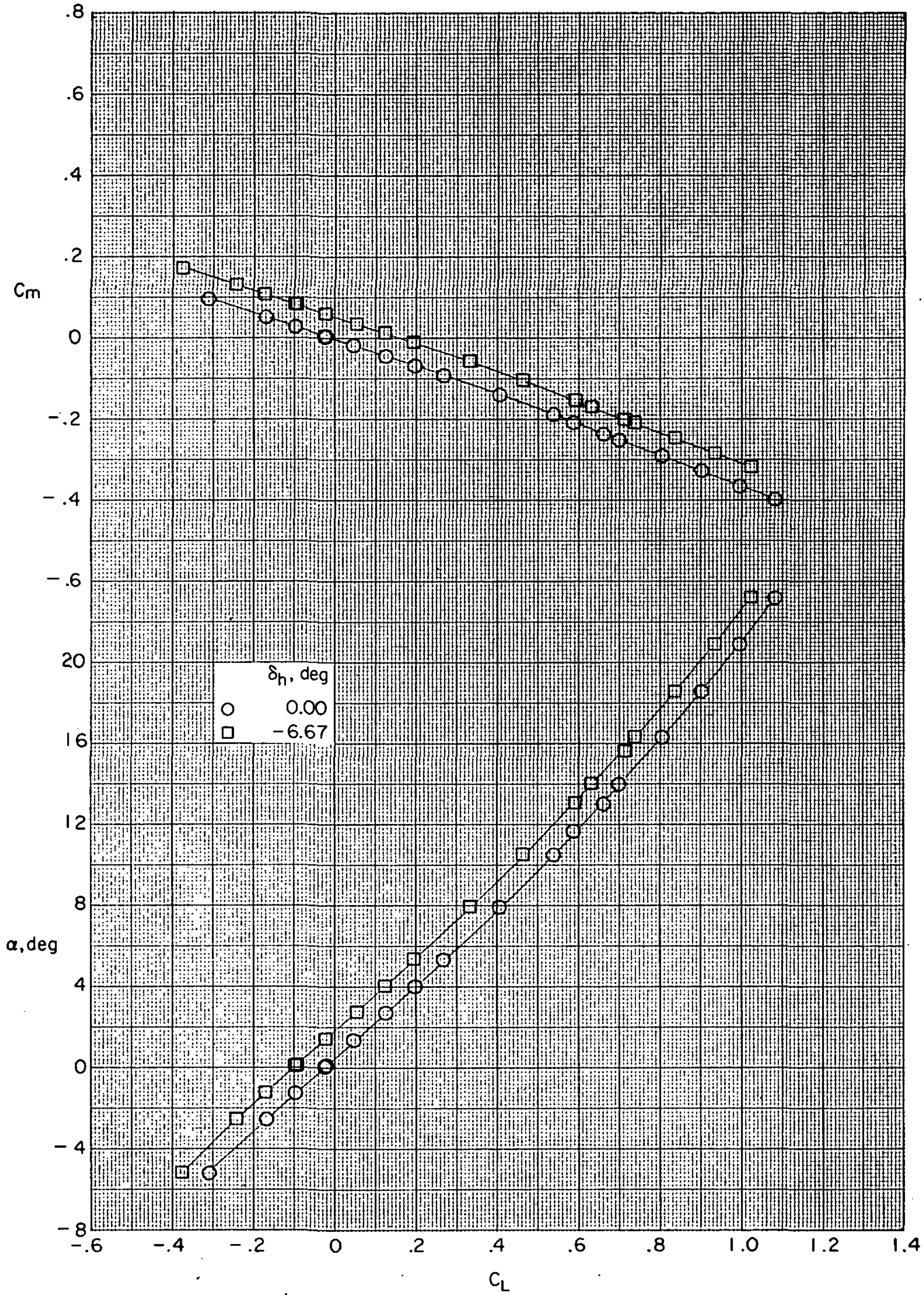

(f) M = 1.80.

Figure 11.- Continued.

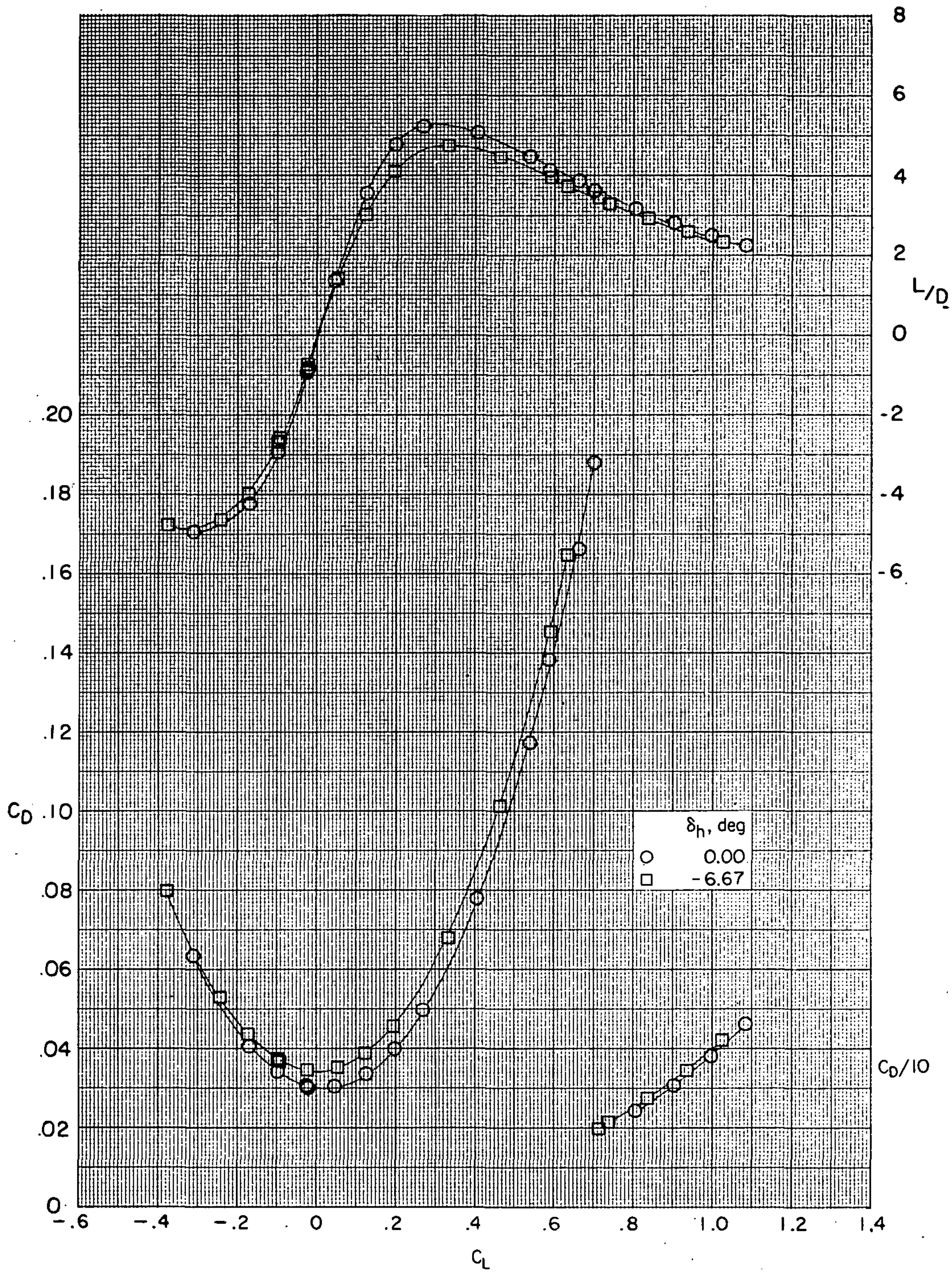

(f) Concluded.

Figure 11.- Continued.

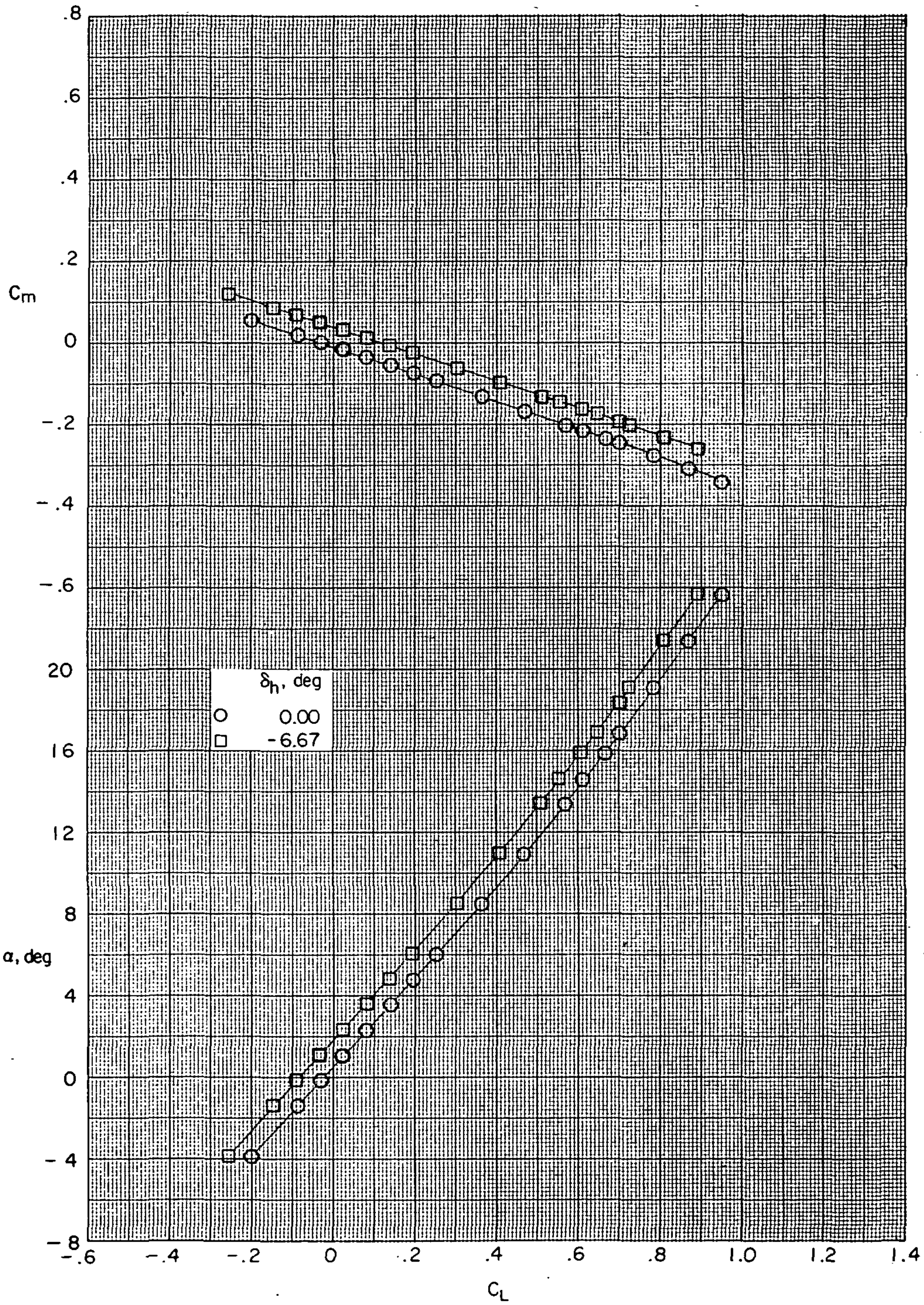

(g) M = 2.16.

Figure 11.- Continued.

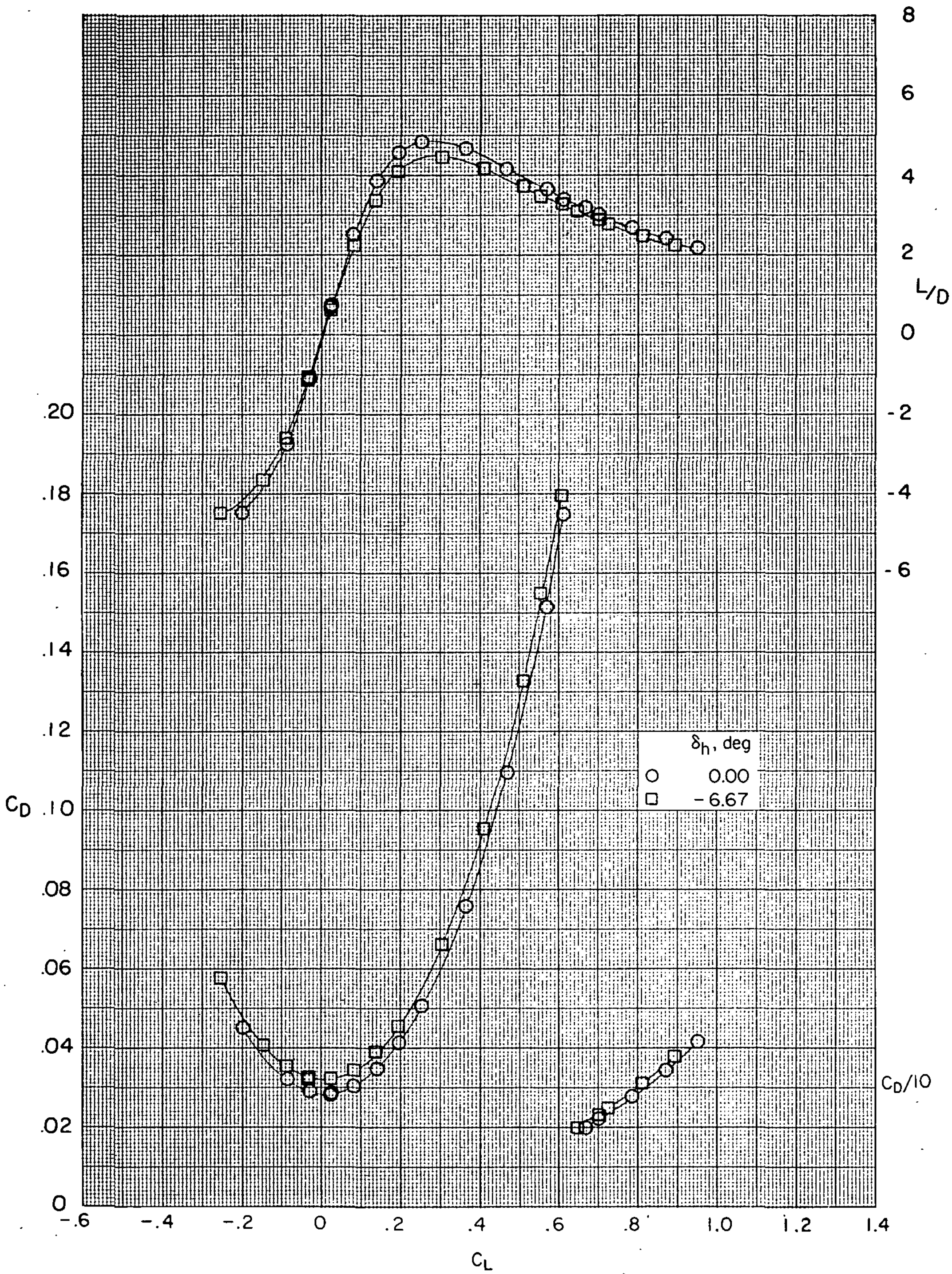

(g) Concluded.

Figure 11.- Concluded.

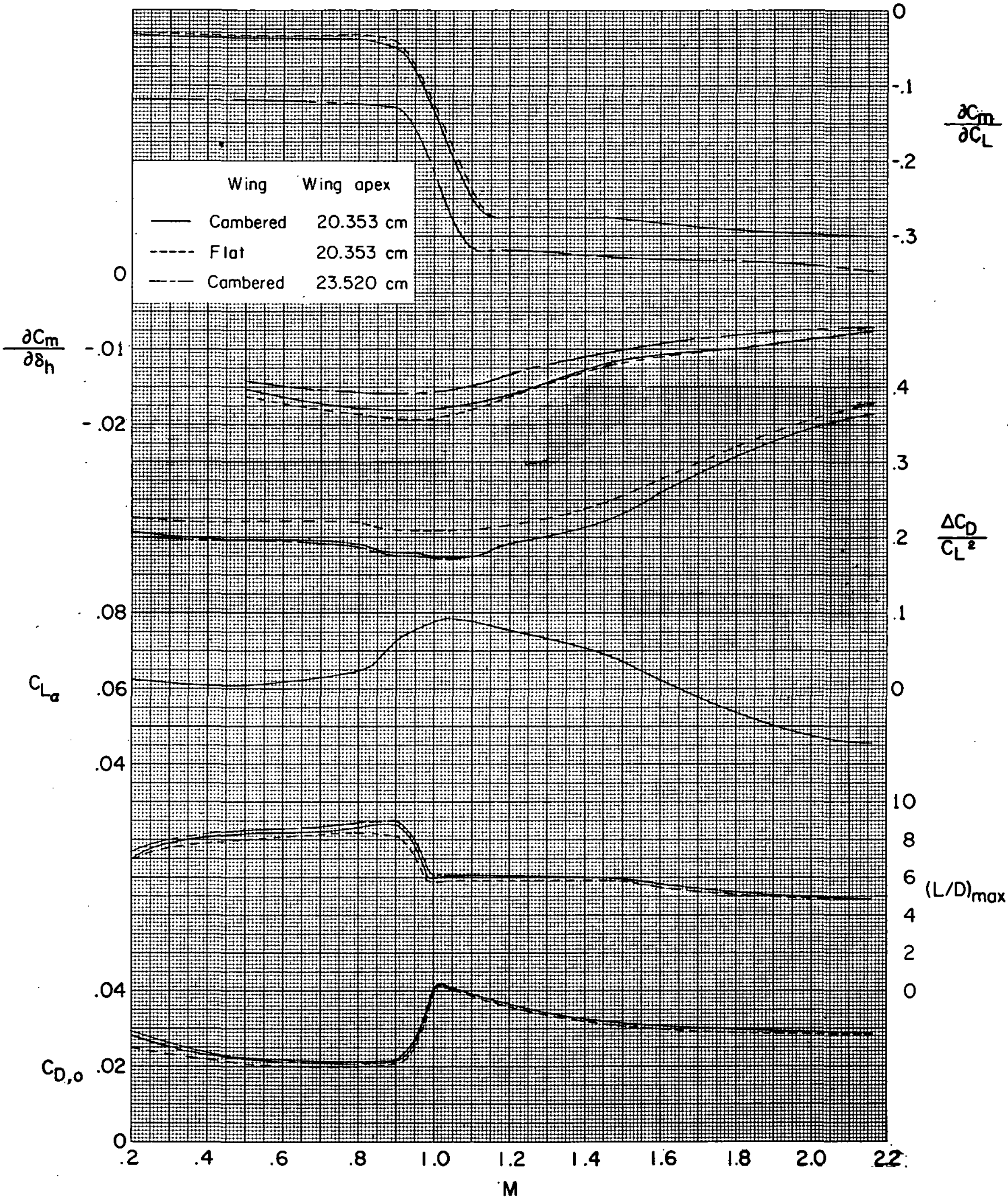

Figure 12.- Summary of pertinent longitudinal data.

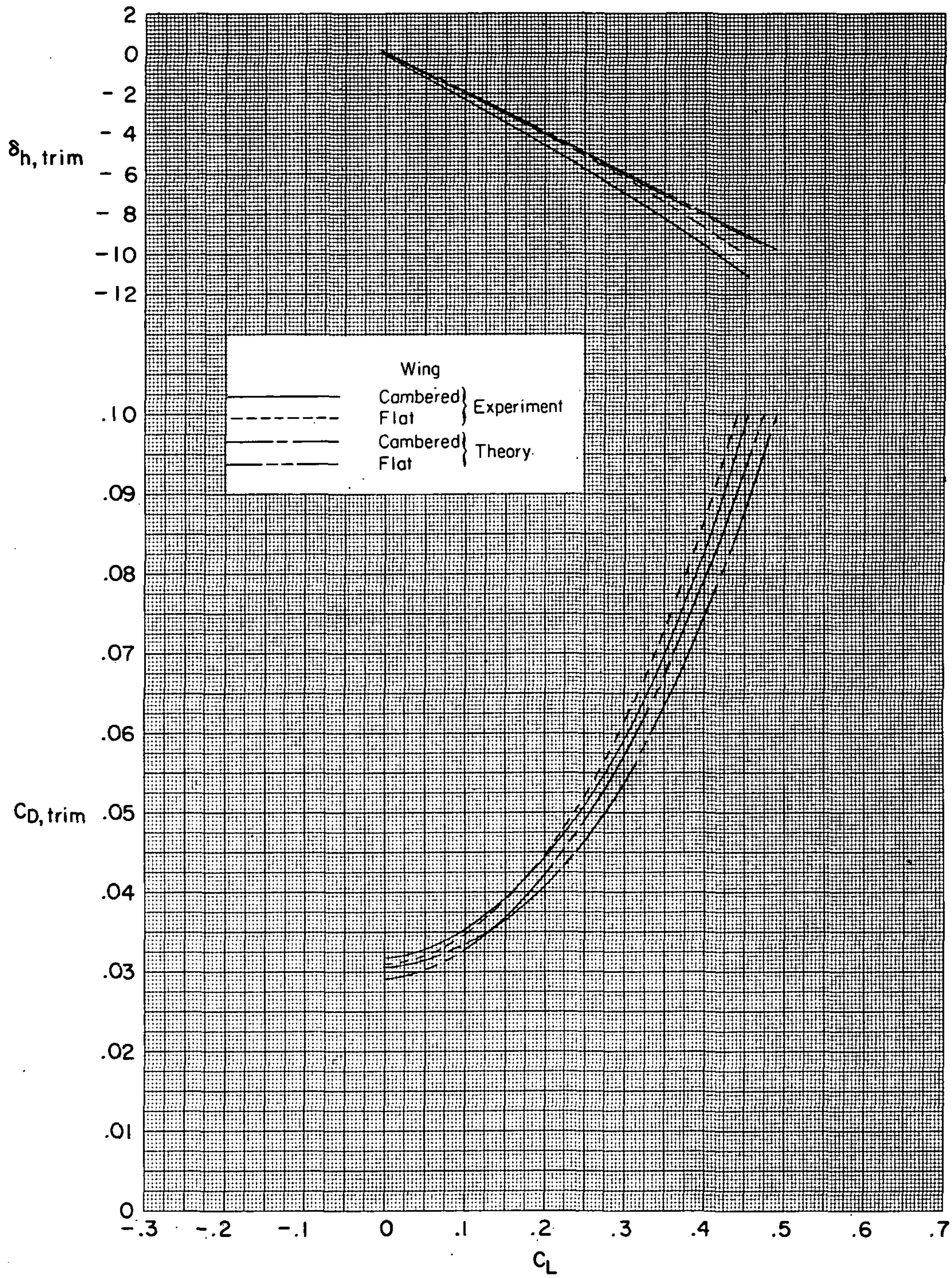

(a) M = 1.47.

Figure 13.- Comparison of experimental and theoretical trim characteristics.

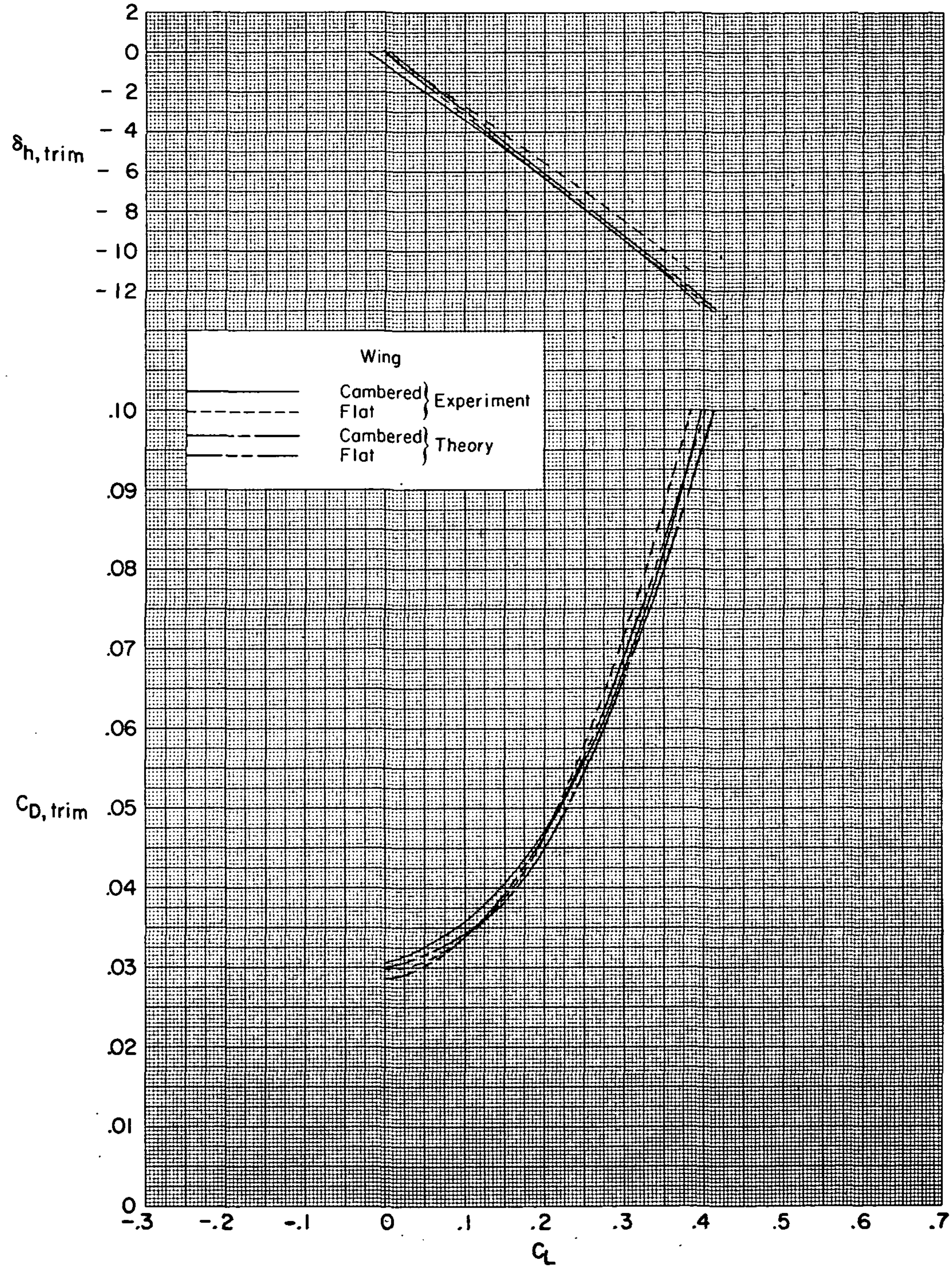

(b) M = 1.80.

Figure 13.- Continued.

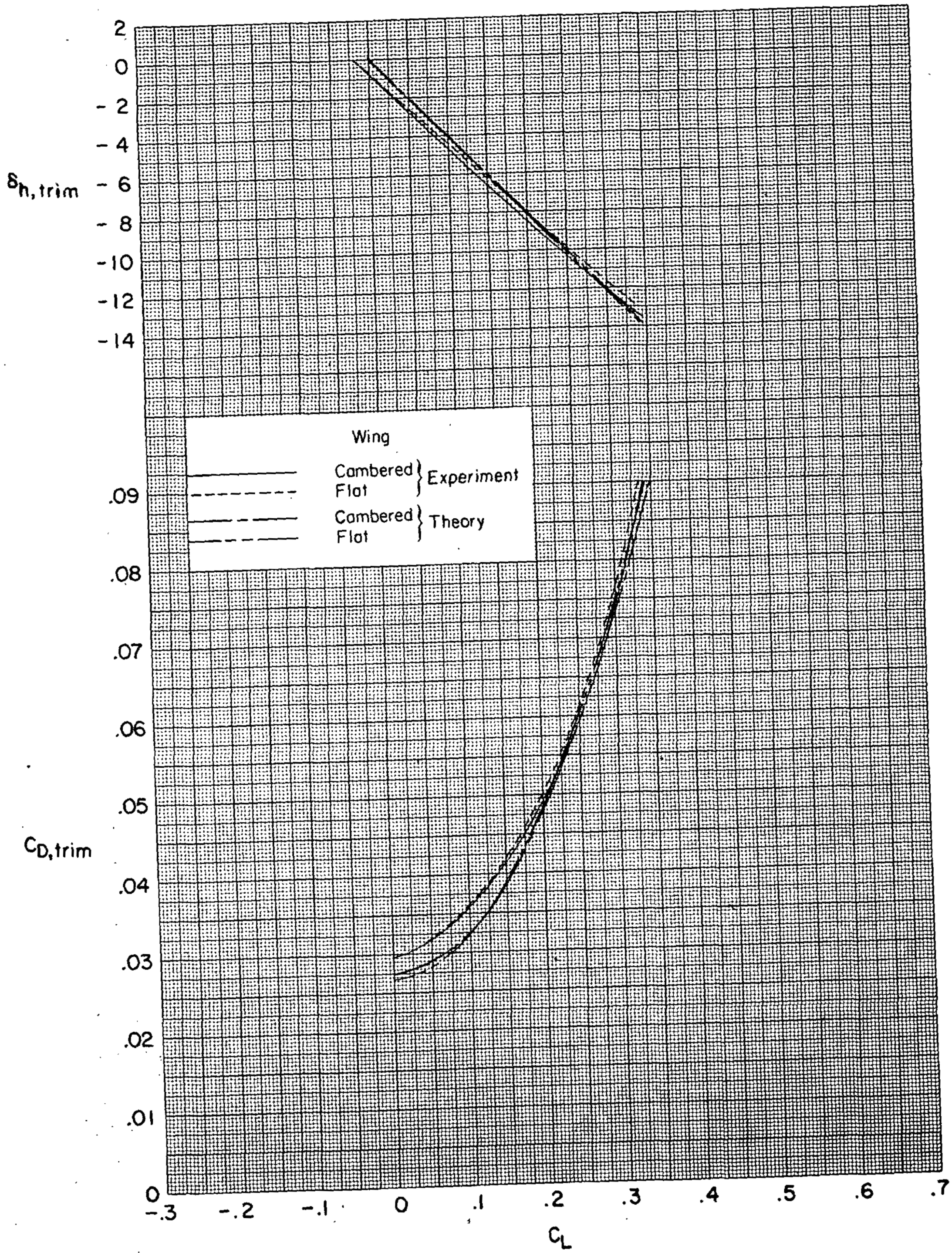

(c) M = 2.16.

Figure 13.- Concluded.

NASA-Langley, 1974 L-9463

"The aeronautical and space activities of the United States shall be conducted so as to contribute . . . to the expansion of human knowledge of phenomena in the atmosphere and space. The Administration shall provide for the widest practicable and appropriate dissemination of information concerning its activities and the results thereof."

—NATIONAL AERONAUTICS AND SPACE ACT OF 1958

NASA SCIENTIFIC AND TECHNICAL PUBLICATIONS

TECHNICAL REPORTS: Scientific and technical information considered important, complete, and a lasting contribution to existing knowledge.

TECHNICAL NOTES: Information less broad in scope but nevertheless of importance as a contribution to existing knowledge.

TECHNICAL MEMORANDUMS: Information receiving limited distribution because of preliminary data, security classification, or other reasons. Also includes conference proceedings with either limited or unlimited distribution.

CONTRACTOR REPORTS: Scientific and technical information generated under a NASA contract or grant and considered an important contribution to existing knowledge.

TECHNICAL TRANSLATIONS: Information published in a foreign language considered to merit NASA distribution in English.

SPECIAL PUBLICATIONS: Information derived from or of value to NASA activities. Publications include final reports of major projects, monographs, data compilations, handbooks, sourcebooks, and special bibliographies.

TECHNOLOGY UTILIZATION PUBLICATIONS: Information on technology used by NASA that may be of particular interest in commercial and other non-aerospace applications. Publications include Tech Briefs, Technology Utilization Reports and Technology Surveys.

Details on the availability of these publications may be obtained from:

SCIENTIFIC AND TECHNICAL INFORMATION OFFICE

NATIONAL AERONAUTICS AND SPACE ADMINISTRATION

Washington, D.C. 20546